SOME NEW HIGH-FREQUENCY EQUIVALENT CIRCUITS FOR JUNCTION TRANSISTORS

by
R. M. SCARLETT

Technical Report No. 103
March 20, 1956

Prepared under Office of Naval Research Contract
N6onr 251 (07), NR 373 360
Jointly supported by the U.S. Army Signal Corps,
the U.S. Air Force, and the U.S. Navy
(Office of Naval Research)

Stanford Electronics Laboratories
STANFORD UNIVERSITY
STANFORD, CALIFORNIA

Stanford Electronics Laboratories
Stanford University
Stanford, California

SOME NEW HIGH-FREQUENCY EQUIVALENT CIRCUITS FOR JUNCTION TRANSISTORS

by

R. M. Scarlett

Technical Report No. 103

March 20, 1956

Prepared under Office of Naval Research Contract
N6onr 251(07), NR 373 360
Jointly supported by the U. S. Army Signal Corps.
the U. S. Air Force, and the U. S. Navy
(Office of Naval Research)

SUMMARY

This report is concerned principally with the characterization of junction transistor triodes at high frequencies by means of small-signal equivalent circuits and associated four-pole parameters. Rational function approximations are developed for the theoretical short-circuit admittance parameters which describe the frequency behavior of an idealized one-dimensional intrinsic transistor. An actual transistor is assumed to be composed of the intrinsic transistor in combination with the collector space charge layer capacitance and base spreading resistance. On this basis, equivalent circuits and four-pole parameters in hybrid form are developed for the overall transistor in each of the three useful configurations. These parameters lend themselves readily to further approximation, and for certain frequency ranges result in some new equivalent circuits of considerably simplified form. The element values in all the circuits are expressed in terms of six fundamental circuit parameters, which are independent of the circuit configuration.

The measurement of transistor small-signal properties is considered. It is shown how the high-frequency short-circuit admittance parameters of the transistor, or any three-terminal network, may be measured directly by the use of a transformer ratio-arm bridge. Methods for measurement of the six fundamental circuit parameters are also given.

Finally, some figures of merit relating to the available high-frequency power gain are obtained in terms of the transistor circuit parameters, and simple design methods for wideband low-pass and bandpass amplifiers are presented. Measurements made on two amplifiers show good agreement with the calculated responses based on the simple equivalent circuits.

ACKNOWLEDGEMENTS

The author is grateful for the helpful guidance and supervision of Dr. J. M. Pettit, and also for the suggestions and corrections made by G. S. Bahrs. This work was sponsored jointly by the U. S. Army Signal Corps, the U. S. Air Force, and the U. S. Navy, under the Office of Naval Research Contract N6onr 251(07), NR 373 360.

TABLE OF CONTENTS

LIST OF ILLUSTRATIONS

LIST OF ILLUSTRATIONS (Cont'd)

I. INTRODUCTION

The purpose of this report is a study of the small-signal properties of junction transistor triodes, leading to equivalent circuits suitable for linear amplifier design.* Attention is directed to those cases where amplification is desired over a band of frequencies which may be a considerable fraction of the maximum possible bandwidth obtainable from the transistor, and where filter-like characteristics are desired; that is, uniform amplification over the band and reasonably rapid attenuation outside the band. Such amplifiers will be referred to as "wideband" and may be either low-pass (video) or band-pass (IF).

Before amplifier design can be intelligently undertaken, the active device to be used, in this case a transistor, must be characterized by an equivalent circuit, which then becomes the basis for the design of associated coupling and feedback networks to control the frequency response. In addition, fundamental limitations on gain and bandwidth, imposed by the device itself, as well as problems of stability can be studied. The emphasis in this report is on the preliminary step of characterization of the device by a convenient equivalent circuit and corresponding four-pole parameters. Associated problems relating to the measurement of these parameters for a particular transistor are also considered.

The transistor for small-signal applications is a linear active four-pole (or, more accurately, a three-terminal network) which can be characterized by a set of four parameters; two describing immittances at the input and output terminals, and two describing forward and reverse transfer properties. As with a triode vacuum tube, there are three useful configurations depending on which of the three terminals is common

---

*The research has been conducted concurrently with that of R. D. Middlebrook, and supports the findings reported in Technical Report No. 83 (N6onr 25107). It also extends and simplifies the results described in TR-No. 83.

to input and output terminal pairs. Each configuration is described by a set of parameters, or an equivalent circuit, and a study of these will suggest the broad area of application of each. One important fact which emerges is that the device is not even approximately unilateral, particularly at high frequencies, in contrast to the pentode vacuum tube where, for example, the property of isolation between interstage circuits makes possible simple stagger-tuning techniques. Consequences of this nonunilateral character, which can be thought of as internal feedback, are excessive complication in design and alignment of amplifiers, and the possibility of instability with certain terminating impedances. As a result, except for some special cases where the reverse transmission can either be ignored, or taken into account in a simple manner, important advantages may result from neutralization where an external network is associated with the device in such a way that the resulting reverse transmission from output to input of the overall circuit is made negligibly small.*

One goal of this report is to obtain equivalent circuits in as simple a form as possible to facilitate circuit design. These equivalent circuits may be of a very approximate nature, since the simpler the circuit the less accurately it represents the transistor. Transistor circuit design is in a sufficiently early stage that the use of an approximate model having only enough complexity to represent the most essential characteristics of the device is distinctly helpful. Restriction of operation to a certain frequency band or to certain external circuit conditions will often permit simplification, just as it does with vacuum tubes. There are also a number of circuits which can be drawn corresponding to identical terminal properties,[1] and

---

*The word "neutralization" is taken to be equivalent to the more descriptive but cumbersome term "unilateralization."

[1]Superscript numerals refer to the numbered references which appear at the end of the report.

one of these will generally be of simpler form than the others, or more directly suited to a particular application. For a given transistor, the element values in the equivalent circuits are determined by certain measurements made on the device. Another aim of this report is to present techniques for making suitable measurements.

Chapter II considers the ideal, one-dimensional junction triode, or "intrinsic" transistor which has been extensively studied theoretically; its small-signal parameters are stated, rather than derived. Since the device is of a distributed nature, however, these parameters are not rational functions of frequency. The problem is considered of how best to approximate these parameters by simple rational functions over the useful frequency range, so that a lumped-network representation may be used. The intrinsic transistor is itself only an approximation to an actual transistor. Extrinsic elements must be added to represent principally base spreading resistance and collector space charge layer capacitance.* Leakage conductance across the collector junction may also be of importance. Chapter III considers the complete transistor in the common-base configuration. Four-pole parameters are derived in such a form that useful approximations which can be made are readily apparent, and several equivalent circuits given. One of these, corresponding to a particular operating point, is of especially simple form, and a series of measurements made on ten high-frequency transistors is presented showing good agreement with the theory. Chapter IV derives approximate equivalent circuits for the common-emitter and the common-collector configurations. In all cases the circuit elements are referred both to measured and physical parameters of the transistor.

---

*The collector space charge layer capacitance is properly an intrinsic effect; for convenience, however, it will be considered separately from the intrinsic transistor and termed "extrinsic."

General considerations relating to transistor measurements are given in Chapter V. Techniques for making four-pole parameter measurements, including bias and termination problems, are discussed. Methods are also shown for the measurement of the fundamental circuit parameters in terms of which all the equivalent circuits of this report are expressed. Chapter VI, making use of the four-pole parameters previously developed, derives expressions for the available power gain of the different transistor configurations under various conditions. A brief investigation is made of the factors limiting bandwidth. Finally, design examples of bandpass and lowpass amplifiers are given, with experimental results.

It is concluded that the simple equivalent circuits presented can yield useful results to the accuracies ordinarily required, when applied to linear-amplifier design of moderately wide bandwidth. Present-day junction triodes are capable of giving reasonable gains over the bandwidths required for television and some radar applications. Owing to certain assumptions employed, the work described appears to be most accurate for conventional alloy-type and surface barrier junction triodes, whose development has been extended well into the radio-frequency range.[2,3] The work should also be applicable to p-n-i-p transistors.[4] However, many grown-type units are not so well represented, nor are junction tetrodes.[5]

II. THE INTRINSIC TRANSISTOR

This chapter considers the ideal one-dimensional transistor triode from the small-signal circuit parameter viewpoint. The theory for this situation is well developed,[6,7] and a brief initial discussion is given of the basic ideas and equations leading to the desired results in the form of four short-circuit admittance parameters. On account of the diffusive nature of the charge carrier motion and the fact that recombination and storage effects are distributed throughout the base region, these parameters are nonrational functions. The problem thus arises of approximating these by rational functions having a simple network representation; the approximations obtained will serve as the basis for later development of equivalent circuits characterizing the overall transistor in the three useful configurations.

Departures from the idealized intrinsic model assumed occur principally because of nonplanar geometry and surface recombination. Convenient visualization of these effects can be achieved by means of an electric circuit analogy for diffusion in the base region, developed in Appendix A; analytical evaluation of surface effects can be obtained for simple geometry, as in Appendix B. However, these considerations are not essential to the present discussion.

A. THE INTRINSIC Y-PARAMETERS

Figure 2.1 shows the simple geometry which will be assumed. The net flow of carriers is supposed to take place entirely in the x-direction. Nonrectifying contacts are attached, and the reference directions of current and voltage shown. For the time being, the base region majority carrier resistance and collector space charge layer capacitance will be ignored.

A p-n-p arrangement is considered for explicitness, although the analysis is of identical form and the results the same for an n-p-n transistor. There exist in each region mobile holes

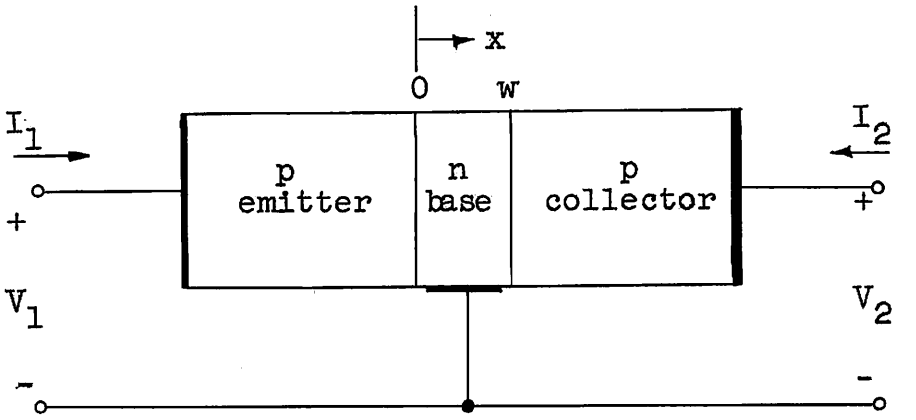

FIG. 2.1.--Intrinsic transistor geometry, with reference directions of terminal voltages and currents.

and electrons which are available for carrying current upon the application of external voltage. Under equilibrium conditions (no applied voltages) the densities of these carriers are uniform throughout each region, except for a small transition region near the junction boundaries which will be neglected in this simplified treatment. Holes predominate in the p-region due to acceptor impurities, and electrons in the n-region due to donor impurities; the product of the density of these majority carriers and the density of the many times less numerous minority carriers is a constant in any region:

$$np = n_i^2 \qquad (2.1)$$

where n is electron density, p is hole density, and $n_i = p_i$ is the density of either holes or electrons in intrinsic, or pure, germanium; $n_i \simeq 2.5 \times 10^{13}$ carriers per c.c. (at $T = 300^{\circ}K$) and is an exponential function of temperature, approximately doubling every $15.5^{\circ}C$. The majority carrier density is very

closely equal to the impurity density, and is measured by the conductivity; for n-type germanium, as an example:

$$\sigma = q\mu_n n = q\mu_n N_d \tag{2.2}$$

where N_d is the density of donor atoms, μ_n is the mobility* of electrons, and q the magnitude of the electronic charge. The conductivities of all three regions are usually great enough that voltage drops occurring in the body of the material can be ignored in comparison to the applied d-c bias potentials,** which thus effectively appear across the transition regions. Negligible electric field appears in the base region, so the flow of carriers occurs only by diffusion instead of by drift.

Diffusive motion is the result of random thermal motion of the charge carriers which, on the average, acts to cause their density to become uniform throughout a region. Thus, net current will flow from areas of high-density to low-density areas. For minority carriers, which provide the basis of transistor action, no charge repulsion effects occur even in high-density areas, provided the density remains much less than that of the majority carriers, which move so as to neutralize the unbalance of charge.[8] Under these conditions, diffusion is a linear phenomenon, and for holes in n-type material can be expressed in the form:***

$$\underline{i}_p = -qD_p \nabla p \tag{2.3}$$

where $\underline{i}_p$ is the current carried per cm^2, owing to a hole density

---

*Mobility is the drift velocity achieved in a unit electric field.

**This is not strictly true for the base region, owing to its small volume, but will be a useful approximation for this section.

***Vector quantities, such as $\underline{i}_p$, will be underlined.

gradient ∇p, and D_p is the diffusion constant for holes which will be taken as 44 cm^2 per sec. in germanium.[9]

When there is an excess of minority carriers over the normal equilibrium concentration, there will be a net rate of hole-electron recombination tending to restore equilibrium. If the excess concentration is small compared to the majority carrier concentration, the net rate of recombination is proportional to the excess concentration, which will decay (if the source providing the excess is removed) according to $\exp[-t/\tau]$. The factor τ is called the lifetime of the minority carriers; for holes in the n-type base it will be written τ_p. Another way of stating this law is that, if no diffusion exists, the rate of change of concentration is proportional to the excess concentration, that is:

$$\frac{\partial p}{\partial t} = - \frac{p - p_n}{\tau_p} \qquad (2.4)$$

where p_n is the equilibrium hole concentration. It will be assumed that this relationship holds uniformly throughout the base region. In addition to the above volume recombination there is surface recombination, an important mechanism occurring at the free surface of the base region. Since this section will consider one-dimensional geometry only, surface recombination does not enter; however, it may be of considerable importance in practical transistors, and further consideration of it is given in Appendices A and B.

The equation describing the flow of minority carriers in the base region can now be formulated. An excess concentration of holes (referring to a p-n-p transistor) in an area tends to diffuse to areas of lower concentration and also to disappear by recombination. Thus, the net rate of decrease in concentration in a small volume is equal to the total current (holes/cm^3/sec) leaving the volume, plus the rate of recombination. Mathematically, using Eq. (2.4):

$$- \frac{\partial p}{\partial t} = \frac{1}{q} \nabla \cdot \underline{i_p} + \frac{p - p_n}{\tau_p} \qquad (2.5)$$

Using Eq. (2.3), and writing p_e for $p - p_n$:

$$\frac{\partial p_e}{\partial t} = - \frac{p_e}{\tau_p} + D_p \nabla^2 p_e \qquad (2.6)$$

This fundamental relationship is known as the diffusion equation, and from its solution the small-signal parameters for the intrinsic transistor directly derive. Equation (2.6) is valid for any geometry since it refers to conditions at a point. The only assumptions inherent in it are, 1) that a recombination mechanism described by Eq. (2.4) exists, characterized by a constant τ_p throughout the region under consideration, and 2) that the minority carrier density p remains much smaller than the majority carrier density n. Because of this last assumption, (2.6) is a linear equation, and its solution can be expressed as the sum of a d-c part depending on the d-c bias voltages applied, and an a-c part (with time dependence $e^{j\omega t}$) depending on small-signal excursions about the operating point. Only the a-c portion is of concern here, and flow will be assumed to take place in the x-direction only, as discussed earlier; hence the operators $\frac{\partial}{\partial t}$ and ∇^2 can be replaced by $j\omega$ and $\frac{\partial^2}{\partial x^2}$ respectively, and (2.6) becomes:

$$L_p^2 \frac{\partial^2 p_e}{\partial x^2} = p_e \ (1 + j\omega\tau_p); L_p \triangleq (D_p \tau_p)^{1/2}; \ p_e \triangleq p - p_n \qquad (2.7)$$

The particular solution of (2.7) depends on the boundary conditions existing at x = 0 and x = w (see Fig. 2.1). As a result of the hole energy distribution, the minority carrier density in the base just inside a junction with p-type material, which is biased V volts with respect to the base, is given by:[10]

$$p = p_n \exp [qV/kT] \qquad (2.8)$$

This nonlinear relation becomes approximately linear for small-signal components; denoting these by p and V, and d-c components by p_0 and V_0, there results:

$$p \simeq p_0 \frac{qV}{kT} \quad \text{if} \quad V \ll \frac{kT}{q} \tag{2.9}$$

where $p_0 = p_n \exp [qV_0/kT]$ $\frac{kT}{q} = 25$ mv. at $T = 300^\circ K$
The emitter region is biased positively with respect to the base by an amount V_e, so that (see Fig. 2.1):

$$p_0 = p_n \exp [qV_e/kT]; \; p \simeq p_0 \frac{qV_1}{kT} \text{ at } x = 0 \tag{2.10}$$

The collector region is biased negatively by a d-c voltage which is usually many times $\frac{kT}{q}$, so that at the collector side of the base region $p_0 \simeq p \simeq 0$ very closely. However, since the width of the collector-base transition region varies with collector voltage V_2, the base width itself varies,[11] and the boundary condition $p = 0$ applies not at $x = w$, but at $x = w + w'$ where w' depends on V_2. Here w is the base width corresponding to the d-c bias voltage, and w' the variation in base width due to the small-signal component V_2. This effect of constant hole density at a varying base width can be approximated by a varying hole density at constant base width w, provided $w' \ll w$. The resultant boundary condition at the collector junction can then be written in a form analogous to (2.10).

$$p \simeq \frac{p_0}{K} \frac{qV_2}{kT} \text{ at } x = w \tag{2.11}$$

where p_0 is given by (2.10), and K is a number expressing the rate of base width change with collector voltage. To a good approximation:

$$1/K = \frac{kT}{q} \frac{1}{w} \frac{\partial w}{\partial V_c} \tag{2.12}$$

which is the fractional change in base width per 25 mv change in collector voltage. The above is a good approximation if $\frac{w}{L_p} \ll 1$, as is generally the case. Typically, K is of the order of several thousand for most junction triodes.

The solution of the diffusion Eq. (2.7) with the boundary conditions (2.10) and (2.11) may now be obtained, giving p as a function of x (and of $j\omega$) throughout the base region. Emitter and collector currents I_1 and I_2 are obtained by evaluating (2.3) at x = 0 and x = w, respectively, and multiplying by the area of the junction.* In this process, p_0, the d-c hole density at the emitter, becomes I_e, the d-c emitter current. Since all the equations for small-signal quantities are linear, and the boundary conditions depend linearly on V_1 and V_2, the resulting expressions for I_1 and I_2 are linear combinations of V_1 and V_2:

$$I_1 = y'_{11} V_1 + y'_{12} V_2$$

$$I_2 = y'_{21} V_1 + y'_{22} V_2 \qquad (2.13)$$

The y' coefficients,** which are the short-circuit admittance

---

*It is here assumed that the emitter current is composed entirely of holes injected into the base, and that the collector current consists entirely of holes collected at the collector-base junction. In other words, the emitter efficiency and collector multiplication factors are assumed to be unity, which is normally a good approximation, as shown in reference 7.

**The prime notation refers to the intrinsic transistor; for example y'_{11} is the short-circuit input admittance for the intrinsic transistor, while y_{11} will refer to the same quantity for the overall transistor.

parameters* of the intrinsic transistor, are given by the following expressions.**

$$y'_{11} = G\,\theta \coth \theta$$

$$y'_{12} = -\frac{G}{K}\,\theta \operatorname{cosech} \theta$$

$$y'_{21} = -\,G\,\theta \operatorname{cosech} \theta$$

$$y'_{22} = \frac{G}{K}\,\theta \coth \theta \qquad (2.14)$$

where $G \triangleq \dfrac{qI_e}{kT}$, I_e = d-c emitter current

$$\theta \triangleq \frac{W}{L_p}\,(1 + j\omega\tau_p)^{1/2}$$

K = space charge layer widening factor, given by (2.12)

The principal assumptions inherent in Eqs.(2.14)(aside from that of small-signal operation) are:

1. Plane parallel geometry exists, as in Fig. 2.1, with one dimensional flow; this implies that no surface effects can enter in.

---

*These parameters are conveniently defined by the following circuit:

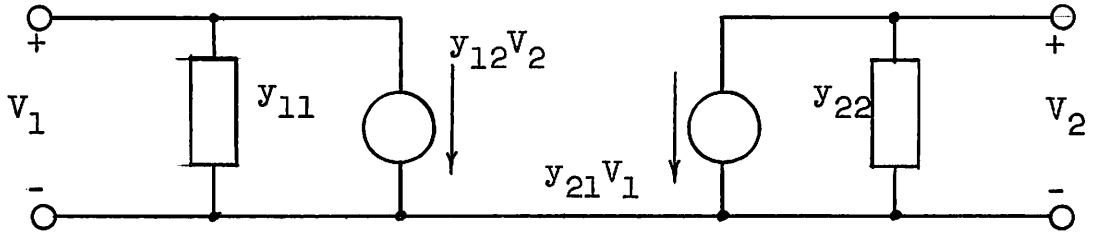

**For a simple derivation of these expressions, and the source of the notation used here, see: J. Zawels, "Physical theory of new circuit representations for junction transistors," J. Appl. Phys., vol. 25, Aug. 1954, pp. 976-981.

2. The minority carrier density in the base is much smaller than the majority carrier density.

3. The emitter efficiency and collector multiplication factor are both unity.

4. The base width w is much less than the diffusion length L_p.

Of these assumptions, 3 and 4 appear to be generally valid for most junction triodes.* Although 2 will be satisfied at low d-c emitter currents, evidence has been presented showing that the minority carrier density may become appreciable at emitter current densities of greater than 0.1 a/cm^2;[12] this corresponds to a total d-c emitter current of only 0.25 ma for a structure 0.020 in. square. Plane parallel geometry is a good approximation for grown units, and for some alloy structures. Where good high-frequency performance is desired, the junctions are made as nearly planar as possible.[13]

Surface recombination is an important phenomenon; in fact, it appears that the loss of minority carriers in the base is due principally to surface effects rather than to volume recombination.[14] However, an analysis given in Appendix B suggests that surface recombination can be taken into account in an approximate manner by supposing it to take place throughout the volume of the base, and ascribing to the volume recombination an effective lifetime which is less than the actual volume lifetime. As an aid to visualizing this mechanism, an electric circuit analog, or equivalent circuit, for diffusion is developed in Appendix A, to which boundary conditions at the surface can readily be applied.

---

*The assumption of unity emitter efficiency may not be valid at very low d-c emitter currents owing to the shunting effect of the emitter-base barrier capacitance.

This section has presented the most important ideas and equations leading to the y'-parameters of Eq. (2.14). Nothing new has been included, the intention being the laying of a foundation for the following work; in particular, the Appendices will utilize the general diffusion Eq. (2.6), together with its boundary conditions (2.10) and (2.11). From now on, except for a brief discussion of the extrinsic elements in section D, the transistor will be regarded as a "black box," characterized by the y-parameters of Eq. (2.14). The task at hand is a suitable approximation of these equations by rational functions, which can then be represented by a network of lumped elements.

B. APPROXIMATION TO THE HYPERBOLIC FUNCTIONS

The y-functions of the intrinsic transistor given in Eq. (2.14) have each a constant admittance factor G or G/K. A symmetry appears in the frequency-dependent portion, y'_{11} and y'_{22} having the common factor:

$$\theta \coth \theta \tag{2.15}$$

and y'_{12} and y'_{21} having the common factor:

$$\theta \operatorname{cosech} \theta \tag{2.16}$$

where:*

$$\theta \triangleq \frac{W}{L} (1 + j\omega\tau)^{1/2} \tag{2.17}$$

Equations (2.15) and (2.16) are regarded as functions of the complex frequency variable θ, and the problem is to obtain approximations to these which are rational functions of $j\omega$, where $j\omega$ and θ are related through (2.17). Fortunately, both coth θ and cosech θ have power series expansions in the region around $\theta = 0$ in which only odd powers of θ appear, so

---

*The subscript p has been dropped from L and τ since it is no longer necessary to consider the transistor to be specifically p-n-p.

that (2.15) and (2.16) are really functions of θ^2. The relation between θ^2 and $j\omega$ is a simple linear one, so that (2.15) and (2.16) can be approximated by functions rational in $j\omega$. There are two principal means of doing this: by using a finite number of terms in the partial fraction expansion,[15] or by using a finite number of terms in the power series expansion of either the function or its inverse. The second method appears to give the most accurate results for a given order of the approximating function, at least for the frequency range under consideration here.

The frequency range over which the approximation is desired to be useful, is from zero to somewhat greater than ω_α, where ω_α is the so-called alpha cut-off frequency. This is defined as the radian frequency at which the magnitude of the short-circuit current gain $\alpha = -y'_{21}/y'_{11}$ drops 3 db below its low-frequency value α_0. Calculations show that this occurs at a frequency such that:[16]

$$\omega_\alpha \tau \left(\frac{W}{L}\right)^2 \triangleq \omega_\alpha \tau_d = 2.43 \tag{2.18}$$

if $\alpha_0 = 1$. The corresponding value of θ^2 is, from (2.18):

$$\theta^2 = \left(\frac{W}{L}\right)^2 + j\omega_\alpha \tau_d \simeq j2.43 \tag{2.19}$$

or

$$|\theta| \simeq 1.56$$

if $\left(\frac{W}{L}\right)^2$ is neglected, which is equivalent to assuming an α_0 of unity. (See Eq. (2.24) later) Thus, in terms of θ, the desired minimum range of approximation is:

$$0 \lesssim |\theta| \lesssim 1.56 \tag{2.20}$$

Consider the function:

$$\theta \coth \theta = \theta \frac{\cosh \theta}{\sinh \theta} \tag{2.15}$$

This function is analytic except for simple poles at the zeros of sinh θ (not including the zero at $\theta = 0$) which occur at $\theta = \pm n\pi j$, $n = 1, 2, \ldots$. The power series (Maclaurin) expansion about $\theta = 0$ therefore converges uniformly for values of $|\theta|$ less than the distance to the nearest pole,[17] i.e. $|\theta| < \pi$, which is about twice the range required by (2.20). The inverse of the function possesses poles at the zeros of cosh θ, which are at $\theta = \pm \frac{2n - 1}{2} \pi j$, $n = 1, 2, \ldots$. The power series expansion for the inverse therefore converges for $|\theta| < \frac{\pi}{2}$ which is barely sufficient. It is thus expected that the expansion of the function itself will yield the best approximation for a given number of terms. This expansion is:[18]

$$\theta \coth \theta = 1 + \frac{1}{3} \theta^2 - \frac{1}{45} \theta^4 + \ldots . \quad |\theta| < \pi$$

The first two terms of this series yield an acceptable approximation up to alpha cut-off as will be shown; using (2.17) and (2.18):

$$\theta \coth \theta \simeq 1 + \frac{1}{3} \theta^2 = 1 + \frac{1}{3} \left(\frac{w}{L}\right)^2 + j\omega \frac{\tau_d}{3} \qquad (2.21)$$

which is a simple first-order rational function.

Consider now the function:

$$\theta \operatorname{cosech} \theta = \frac{\theta}{\sinh \theta} \qquad (2.16)$$

This function again possesses poles at the zeros of sinh θ (except at $\theta = 0$) so that its power series representation converges for $|\theta| < \pi$. However, the inverse of (2.16) is analytic everywhere in the finite θ-plane so that its power series converges for any finite θ. It is thus expected that the series for the inverse function will provide a more efficient approximation:

$$\frac{\sinh \theta}{\theta} = 1 + \frac{1}{6} \theta^2 + \frac{1}{120} \theta^4 + \ldots .$$

Using the first two terms yields the approximation:

$$\theta \operatorname{cosech} \theta \simeq \frac{1}{1 + \frac{1}{6}\theta^2} = \frac{1}{1 + \frac{1}{6}\left(\frac{W}{L}\right)^2 + j\omega \frac{\tau_d}{6}} \tag{2.22}$$

which is again a simple first-order rational function.

Equations (2.21) and (2.22) are the basic approximations which will be used to obtain equivalent circuit representations; however they can be put in more convenient form. Each involves the quantities $\left(\frac{W}{L}\right)^2$ and $\tau_d \triangleq \tau \left(\frac{W}{L}\right)^2$ which are constants for a particular transistor. These constants can be related to the more useful (for circuit applications) and easily measurable parameters α_0 and ω_α through the expression for α:

$$\alpha = \frac{-y'_{21}}{y'_{11}} = \operatorname{sech} \theta = \frac{1}{\cosh \theta} \tag{2.23}$$

At very low frequencies, there results:

$$\alpha_0 = \frac{1}{\cosh \frac{W}{L}} \simeq \frac{1}{1 + \frac{1}{2}\left(\frac{W}{L}\right)^2} \approx 1 - \frac{1}{2}\left(\frac{W}{L}\right)^2 \tag{2.24}$$

Equation (2.24) directly relates α_0 and $\left(\frac{W}{L}\right)^2$, and Fig. 2.2 shows this relation as computed from the exact expression, as well as the approximation indicated. The frequency at which the magnitude of (2.23) is down by a factor of 0.707 (3 db) from its low-frequency value α_0, ω_α by definition, is conveniently expressed in terms of τ_d by:

$$\omega_\alpha = \frac{\kappa}{\tau_d} \tag{2.25}$$

where κ is a number depending somewhat on α_0, being 2.43 for

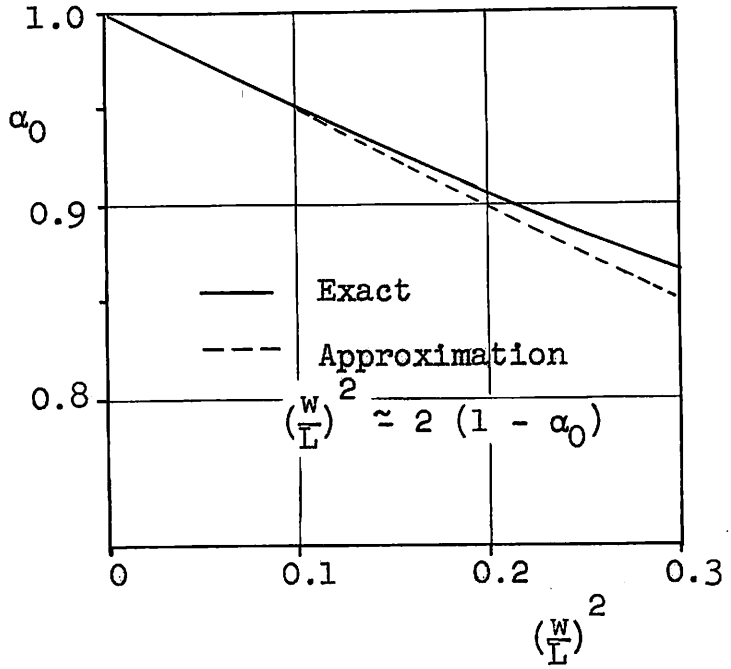

FIG. 2.2.--Relation between low-frequency current-gain α_0 and ratio of base width to difussion length w/L.

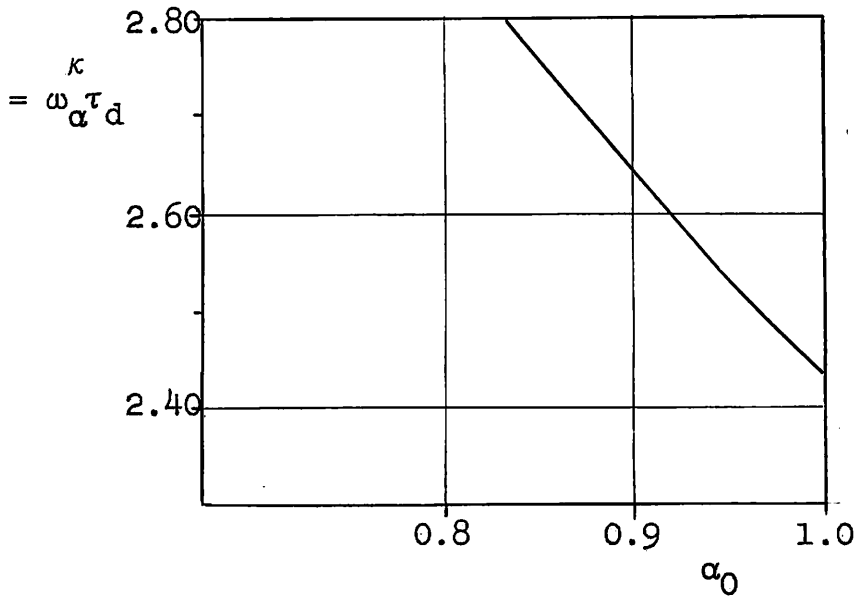

FIG. 2.3.--Relation between alpha cut-off frequency ω_α and diffusion time constant τ_d as a function of α_0.

$\alpha_0 = 1$, as indicated in Eq. (2.19). The factor κ cannot be expressed in a simple analytic fashion, but can be determined for various values of α_0 by a straightforward but tedious calculation, the details of which will not be given here. Figure 2.3 shows κ as a function of α_0, and is taken from published data,[19,20] checked by independent calculation.

The approximations (2.21) and (2.22) can now be plotted in terms of ω_α for various values of α_0, along with the exact expressions for comparison. Figure 2.4 shows real and imaginary parts of both sides of Eq. (2.21) as a function of normalized frequency ω/ω_α; Fig. 2.5 is a similar plot for the reciprocal of Eq. (2.22). Two values of α_0 are shown in each case, 0.99 and 0.90 representing about the limits of this parameter found in useful transistors. If these approximations are used to calculate the intrinsic h-parameters, as will be done in section C, the resulting expressions approximate the exact h-parameters more closely than might be expected from the curves of Figs. 2.4 and 2.5. This is fortunate, since, as will be seen, the h-parameters seem to be the most significant from a circuit viewpoint. (refer to Figs. 2.7 and 2.8)

The conclusions to be drawn from Figs. 2.4 and 2.5 are as follows: In both cases the approximation is reasonably good, considering that only a first-order function is used. The imaginary part is particularly good, and it is apparent that the curve for $\alpha_0 = 0.99$ also provides an acceptable approximation for $\alpha_0 = 0.90$. This means that a single value of κ corresponding to $\alpha_0 \simeq 1$ can be used; thus $\omega_\alpha \simeq \frac{2.43}{\tau_d}$. In Fig. 2.5, the real part is nearly independent of α_0, so that the approximation can be written:

$$\theta \operatorname{cosech} \theta \simeq \frac{1}{1 + 0.405\, j\, \omega/\omega_\alpha} \qquad (2.26)$$

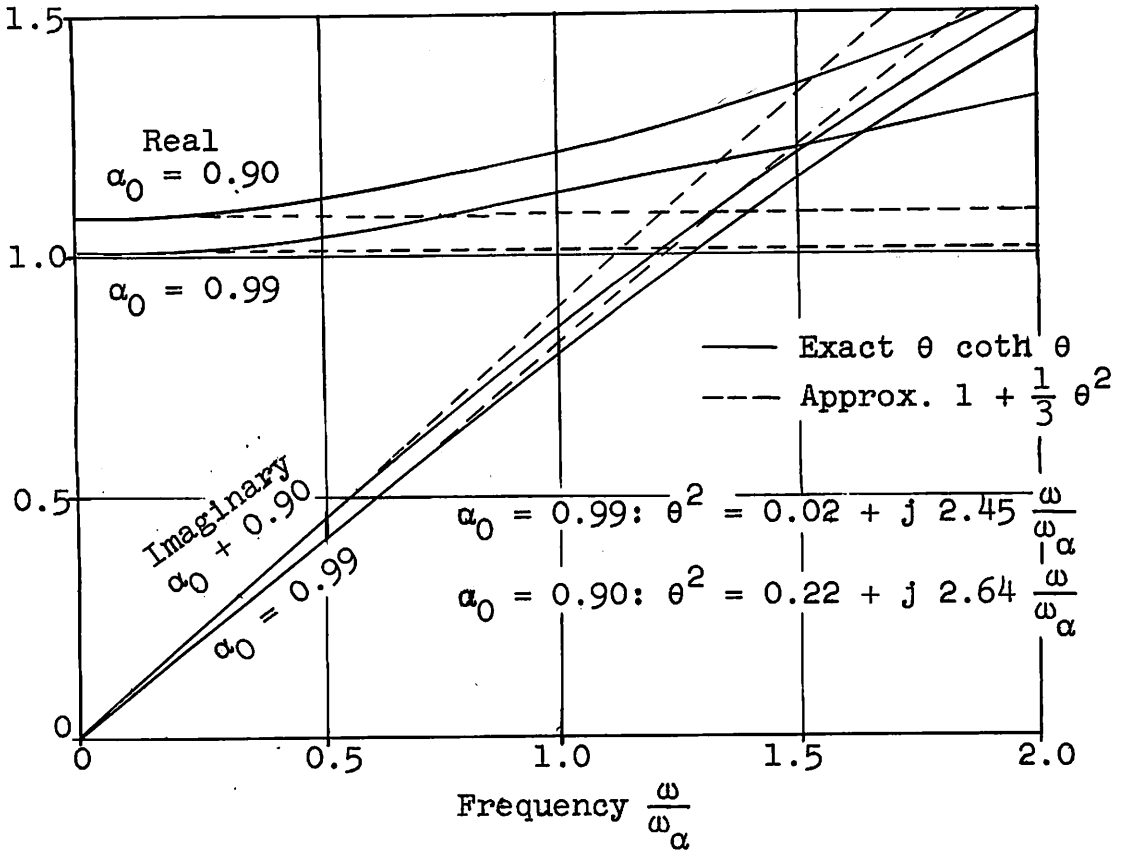

FIG. 2.4.--Real and imaginary parts of θ coth θ and approximation.

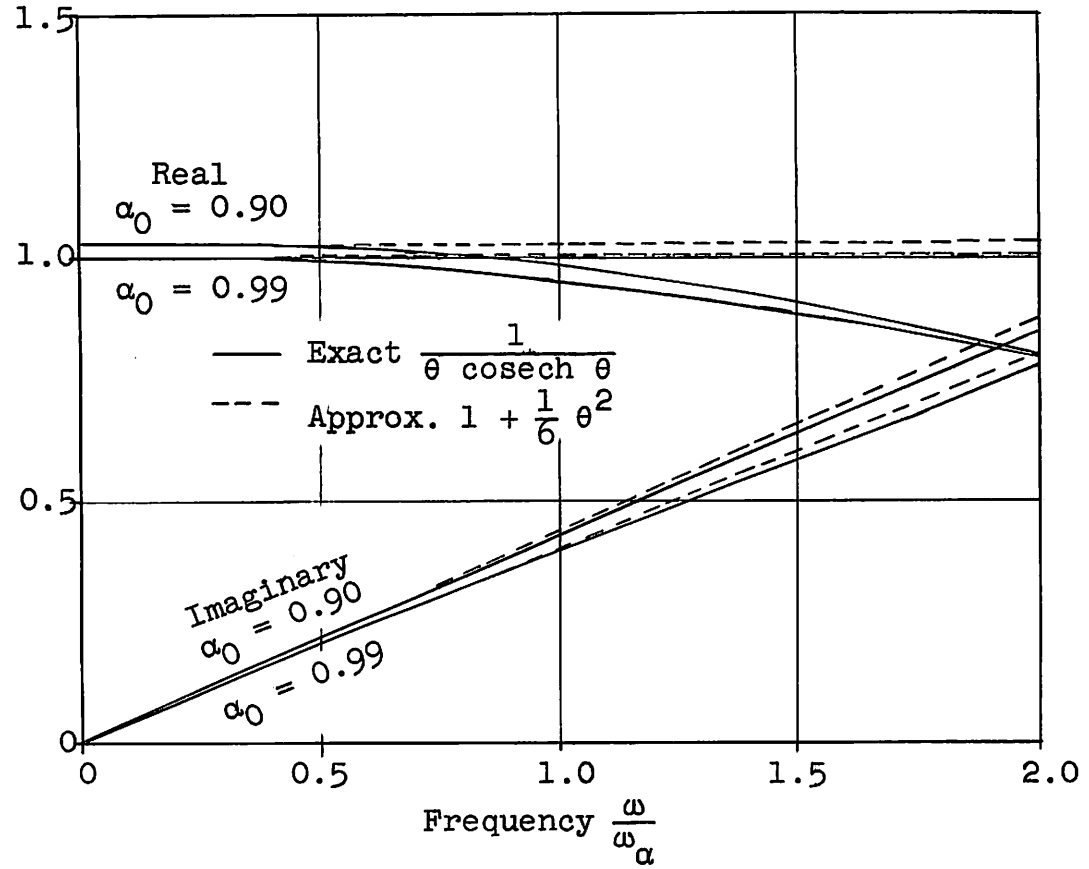

FIG. 2.5.--Real and imaginary parts of $\frac{1}{\theta \text{ cosech } \theta}$ and approximation.

In Fig. 2.4, the real part is somewhat more dependent on α_0. However, for most purposes of this report, the approximation will still be satisfactory if this dependence is ignored. Thus:

$$\theta \coth \theta \simeq 1 + 0.81\ j\ \omega/\omega_\alpha \tag{2.27}$$

Finally, an expression for θ^2 in terms of α_0 and ω_α will be required in order to obtain approximations for the intrinsic h-parameters. From Eq. (2.17), using the approximation to $(\frac{w}{L})^2$ indicated in Fig. 2.2:

$$\theta^2 \simeq 2(1 - \alpha_0) + 2.43\ j\ \omega/\omega_\alpha \tag{2.28}$$

Equations (2.26) to (2.28) are the final results of this section, and are thought to constitute a more efficient set of approximations than any published to date.

C. THE INTRINSIC H-PARAMETERS

In section B approximations were derived for the y-parameters of the intrinsic transistor, which will be of use primarily in determining equivalent circuits for the common-emitter and common-collector configurations to be discussed in Chapter IV. For common-base considerations, it will turn out to be considerably more convenient to work in terms of the h-parameters, which can be defined by the following equations:

$$\begin{aligned} V_1 &= h_{11}\ I_1 + h_{12}\ V_2 \\ I_2 &= h_{21}\ I_1 + h_{22}\ V_2 \end{aligned} \tag{2.29}$$

The V's and I's have reference directions shown in Fig. 2.6,

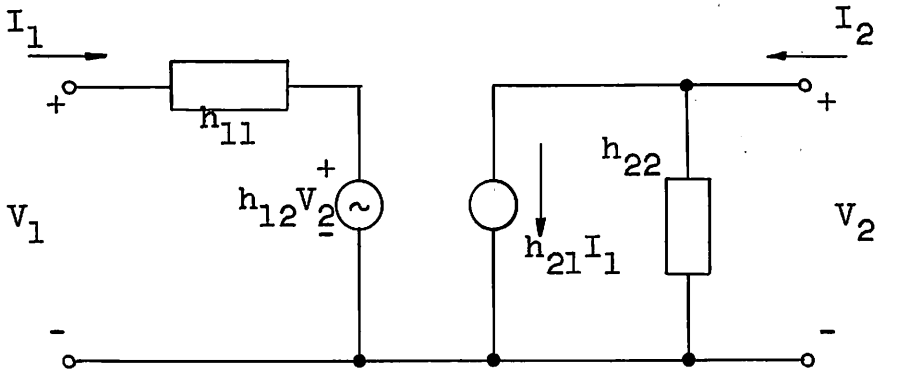

FIG. 2.6.--Circuit defining the hybrid (h) parameters.

which also gives an equivalent circuit defining the h-parameters. In terms of y-parameters, the h-parameters are given by:*

$$h_{11} = \frac{1}{y_{11}} \qquad h_{12} = \frac{-y_{12}}{y_{11}}$$

$$h_{21} = \frac{y_{21}}{y_{11}} \qquad h_{22} = \frac{\Delta^y}{y_{11}}$$

$$\Delta^y = y_{11}\, y_{22} - y_{12}\, y_{21} \tag{2.30}$$

The calculation of the intrinsic h-functions proceeds by substitution of the intrinsic y's of (2.14) into (2.30), and then employment of the previously developed approximations

*A convenient source of such matrix interrelations is R. F. Shea et. al., Principles of Transistor Circuits, John Wiley and Sons, Inc., New York, 1953, p. 335. See also E. A. Guillemin, Communication Networks, vol. II, John Wiley and Sons, Inc., New York, p. 132-139, but note that only passive networks are considered therein, where $y_{12} = y_{21}$.

(2.26) to (2.28). In the first step, one obtains:*

$$\Delta^{y'} = \frac{G^2\theta^2}{K}\left[\coth^2\theta - \operatorname{cosech}^2\theta\right] = \frac{G^2\theta^2}{K}$$

$$h'_{11} = \frac{1}{G\ \theta\ \coth\ \theta} \triangleq \frac{r_e'}{\theta\ \coth\ \theta}$$

$$h'_{12} = \frac{\operatorname{sech}\ \theta}{K} = \frac{\alpha}{K}$$

$$h'_{21} = -\ \operatorname{sech}\ \theta = -\ \alpha$$

$$h'_{22} = \frac{G}{K}\frac{\theta}{\coth\ \theta} \qquad (2.31)$$

The approximation process yields:

$$h'_{11} \simeq \frac{r_e'}{1 + 0.81\ j\ \omega/\omega_\alpha}$$

$$h'_{12} = \frac{1}{K}\frac{\theta\ \operatorname{cosech}\ \theta}{\theta\ \coth\ \theta} \simeq \frac{1}{K}\frac{\alpha_0}{(1 + 0.81\ j\ \omega/\omega_\alpha)(1 + 0.405\ j\ \omega/\omega_\alpha)}$$

$$\approx \frac{1}{K}\frac{\alpha_0}{1 + 1.21\ j\ \omega/\omega_\alpha}$$

$$h'_{21} \simeq \frac{-\ \alpha_0}{(1 + 0.81\ j\ \omega/\omega_\alpha)(1 + 0.405\ j\ \omega/\omega_\alpha)} \approx \frac{-\ \alpha_0}{1 + 1.21\ j\ \omega/\omega_\alpha}$$

$$h'_{22} = \frac{1}{Kr_e'}\frac{\theta^2}{\theta\ \coth\ \theta} \simeq \frac{1}{Kr_e'}\frac{2(1 - \alpha_0) + 2.43\ j\ \omega/\omega_\alpha}{1 + 0.81\ j\ \omega/\omega_\alpha}$$

$$\simeq \frac{1}{Kr_e'}\frac{1}{\frac{1}{3} + \frac{1}{2(1 - \alpha_0) + 2.43\ j\ \omega/\omega_\alpha}} \qquad (2.32)$$

---

*It is generally more convenient to deal with the reciprocal of G, and the symbol for this is chosen to be r_e' which is used fairly extensively throughout the literature.

Here the factor α_0 has been included in h'_{12} and h'_{21} so they will possess the correct low-frequency values. The further approximations shown for h'_{12} and h'_{21} are useful for $\frac{\omega}{\omega_\alpha} < 0.5$, or so. Equations (2.32) are the desired functions which will be used in Chapter III to obtain h-functions for the complete transistor.

Since the intrinsic h-parameters will be important to the study of common-base equivalent circuits, it is desirable to obtain an indication of the accuracy of the approximations used (Eq. 2.32), as was done for the y'-parameters in Figs. 2.4 and 2.5. Since h'_{11} corresponds to $\frac{1}{y'_{11}}$, the curves of Fig. 2.4 apply; but the other h'-parameters involve different functions, which are, from Eq. (2.31) (Note that h'_{12} and h'_{21} are essentially the same function):

$$\text{sech } \theta = \alpha$$

$$\frac{\theta}{\coth \theta}$$

where $\theta^2 = \left(\frac{W}{L}\right)^2 + j\omega\tau_d$

The approximations used for the above functions are, from Eq. (2.32):*

$$\alpha = \text{sech } \theta \simeq \frac{\alpha_0}{(1 + 0.81\ j\ \omega/\omega_\alpha)(1 + 0.405\ j\ \omega/\omega_\alpha)}$$

$$\approx \frac{\alpha_0}{1 + 1.21\ j\ \omega/\omega_\alpha} \qquad (2.33)$$

where α_0 and ω_α are defined by Figs. 2.2 and 2.3.

---

*A different approximation to alpha has been given by R. D. Middlebrook and R. M. Scarlett, "An approximation to alpha of a junction transistor," Trans. IRE, PGED, vol. ED-3, January 1956, pp. 25-29.

$$\frac{\theta}{\coth \theta} \simeq \frac{1}{\frac{1}{3} + \frac{1}{2(1 - \alpha_0) + 2.43\ j\ \omega/\omega_\alpha}}$$

For plotting purposes, it is convenient to rearrange the last equation thus:

$$\frac{1}{\frac{\theta}{\coth \theta} - \frac{1}{3}} \simeq 2(1 - \alpha_0) + 2.43\ j\ \omega/\omega_\alpha \qquad (2.34)$$

Figure 2.7 shows both sides (exact and approximate) of Eq. (2.33) plotted against normalized frequency ω/ω_α in terms of magnitude and phase (for two values of α_0), this being the most convenient representation for alpha, which is a current gain (numeric) rather than an immittance. In all cases, the curves have been normalized to unity at zero frequency. It is evident that the first approximation is excellent over the entire range,* and the second is useful up to perhaps $0.5\omega_\alpha$.

Figure 2.8 shows curves corresponding to Eq. (2.34). It may be seen the approximation is quite good up to ω_α, but departs appreciably from reality at $2\omega_\alpha$. However, the important frequency region is from zero to ω_α, and here the approximation is quite satisfactory.

D. EXTRINSIC ELEMENTS

The complete transistor differs from the intrinsic transistor principally by possessing base spreading resistance and collector space charge layer capacitance, which will be referred to as extrinsic elements. The base resistance arises from the fact that the base is of small volume and has a relatively small conductivity, hence it offers an appreciable

---

*For an approximation to alpha of somewhat different form, but about equally as accurate in this region, see R. D. Middlebrook, reference 7; p. 68. See also footnote on p. 24.

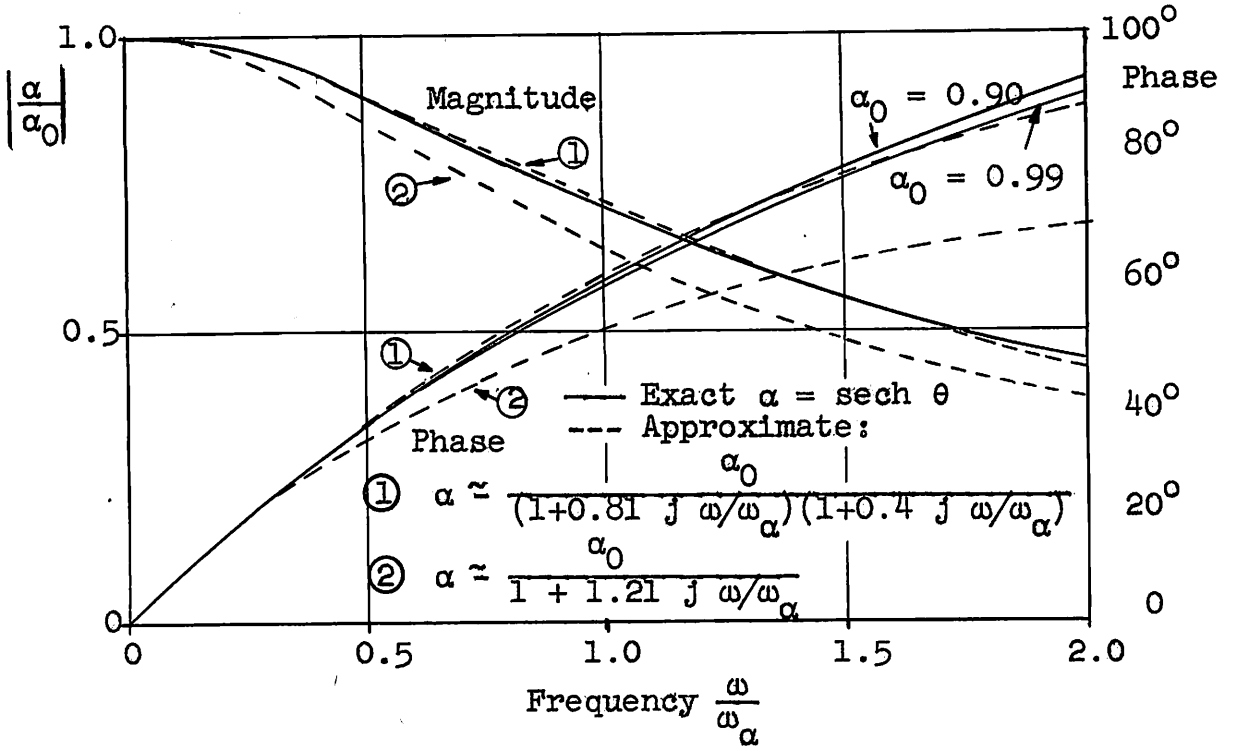

FIG. 2.7.--Magnitude and phase of α = sech θ and approximations.

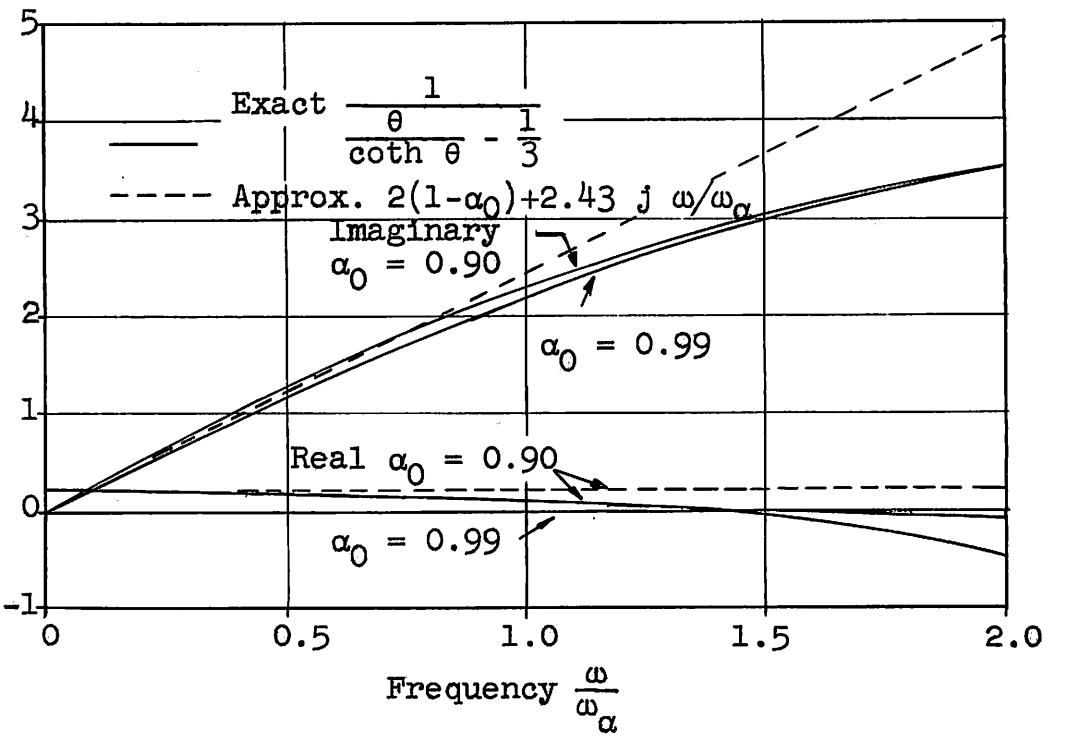

FIG. 2.8.--Real and imaginary parts of $1/[\frac{\theta}{\coth\ \theta} - \frac{1}{3}]$ and approximation.

resistance to the majority carrier recombination current flow. This effect can be approximated by a resistance r_b' in series leading to the external base terminal, as shown in Fig. 2.9. The recombination current is actually distributed through the base volume, and in grown-junction structures of very small base width it may be necessary to consider this distributed effect, leading to an effective complex base impedance.[21] In alloy transistors and many grown transistors, however, the assumption of a constant r_b' appears to be an excellent one.

The other important extrinsic element is the capacitance across the collector junction owing to the depletion layer of mobile carriers, which leaves a dipole layer of charge whose width is dependent on the d-c collector-to-base voltage. The capacitance is really nonlinear, but for small-signal a-c variations can be considered linear, and its value will be denoted by C_c. It appears from the collector to the intrinsic base terminal b', as shown in Fig. 2.9. A similar capacitance C_e exists across the emitter junction, but is generally small enough to be ignored* because of the small emitter impedance across which it appears,** unless the d-c emitter current is very small. However, in p-n-i-p transistors, C_e appears to be important.[22]

Various small parasitic capacitances between the external terminals exist on account of the mounting structure and proximity of the leads, and for some grown-junction units the effect of base contact overlap provides additional capacitance.[23] Evidence has been presented indicating that

---

*See, however, Chapter V for the possible effect of C_e on h_{22}. Refer to p. 107.

**This depletion layer capacitance must be distinguished from the emitter diffusion capacitance whose susceptance is given by the imaginary part of y_{11}' (Eq. 2.14). The latter is normally much larger and cannot be neglected. A similar diffusion capacitance appears at the collector, but is normally small compared to C_c. See p. 36.

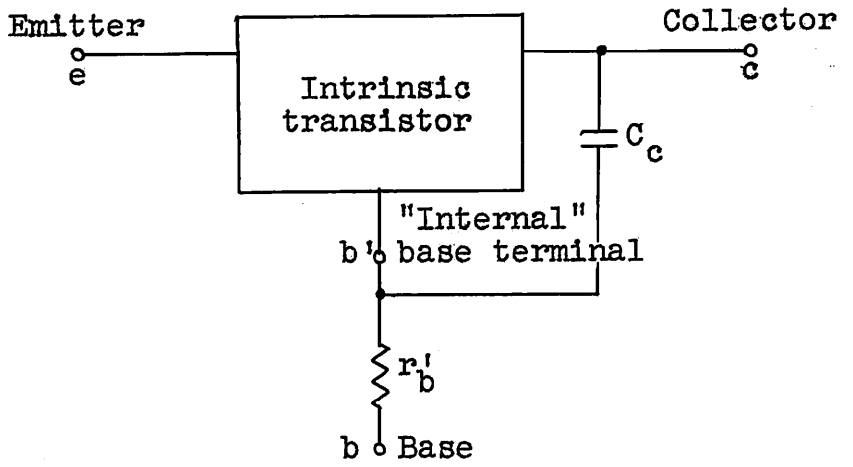

FIG. 2.9.--Showing the addition of the extrinsic elements r_b' and C_c to the intrinsic transistor.

the effect of C_{bc} (collector-base parasitic capacity) is appreciable at high frequencies in grown junction transistors.[24] Parasitic capacities will not be considered explicitly in this report; however they will undoubtedly become more important as transistor development is extended to higher frequencies.

The transistor can now be considered solely in terms of its circuit properties. Equivalent circuits will be derived from consideration of Fig. 2.9, where expressions for the intrinsic parameters have already been developed earlier in this chapter. The problem is now to determine circuit parameters for the overall transistor in the three useful configurations, and to make appropriate approximations. The most convenient approach in each case is somewhat different; Chapter III considers the common-base, and Chapter IV, the common-emitter and common-collector configurations.

E. CONCLUSIONS

A brief description has been given of the physical processes in an idealized one-dimensional junction transistor, leading to the fundamental equation for minority carrier motion and its appropriate boundary conditions. The small-signal solution to this equation for terminal currents in terms of applied voltages was stated in the form of four short-circuit admittance, or y-parameters. Approximations to these parameters which are simple rational functions of frequency were developed and shown to correspond reasonably closely to the exact expressions. The hybrid, or h-parameters for the intrinsic transistor were derived from the y-parameters in both exact and approximate form. Finally, in preparation for the next two chapters, the extrinsic elements necessary in a complete transistor were briefly discussed. Figure 2.9 shows the general equivalent circuit, which will be reduced to useful forms for common-base, common-emitter and common-collector configurations.

III. COMMON-BASE EQUIVALENT CIRCUITS

In the previous chapter the small-signal four-pole parameters of the intrinsic transistor have been given, and rational function approximations developed for these parameters which are fundamental to the study of equivalent circuits for any configuration. This chapter considers the common-base configuration; for this purpose the most convenient parameters to work with appear to be the h-parameters.

The model for the complete transistor considered in this report is shown in Fig. 3.1 for the common-base situation. From this circuit, overall h-parameters will be derived (in terms of the intrinsic h-parameters and the extrinsic elements r_b' and C_c), which will characterize the transistor over the entire useful frequency range from zero to somewhat above the alpha cut-off frequency. These overall h-parameters will be the basis for the synthesis of equivalent circuits and for the derivation of the corresponding y-parameters for comparison with those determined by R. D. Middlebrook.[7]

It will be found that, under certain restrictions in frequency range, or circuit conditions, considerable simplification in equivalent circuits and their representative h-parameters is possible. The development of these simplified circuits is a major goal of this report. At one particular operating point, an especially simple high-frequency circuit results, and measurements, designed to verify this circuit, are presented, which are made on a selection of 11 transistors.

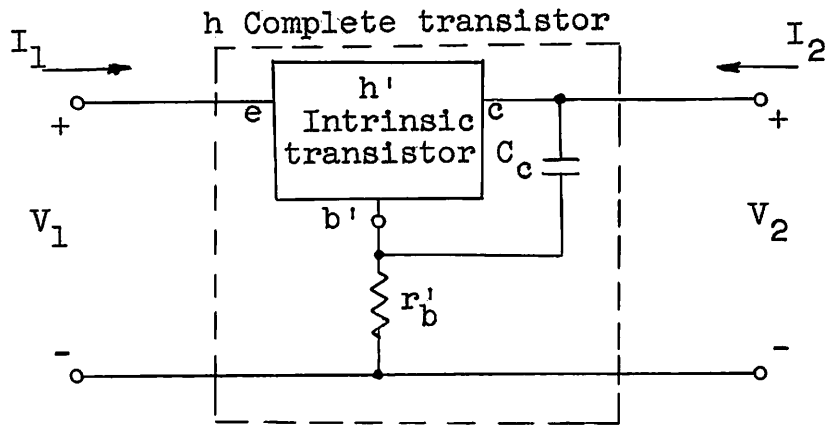

FIG. 3.1.--Common-base configuration for the complete transistor.

A. THE H-PARAMETERS OF THE COMPLETE TRANSISTOR

The immediate problem is to determine the h-parameters of the overall structure of Fig. 3.1, where the parameters of the h' network are known, and the elements r'_b and C_c are connected as shown. In general terms, the derivation proceeds in a straightforward manner. The element C_c is absorbed by adding its admittance $j\omega C_c$ to h'_{22}, the other h'-parameters being unaffected by this step. The set h'_{11}, h'_{12}, h'_{21}, and $h'_{22} + j\omega C_c$ is then converted to the corresponding set of open-circuit impedance, or z-parameters,* whereupon r'_b is absorbed by simple addition to each of the z's. The resultant set is then converted back to its equivalent h-form. The results for the situation of Fig. 3.1 have been given by Pritchard,[19] and are as follows:

*See footnote on page 22.

$$h_{11} = h'_{11} + \frac{r'_b\,(1 + h'_{21})(1 - h'_{12})}{1 + r'_b\,(h'_{22} + j\omega C_c)}$$

$$h_{12} = \frac{h'_{12} + r'_b\,(h'_{22} + j\omega C_c)}{1 + r'_b\,(h'_{22} + j\omega C_c)}$$

$$h_{21} = \frac{h'_{21} - r'_b\,(h'_{22} + j\omega C_c)}{1 + r'_b\,(h'_{22} + j\omega C_c)}$$

$$h_{22} = \frac{h'_{22} + j\omega C_c}{1 + r'_b\,(h'_{22} + j\omega C_c)} \qquad (3.1)$$

The h'-parameters have been given in exact and approximate form by Eqs. (2.31) and (2.32), respectively, which can now be substituted in Eq. (3.1) to obtain explicit h-parameters. A number of useful approximations can be made at this point. It is to be noted that the quantity $1 + r'_b\,(h'_{22} + j\omega C_c)$ appears in all the expressions. From Eq. (2.32):

$$h'_{22} \simeq \frac{1}{Kr'_e}\,\frac{2(1 - \alpha_0) + 2.43\ j\ \omega/\omega_\alpha}{1 + 0.81\ j\ \omega/\omega_\alpha} \qquad (3.2)$$

This quantity has a magnitude of $\frac{2(1 - \alpha_0)}{Kr'_e}$ at $\omega = 0$ increasing to a maximum magnitude of $\frac{3}{Kr'_e}$ with increasing frequency.* Thus the maximum magnitude of the quantity $r'_b\,h'_{22}$ is $\frac{3r'_b}{Kr'_e}$. For all good

*It should be understood that Eq. (3.2) is an approximation, and valid only up to a frequency of the order of $2\omega_\alpha$. It does <u>not</u> correctly indicate the asymptotic behavior of h_{22} for $\omega \to \infty$.

junction triodes at the present time, $\frac{r_b'}{r_e'} < 10$, $K > 10^3$, so that $|r_b' h_{22}'| < 0.03$ (probably considerably less), and hence to a good approximation:

$$1 + r_b' (h_{22}' + j\omega C_c) \simeq 1 + j\omega r_b' C_c \tag{3.3}$$

In many cases, the imaginary part of (3.3) can also be discarded, particularly at low frequencies. Its value at alpha cut-off, $\omega_\alpha r_b' C_c$, is a quantity which occurs frequently in transistor circuit theory, and is conveniently denoted by a single symbol:*

$$\partial \triangleq \omega_\alpha r_b' C_c \tag{3.4}$$

This quantity is a fundamental constant of a transistor and enters into all high-frequency performance calculations, as will become apparent in Chapter VI. For most high-frequency transistors, ∂ is generally less than 0.1, and to a fair approximation one can write:

$$1 + r_b' (h_{22}' + j\omega C_c) \simeq 1 + j\omega r_b' C_c = 1 + j\partial \omega/\omega_\alpha \approx 1 \tag{3.5}$$

for $\frac{\omega}{\omega_\alpha} < 1$. However, the term in ∂ will be retained in some of the expressions where it is of importance. It is also convenient to define a normalized complex frequency variable, which in the sinusoidal steady state case is:

$$s \triangleq j \frac{\omega}{\omega_\alpha} \tag{3.6}$$

Thus Eq. (3.5) is written:

$$1 + r_b' (h_{22}' + j\omega C_c) \simeq 1 + \partial s \tag{3.7}$$

---

*Middlebrook (see reference 7) uses the same symbol for a very similar, but slightly more complicated expression.

The factor $1 - h'_{12}$ in the expression for h_{11} is very nearly equal to unity, as h'_{12} is of magnitude $\frac{1}{K}$ and decreases with frequency. Using Eq. (2.32) and the notation of Eq. (3.6), the relation $1 + h'_{21} = 1 - \alpha$ can be expressed as:

$$1 + h'_{21} = (1 - \alpha_0) \frac{1 + \frac{1.21}{1 - \alpha_0} s + \frac{0.33}{1 - \alpha_0} s^2}{1 + 1.21s + 0.33s^2}$$

The dominant term here in the frequency range of interest is $\frac{1.21}{1 - \alpha_0}s$, and, to a good approximation, the terms in s^2 may be ignored; thus:

$$1 + h'_{21} \simeq (1 - \alpha_0) \frac{1 + \frac{1.21}{1 - \alpha_0} s}{1 + 1.21\ s} \qquad (3.8)$$

With the aid of Eq. (2.33), (3.5) and (3.8) in (3.1), h_{11} becomes:

$$h_{11} \simeq \frac{r'_e}{1 + 0.81s} + r'_b\ (1 - \alpha_0) \frac{1 + \frac{1.21}{1 - \alpha_0} s}{1 + 1.21s}$$

The first term is the emitter diffusion impedance h'_{11}. The second term results from the difference of collector and emitter currents flowing through the extrinsic base resistance r'_b. It is convenient to combine these terms, and it is then found that the following expression provides an acceptable approximation:

$$h_{11} \simeq \frac{r'_e + r'_b\ (1 - \alpha_0) + 1.21\ r'_b\ s}{1 + s} \qquad (3.9)$$

The parameter h_{12} is found by substituting from Eqs.(2.32) and (3.5) into (3.1), and using the definitions of Eqs. (3.4) and (3.6). After some manipulation, the result can be written in the form:

$$h_{12} = \frac{\alpha_0/K}{(1 + 0.81s)(1 + 0.405s)} + \frac{\dfrac{2r_b' (1 - \alpha_0)}{Kr_e'}}{1 + 0.81s} + \frac{3r_b'}{Kr_e'} \frac{0.81s}{1 + 0.81s}$$

$$+ \frac{\partial s}{1 + \partial s} \qquad (3.10)$$

As can be seen from the circuit of Fig. 2.6, h_{12} is an open-circuit voltage feedback parameter. In the above expression, the first term is the feedback component of the intrinsic transistor alone, owing to space charge layer widening. The second and third terms, separated for convenience in later work, represent the voltage developed across r_b' which is due to current flowing through it by way of the collector diffusion admittance h_{22}'. The fourth term is a feedback voltage developed by current flowing through r_b' from the collector space charge layer capacitance C_c. This fourth term is nearly always the dominant one at high frequencies. A plot of typical magnitudes of these four components vs frequency is shown in Fig. 3.2, where it is apparent that the fourth term $\partial s/1 + \partial s$ becomes predominant at frequencies such that $\omega/\omega_\alpha > \frac{1}{K\partial}$. A good approximation to h_{12} may be obtained by first taking a constant term representing the zero-frequency value of the first and second terms, then noting that the third term becomes dominant over the first two before the latter decrease with frequency. Thus the frequency variation of the first two terms need not be included, and one obtains:

$$h_{12} \simeq \frac{\alpha_0 + \dfrac{2r_b' (1 - \alpha_0)}{r_e'}}{K} + \frac{3r_b'}{Kr_e'} \frac{0.81s}{1 + 0.81s} + \frac{\partial s}{1 + \partial s} \qquad (3.11)$$

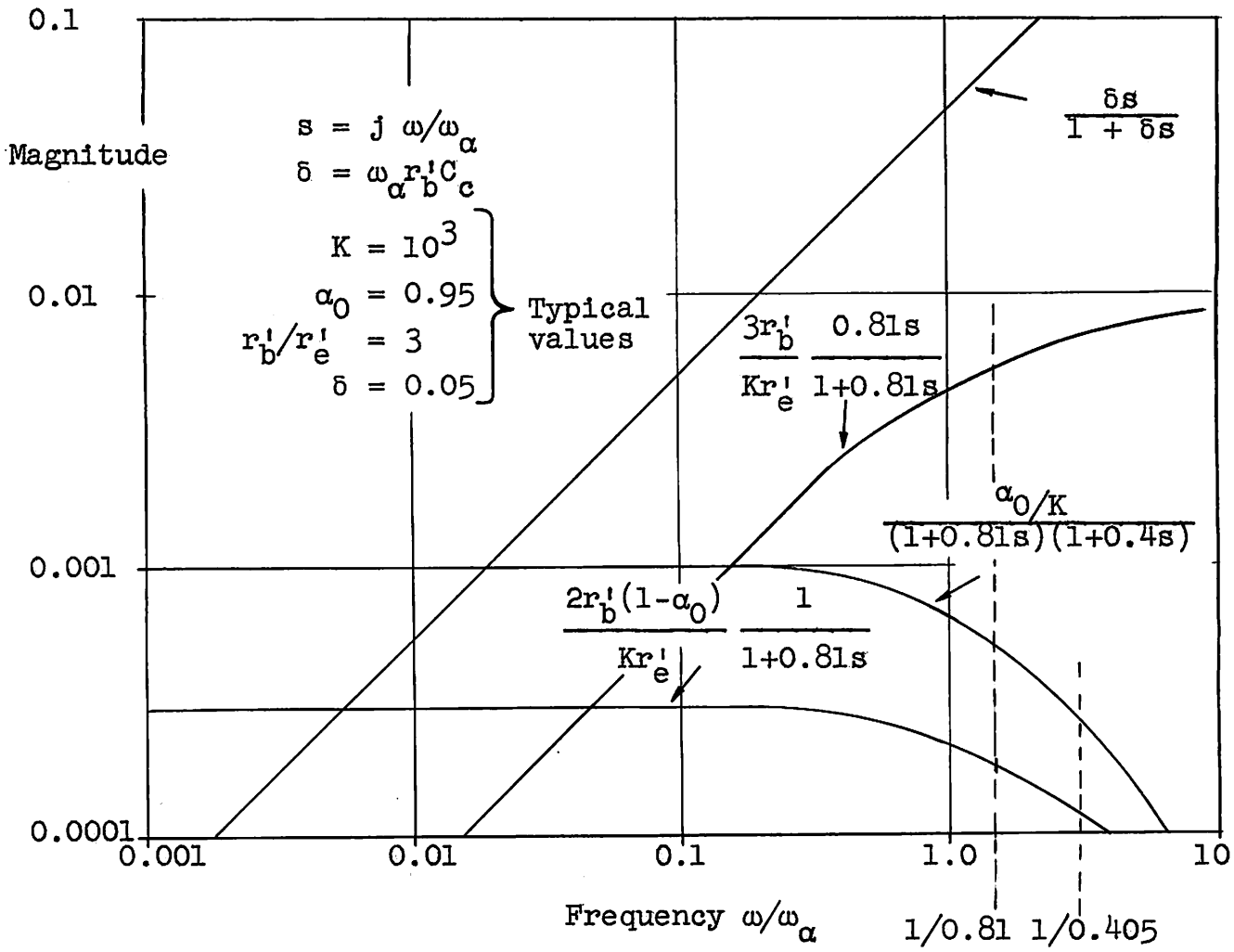

FIG. 3.2.--Frequency variation of the four components of h_{12}. (From Eq. (3.10); magnitude only.)

In many situations, the second term of the above may be ignored if $K\delta \gg \frac{2.43 r'_b}{r'_e}$, which is equivalent to writing $C_c \gg \frac{2.43}{K\omega_\alpha r'_e}$.

The quantity $\frac{2.43}{K\omega_\alpha r'_e}$ is the collector diffusion capacitance C_d, which is small compared with C_c if the minority carrier concentration in the base is small relative to the majority carrier concentration.* Thus, the above criterion is satisfied

*R. L. Pritchard, reference 19, pp. 798-799.

under the assumptions of this report. However, in a case where the real part of h_{12} for $s = j\,\omega/\omega_\alpha$ is of importance, the second term cannot be neglected.* This generally occurs only when one is interested in maximum performance at a single frequency, and does not arise in wideband work. The form of Eq. (3.11) will be retained for generality.

Consider now the expression for h_{21} given in Eq. (3.1). Since h'_{21} is of order unity, the quantity $h'_{21} - r'_b\,(h'_{22} + j\omega C_c)$ can be approximated by $h'_{21} - j\omega r'_b C_c$ in the same manner as discussed in connection with Eq. (3.3). Using Eq. (2.32), there results:

$$h_{21} = -\frac{\alpha_0 + \partial s(1 + 0.81s)(1 + 0.405s)}{(1 + 0.81s)(1 + 0.405s)(1 + \partial s)}$$

This quantity is conveniently separated into two parts, and the factor $1 + \partial s$ in the denominator of the first part replaced by unity, so that:

$$h_{21} \simeq -\alpha - \frac{\partial s}{1 + \partial s} = -\frac{\alpha_0}{(1 + 0.81s)(1 + 0.405s)} - \frac{\partial s}{1 + \partial s} \qquad (3.12)$$

As a further approximation, the second term can be ignored.**

The relation for h_{22} results from substituting Eqs. (2.32) and (3.3) into (3.1); using the notation of Eqs. (3.4) and (3.6) one obtains:

$$h_{22} = \frac{2(1 - \alpha_0)/Kr'_e}{1 + 0.81s} + \frac{3}{Kr'_e}\,\frac{0.81s}{1 + 0.81s} + \frac{1}{r'_b}\,\frac{\partial s}{1 + \partial s} \qquad (3.13)$$

---

*The magnitude and imaginary part of the second term of Eq. (3.11) may be ignored compared with the corresponding parts of the third term if $C_d \ll C_c$. For the real parts, however, the criterion is $C_d \ll \partial C_c$, which is not satisfied.

**This second term is, however, of some importance in the relation between apparent and actual alpha cut-off frequency, as will be considered in Chapter V. Also see R. L. Pritchard, reference 19, pp. 789.

The first two terms represent the diffusion admittance of the intrinsic transistor, and the last term is the contribution to h_{22} produced by the elements r_b' and C_c. It is to be noted that the above is identical to the last three terms of h_{12} in Eq. (3.10), except for a constant factor r_b'. Thus the approximation procedure discussed for Eq. (3.10) and the plots of Fig. 3.2 are applicable here, resulting in:

$$h_{22} \simeq \frac{2(1 - \alpha_0)}{Kr_e'} + \frac{3}{Kr_e'} \frac{0.81s}{1 + 0.81s} + \frac{1}{r_b'} \frac{\partial s}{1 + \partial s} \tag{3.14}$$

The entire set of h-parameters has now been determined, as given by Eqs. (3.9), (3.11), (3.12) and (3.14). For circuit applications, it is desirable to simplify the notation somewhat by defining the following symbols for the low-frequency values:*

$$\text{For } s = 0: \qquad h_{11} = r_e' + r_b' (1 - \alpha_0) \triangleq r_h$$

$$h_{12} = \frac{\alpha_0}{K} + \frac{2r_b' (1 - \alpha_0)}{Kr_e'} \triangleq \mu_b$$

$$h_{21} = - \alpha_0$$

$$h_{22} = \frac{2(1 - \alpha_0)}{Kr_e'} \triangleq \frac{1}{r_c} \tag{3.15}$$

Using these definitions, the complete set of h-parameters becomes:

---

*This is essentially the same notation as used by R. F. Shea, Transistor Audio Amplifiers, John Wiley and Sons, New York, 1955, p. 73.

$$h_{11} = r_h \frac{1 + \frac{1.21 r_b'}{r_h} s}{1 + s}$$

$$h_{12} = \mu_b + \frac{1.21 r_b'}{(1 - \alpha_0) r_c} \frac{s}{1 + 0.81s} + \frac{\partial s}{1 + \partial s}$$

$$h_{21} = \frac{-\alpha_0}{(1 + 0.81s)(1 + 0.405s)} - \frac{\partial s}{1 + \partial s}$$

$$h_{22} = \frac{1}{r_c} + \frac{1.21}{(1 - \alpha_0) r_c} \frac{s}{1 + 0.81s} + \frac{1}{r_b'} \frac{\partial s}{1 + \partial s} \qquad (3.16)$$

Where: $s = j\,\omega/\omega_\alpha$ in the sinusoidal steady state,

$$\partial = \omega_\alpha r_b' C_c$$

Equation set (3.16) is the principal result of this section and completely describes the small-signal properties of the junction triode over a frequency range from zero to somewhat above the alpha cut-off frequency, ω_α. Numerous approximations have been used to obtain these parameters, the principal ones being the approximations of Eq. (2.32) to the intrinsic h-parameters, which involve more error than those used to reduce Eq. (3.1) to a reasonably simple form. It is believed that the form of the common-base h-parameters given in Eq. (3.16) is new, and conveniently leads to further approximation for various frequency ranges and circuit configurations.*

From Eq. (3.16), the number of independent quantities necessary to specify the transistor are apparently seven:

r_h, μ_b, α_0, r_c, r_b' ω_α, ∂

*A set of simplified h-parameters which is somewhat similar, but involving different approximations, has been given by R. L. Pritchard; see reference 25.

However, of the first five quantities above, which are the low-frequency h-parameters and the extrinsic base resistance, only four are independent as may be seen from Eq. (3.15).* Thus a total of six quantities characterize a transistor. Using relations brought out in Chapter II, a set of six independent quantities convenient for circuit applications may be written:

$$r_e' = \frac{kT}{qI_e} \qquad \text{(Eq. 2.14)}$$

$$\alpha_0 = \operatorname{sech} \frac{W}{L} = \operatorname{sech} \frac{W}{\sqrt{D\tau}} \qquad \text{(Eq. 2.24)}$$

$$\omega_\alpha = \frac{\kappa}{\tau_d} = \frac{\kappa D}{W^2} \qquad \text{(Eq.(2.25) and Fig. 2.3)}$$

$$r_c = \frac{Kr_e'}{2\,(1 - \alpha_0)} \qquad \text{(Eq. 2.12 and 3.15)}$$

$$r_b'$$

$$C_c \qquad (3.17)$$

These equations relate the circuit parameters to the physical constants, or device parameters of the transistor.

It is instructive to synthesize equivalent circuits representing the h-parameters of Eq. (3.16). The simplest approach is to determine an h-type circuit directly from these equations; thus h_{11} is written as: (for $1.21r_b' > r_h$).

---

*This implies that any low-frequency h-parameter may be predicted from knowledge of the other three and the extrinsic base resistance. In practical transistors, this generally cannot be done very accurately, owing principally to surface recombination effects. See Appendix B for a brief discussion of this.

$$h_{11} = r_h + \frac{(1.21r_b' - r_h)\ s}{1 + s} \qquad s = j\ \omega/\omega_\alpha$$

which can be recognized as a resistance r_h in series with a parallel combination of resistance $1.21r_b' - r_h$ and inductance

$$\frac{1.21r_b' - r_h}{\omega_\alpha}$$

Similarly, h_{22} can be recognized as parallel combinations of a resistance and two series resistance-capacitance branches. The result is shown in Fig. 3.3; observe the notation C_d for the collector diffusion capacitance (refer to the discussion following Eq. (3.11). Since C_d is generally much smaller than C_c, the C_d-branch may often be ignored, as may the resistance r_b' in series with C_c.

The equivalent circuit of Fig. 3.3 has two frequency-dependent generators, whereas a circuit containing only one generator is more useful in visualizing terminal effects. One simple approach to such a circuit is to return to the situation of Fig. 3.1 and synthesize a T-circuit from the intrinsic parameters of Eq. (2.32). These are first converted to open-circuit impedance, or z-parameters, and the relationships shown in Fig. 3.4 applied.* The approximations $z_{12}' \ll z_{21}', z_{22}'$ may be employed, and after some minor approximations in the expression for z_{12}', the circuit of Fig. 3.5 results. This circuit bears a close similarity to one described by Early,** from which the notation r_e'' and r_b'' is taken. The present circuit is somewhat more accurate, and differs in having capacitance across r_e'' and r_b'', as well as the C_d-branch across r_c. It is interesting to note, however, that the circuit of Early, which was derived on a very approximate basis, still represents a useful model.

---

*See reference 1.

**See reference 11.

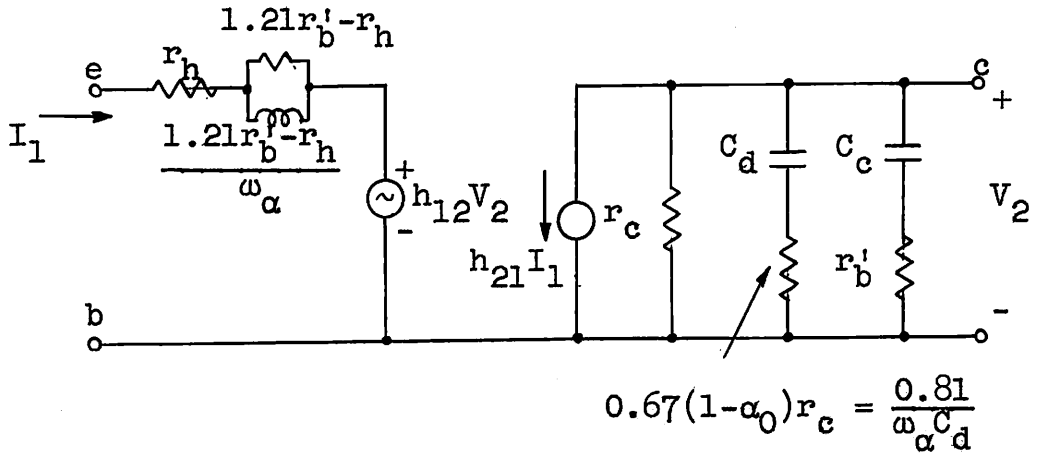

$r_h = r'_e + r'_b(1-\alpha_0)$ $\quad C_d = \dfrac{1.21}{(1-\alpha_0)\omega_\alpha r_c}$ $\quad h_{12}, h_{21}$: See Eq. (3.16)

FIG. 3.3.--Equivalent-h circuit for the complete common-base transistor.

Another circuit which can be derived is a pure T-circuit, obtained from consideration of the overall z-parameters (calculated from the h-parameters of Eq. 3.16) in the same manner as illustrated in Fig. 3.4 for the intrinsic z-parameters. The resulting circuit is given in Fig. 3.6, and has the advantage that the character of the internal feedback is clearly displayed by the impedance in series with the base lead. At very low frequencies, this impedance is seen to have the value $r''_b + r'_b$, where r''_b accounts for the reverse transmission in the intrinsic transistor owing to space charge layer widening, and is typically

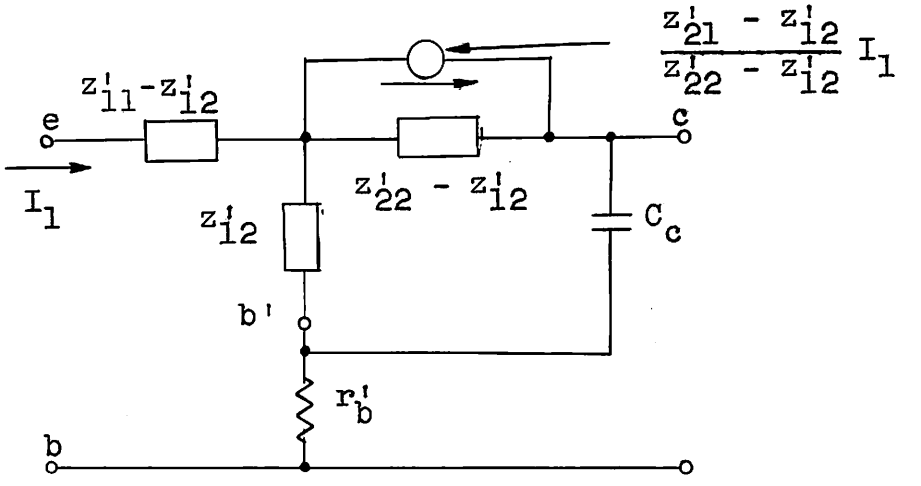

FIG. 3.4.--Common-base equivalent circuit in terms of intrinsic z parameters.

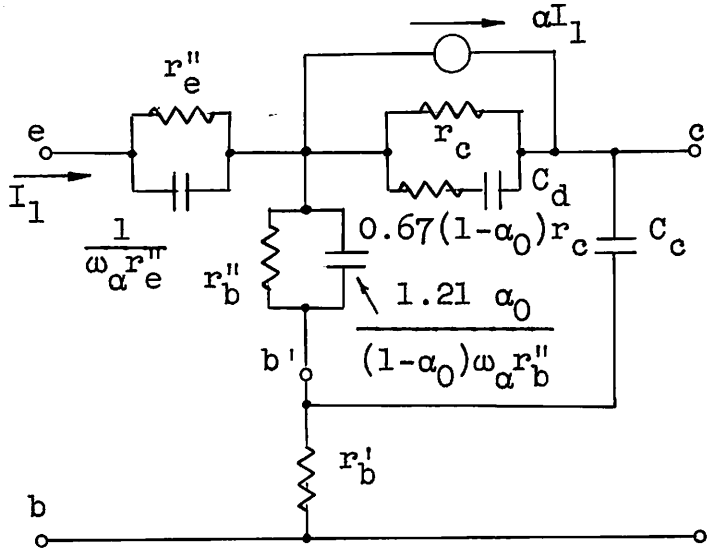

$$r''_e = r'_e\left(1 - \frac{\alpha_0}{2}\right) \qquad r''_b = \frac{\alpha_0 r'_e}{2(1-\alpha_0)} \qquad C_d = \frac{1.21}{(1-\alpha_0)r_c\omega_\alpha}$$

α: see Eq. (2.33)

FIG. 3.5.--A common-base equivalent circuit. (explicit form of Fig. 3.4)

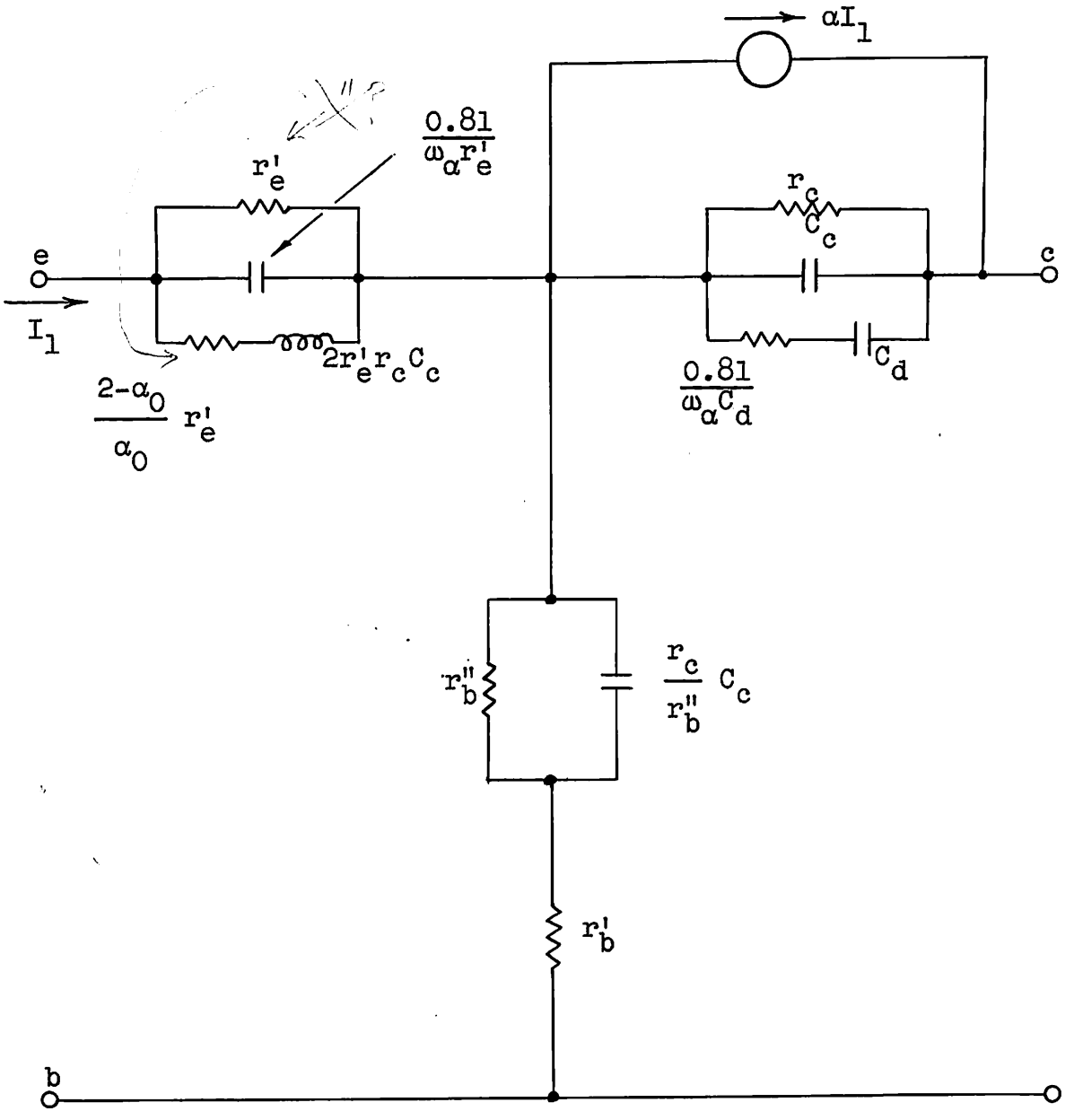

$$r''_b = \frac{\alpha_0 r'_e}{2(1 - \alpha_0)} \qquad C_d = \frac{1.21}{(1 - \alpha_0)\omega_\alpha r_c} \qquad \alpha\text{: Eq. (2.33)}$$

FIG. 3.6.--Common-base equivalent T-circuit.

several times as large as r_b'. However, r_b'' has a capacitance shunting such that the resulting time constant is $r_c C_c$, and the frequency corresponding to this time constant is usually of the order of tens of kc. At frequencies much greater than this, or above perhaps 100 kc , the effective base impedance is r_b' alone. Thus at medium and high frequencies, the space charge layer widening feedback can be ignored.* Also, at these frequencies, the inductive branch of the emitter impedance can be neglected, since a similar time constant is involved. The simplified circuit which results is given in Section B.

It is now desirable to calculate the y-parameters corresponding to the complete h-parameters of Eq. (3.16) in order to effect a comparison with y-parameters obtained from TR-No. 83.** The y-parameters are derived here, and the comparison made, with a change of notation, in Appendix C. The standard conversion relations are:***

$$y_{11} = \frac{1}{h_{11}},\quad y_{12} = \frac{-h_{12}}{h_{11}},\quad y_{21} = \frac{h_{21}}{h_{11}},\quad y_{22} = \frac{\Delta^h}{h_{11}}$$

$$\text{where}\quad \Delta^h = h_{11}h_{22} - h_{12}h_{21}$$

In the interests of simplicity, it is desirable to employ an approximation for h_{21} which is different from the one given in Eq. (3.16). The following is essentially similar to an expression due to R. D. Middlebrook:**

$$h_{21} \simeq -\alpha_0 \frac{1 - 0.2s}{1 + s} \qquad (3.18)$$

---

*Early has also pointed this out, and given expressions for the z-parameters which are similar to those involved in Fig. 3.6, z_{12} being identical. See reference 11, pp. 1404.

**R. D. Middlebrook, reference 7.

***See footnote on page 22.

Using this approximation and Eq. (3.16), the y-parameters become:

$$y_{11} = \frac{1}{r_h} \frac{1 + s}{1 + \frac{1.21 r_b'}{r_h} s}$$

$$y_{21} = -\frac{\alpha_0}{r_h} \frac{1 - 0.2s}{1 + \frac{1.21 r_b'}{r_h} s}$$

$$y_{12} = -\frac{\mu_b}{r_h} \frac{1 + \frac{\partial}{\mu_b} s \frac{\partial}{\mu_b} s^2}{1 + \frac{1.21 r_b'}{r_h} s}$$

$$y_{22} = \frac{1}{r_c} \frac{r_h + r_c \alpha_0 \mu_b}{r_h} \frac{1 + \frac{r_c}{r_b'} \frac{\alpha_0 r_b' + r_h}{r_h + r_c \alpha_0 \mu_b} \partial s + \frac{r_c}{r_h + r_c \alpha_0 \mu_b} \partial s^2}{1 + \frac{1.21 r_b'}{r_h} s} \qquad (3.19)$$

where $s = j\, \omega/\omega_\alpha$ for real frequencies

$$\partial = \omega_\alpha\, r_b'\, C_c$$

In deriving the expressions for y_{12} and y_{22}, the approximation $\partial \gg \mu_b$ has been utilized, typical values for these quantities being 5×10^{-2} and 10^{-3}, respectively. In addition, the second terms of the expressions for h_{12} and h_{22} of Eq. (3.16) have been neglected relative to the third terms. As discussed following

Eq. (3.11), this approximation is valid, except for the real parts of these parameters. Thus, Eq. (3.19) above is not fully equivalent to Eq. (3.16), being slightly less general. Circuits representing the above y-parameters are given in Appendix C, which shows substantial agreement with the results of TR-No. 83.

This section has considered the complete transistor in the common-base connection. Making use of the approximate intrinsic h-parameters developed in Chapter II (Eq. 2.32), the h-parameters for the overall transistor including collector capacitance and extrinsic base resistance were developed and presented in relatively simple form, in Eq. (3.16). The form of these is thought to be new, and clearly points out the principal components of each parameter, as well as facilitating further approximation. From these h-parameters, a number of equivalent circuits were synthesized representing the transistor over the entire useful frequency range. Finally, the corresponding y-parameters were obtained, and compared in Appendix C with the y-parameters of TR-No. 83. The next section will consider further approximations which can be made when operation is restricted to certain frequency ranges and circuit conditions.

B. COMMON-BASE APPROXIMATE CIRCUITS

The equivalent circuits and associated h-parameters derived in section A represent the transistor from zero-frequency to somewhat above alpha cut-off frequency. In a particular circuit application, the frequency range desired may often be considerably less than this; hence it is useful to consider what simplifications can be made for certain restricted frequency ranges. In addition, for certain terminating impedances the previous equivalent circuits may prove more complex than necessary. In the present section a number of simplified circuits applicable under such restricted conditions are developed.

Low frequency operation will be considered first. If the frequency is low enough, all the four-pole parameters are resistive, and a number of equivalent circuits such as the T- or the π-equivalents may be easily drawn.* The frequency range over which such a resistive circuit is valid may be obtained from Fig. 3.6, where it is observed that the low-frequency time constant involved in each arm is $r_c C_c$, or very nearly so. Thus at (radian) frequencies considerably below $\frac{1}{r_c C_c}$, the equivalent circuit can be considered to be purely resistive, and the circuit of Fig. 3.7 results, which is the familiar low-frequency equivalent-T. Since the alpha cut-off frequency is very much greater than $\frac{1}{r_c C_c}$, alpha can be considered a real constant α_0. In terms of the T-resistances, the h-parameters are, very closely:

$$h_{11} = r_h = r_e + r_b(1 - \alpha_0) = r_e' + r_b'(1 - \alpha_0)$$

$$h_{21} = - \alpha_0$$

$$h_{12} = \mu_b = r_b/r_c$$

$$h_{22} = 1/r_c \qquad (3.20)$$

---

*The equivalent T will be emphasized here, since it is convenient to work with and more or less directly corresponds to the underlying physical situation. It is also probably the most familiar, having been extensively used in early transistor literature. Thus see: R. M. Ryder and R. J. Kircher, "Some circuit properties and applications of n-p-n transistors," Bell Syst. Tech. Jour., vol. 30, July 1951, pp. 537; also Proc. IRE, vol. 39, July 1951, pp. 760; W. A. Shockley, Electrons and Holes in Semiconductors, D. Van Nostrand Co., Inc., New York, 1950, pp. 37-41.

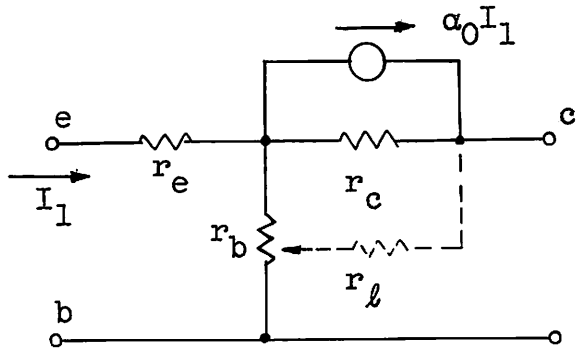

$$r_e = r_e' \left(1 - \frac{\alpha_0}{2}\right) \qquad r_b = r_b' + r_b''$$

$$r_b'' = \frac{\alpha_0 r_e'}{2(1 - \alpha_0)} \qquad \text{Valid for } \omega \ll \frac{1}{r_c C_c}$$

FIG. 3.7.--Low-frequency equivalent T.

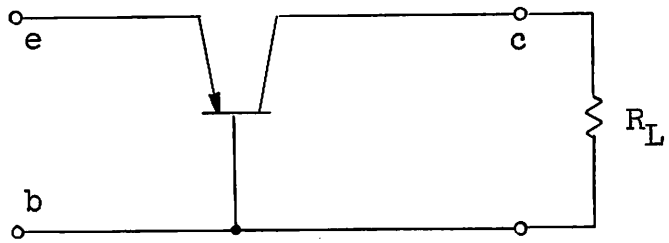

FIG. 3.8.--Terminated common-base stage.

In practical transistors, there may be a leakage resistance across the collector junction which is of the same order of magnitude as r_c. This situation is indicated in Fig. 3.7, where the leakage resistance is tapped to some indefinite point on r_b. Of course, this additional resistance may be absorbed to obtain a new equivalent T, but then the relations for r_e and r_b'', shown in Fig. 3.7, are no longer true. They are also invalid if surface recombination is present.*

The frequency limitation obtained above, $\omega r_c C_c \ll 1$, is actually unduly restrictive under typical operating conditions. Thus consider the situation of Fig. 3.8 showing the transistor terminated in a resistance R_L, which may be a bias resistor supplying current to the collector. The h-parameters of the combination are, from Eq. (3.16), and for $\omega \ll \omega_\alpha$:

$$h_{11} = r_h \qquad h_{12} = \mu_b + j\omega r_b' C_c, \ \mu_b = \frac{r_b}{r_c}$$

$$h_{21} = -\alpha_0, \ h_{22} = \frac{1}{r_c} + \frac{1}{R_L} + j\omega C_c \tag{3.21}$$

If now $R_L \ll r_c$, which limits R_L to a maximum of perhaps 100 K ohms, the determinant of the above h-matrix is:

$$\Delta^h = h_{11}h_{22} - h_{12}h_{21} = \frac{r_h}{R_L} + \frac{\alpha_0 r_b}{r_c} + j\omega C_c(r_h + \alpha_0' r_b')$$

$$\simeq \frac{r_h}{R_L} + j\omega C_c \ (r_h + \alpha_0 r_b')$$

$$\simeq \frac{r_h}{R_L} \quad \text{if } \omega R_L C_c \ll 1$$

---

*This implies that any low-frequency h-parameter may be predicted from knowledge of the other three and the extrinsic base resistance. In practical transistors, this generally cannot be done very accurately, owing principally to surface recombination effects. See Appendix B for a brief discussion of this.

Thus, h_{12} can be assumed to be simply $j\omega r_b' C_c$, or in the latter case zero, since the above Δ^h-expressions would result from these assumptions.* The equivalent circuits obtained from these considerations are shown in Fig. 3.9, and are of considerable utility in the audio-frequency range. It should be noted that circuits B and C are equivalent, but circuit C will generally be more convenient to use, lending itself naturally to nodal analysis. This circuit may readily be derived from Eq. (3.21), taking $\mu_b = 0$, or perhaps more directly from the y-parameters of Eq. (3.19). The h-parameters for circuit C are as follows:

$$h_{11} = r_h$$

$$h_{12} = \partial s$$

$$h_{21} = -\alpha_0$$

$$h_{22} = \frac{1}{r_b'} \partial s$$

$$R_L \ll r_c, \ \omega \ll \omega_\alpha \qquad (3.22)$$

The medium- and high-frequency range will now be considered. For frequencies such that $\omega r_c C_c \gg 1$, the complete circuit of Fig. 3.6 simplifies to that shown in Fig. 3.10.** This frequency range, from a few hundred kc to above alpha cut-off, is the important region for wideband operation. The h-parameters for

---

*This is due to the fact that h_{12} enters into the properties of a four-terminal network, such as input and output impedances and gain, only through the expression Δ^h. See page 336 of the footnote reference on page 22.

**R. L. Pritchard has derived a circuit essentially similar to the one shown in Fig. 3.10; see reference 25. Also see R. L. Pritchard, "High-frequency power gain of junction transistors," Proc. IRE, vol. 43, Sept. 1955, pp. 1085.

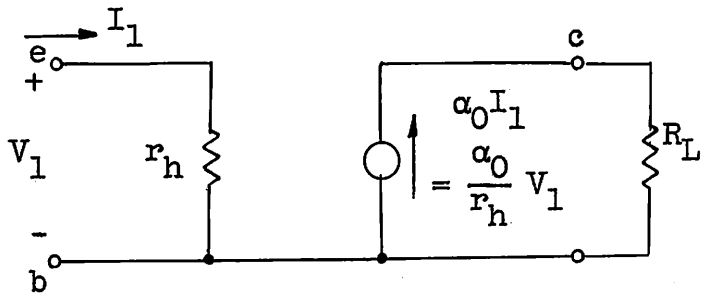

$$r_h = r'_e + r'_b (1 - \alpha_0)$$

Valid for $R_L \ll r_c$, $\omega \ll \frac{1}{R_L C_c}$ and $\omega \ll \omega_\alpha$

a.

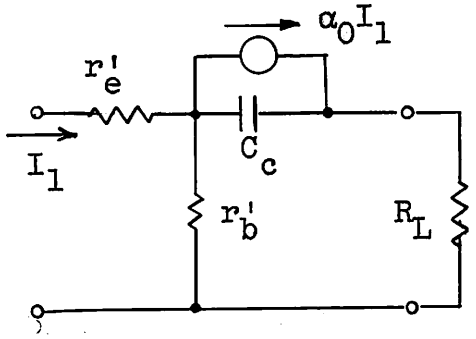

Valid for $R_L \ll r_c$, $\omega \ll \omega_\alpha$

b.

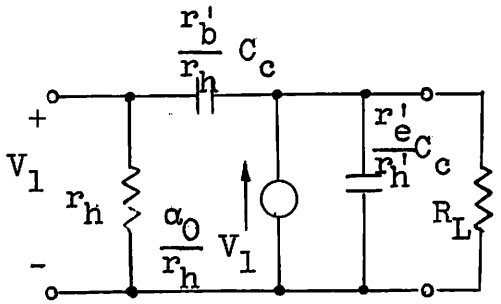

c.

FIG. 3.9.--Low-frequency common-base equivalent circuits.

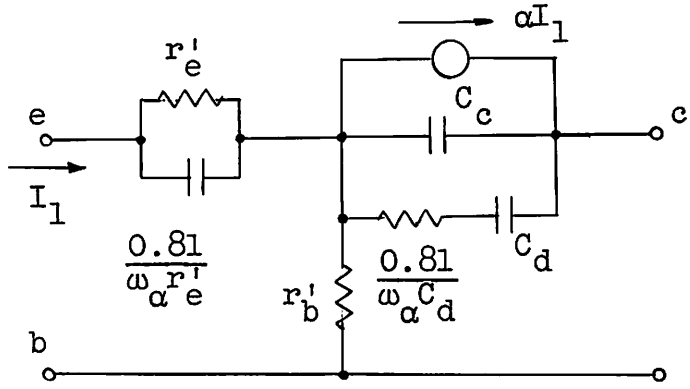

α: see Eq. (2.33)
Valid for $\omega \gg \frac{1}{r_c C_c}$

FIG. 3.10.--High-frequency equivalent T.

this region are, from Eq. (3.16):

$$h_{11} = r_h \frac{1 + \frac{1.21 r'_b}{r_h} s}{1 + s}$$

$$h_{12} = \frac{\omega_\alpha r'_b C_d s}{1 + 0.81s} + \frac{\partial s}{1 + \partial s}$$

$$h_{21} = \frac{-\alpha_0}{(1 + 0.81s)(1 + 0.405s)} - \frac{\partial s}{1 + \partial s}$$

$$h_{22} = \frac{\omega_\alpha C_d s}{1 + 0.81s} + \frac{1}{r'_b} \frac{\partial s}{1 + \partial s} \qquad (3.23)$$

Some simplification is possible in these equations. If $\omega < \omega_\alpha/2$, a good approximation to h_{21} is given by:

$$h_{21} \simeq \frac{-\alpha_0}{1 + 1.21s} \qquad (3.23a)$$

This result is obtained by ignoring the term in s^2, and also ∂s, in the expression for h_{21} of Eq. (3.23). A considerably cruder approximation, but one which has been widely used and

can yield simple and useful results, is:*

$$h_{21} \simeq \frac{-\alpha_0}{1+s} - \partial s \qquad (3.23b)$$

The first term represents quite accurately the magnitude of alpha well beyond ω_α, but has a considerable phase error amounting to about 12° at ω_α.** The second term can be ignored to obtain the simplest results, but is necessary in considering the relation between the h_{21} cut-off frequency, which can be measured directly, and the alpha cut-off frequency, which cannot. As shown in Chapter V, if $\partial = 0.05$, $\omega_{h_{21}}$ is about 10 per cent lower than ω_α.

A further simplification results from discarding the first terms of h_{12} and h_{22} in Eq. (3.23), which is equivalent to discarding the branch containing C_d in the circuit of Fig. 3.10. In addition, the quantity $1 + \partial s$ may be replaced by unity. The above two approximations are excellent as far as the magnitudes of h_{12} and h_{22} are concerned; if the real parts are desired, the full form of Eq. (3.23) should be used. This situation does not arise when one is interested in moderately wide bandwidths, the real parts being of importance only if the maximum single-frequency power gain is to be calculated. Thus useful approximations to Eq. (3.23) are:***

$$h_{11} = r_h \frac{1 + \frac{1.21 r_b'}{r_h} s}{1+s}$$

$$h_{12} \simeq \partial s$$

$$h_{21} \simeq \frac{-\alpha_0}{1 + 1.21s} \text{ for } \omega < \omega_\alpha/2$$

$$\approx \frac{-\alpha_0}{1+s} - \partial s \text{ for } \omega < 2\omega_\alpha$$

$$h_{22} \simeq \frac{1}{r_b'} \partial s \qquad (3.24)$$

---

*The approximation to alpha implied by Eq. (3.23b) has been used, for example, by D. E. Thomas, "Transistor amplifier—cutoff frequency," Proc. IRE, vol. 40, Nov. 1952, pp. 1481-1483.

**R. L. Pritchard, reference 19, p. 789.

***A set of h-parameters substantially equivalent to those of Eq. (3.24) has been given by Stern, Aldridge and Chow; reference 24, p. 844.

These expressions are valid from $\omega >> \frac{1}{r_c C_c}$ to an upper limit depending on the approximation used for h_{21}, as noted above. An equivalent circuit representing the above equations is obtained from Fig. 3.10 by omitting the C_d branch across C_c. Another equivalent circuit, useful when the transistor is to be driven from a relatively high impedance $|Z_G| >> |h_{11} - r_b'|$, is given in Fig. 3.11. The impedance $h_{11} - r_b'$ will generally contain negative resistances, so that this circuit is not particularly useful in the general case.

An interesting simplification results if the d-c emitter current is restricted to a particular value. The expression for the resistance r_h involved in h_{11} is given by Eq. (3.15) as $r_h = r_e' + r_b' (1 - \alpha_0)$, and from Eq. (3.17), $r_e' = kT/qI_e$. Thus, by controlling the d-c emitter current I_e, r_e' and hence r_h can be varied over a moderately wide range. Now suppose by choice of I_e, $r_h = 1.21 r_b'$. Then from Eq. (3.24), h_{11} becomes simply:

$$h_{11} = r_h = 1.21 r_b' \tag{3.25}$$

With this restriction, especially simple equivalent circuits result. Figure 3.12 shows a circuit which is equivalent (to a good approximation) to the general high-frequency T of Fig. 3.10. The form is essentially that of a π-circuit, with the alpha generator now applied directly across the output terminals. A useful approximate form of this circuit is obtained by ignoring the C_d-branch, as before, in which case a pure π-circuit may be drawn, as in Fig. 3.13a. Such a circuit lends itself most readily to nodal analysis, and, for this purpose, a generator controlled by the input voltage, rather than current, is desirable. A circuit with this property can be obtained by

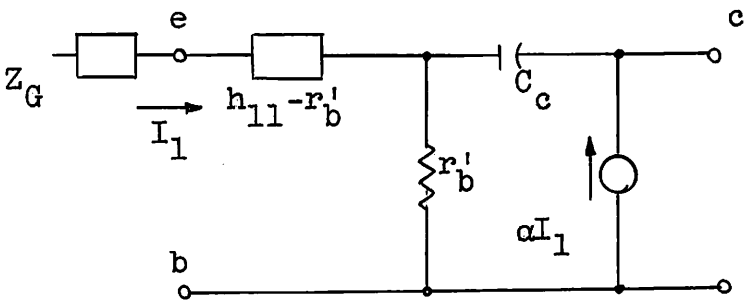

α: See Eq. (2.33)

FIG. 3.11.--Approximate high-frequency equivalent circuit for large driving impedances.

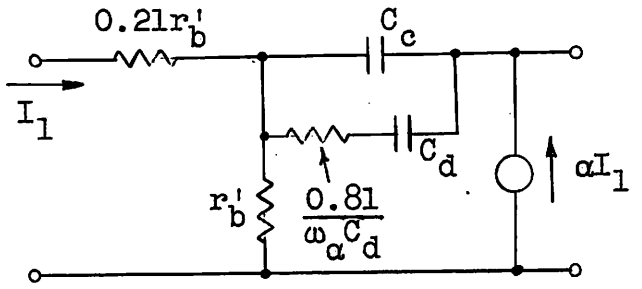

FIG. 3.12.--High-frequency equivalent when $h_{11} = 1.2\ r_b'$.

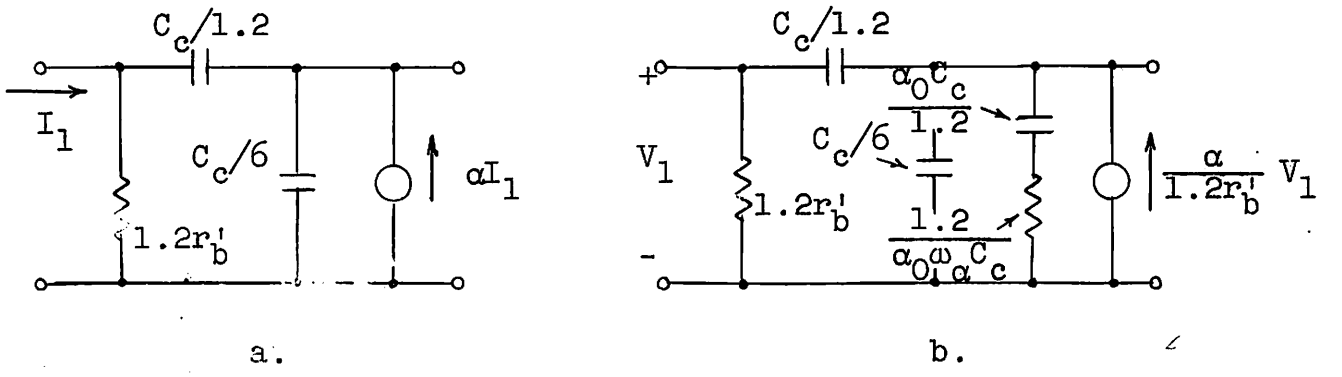

FIG. 3.13.--Approximate equivalents to Fig. 3.12.

considering the y-parameters corresponding to Eq. (3.24), with $h_{11} = 1.2r_b'$:

$$y_{11} = \frac{1}{h_{11}} = \frac{1}{1.2r_b'}$$

$$y_{12} = \frac{-h_{12}}{h_{11}} = \frac{-j\omega C_c}{1.2}$$

$$y_{21} = \frac{h_{21}}{h_{11}} \simeq \frac{-\alpha}{1.2r_b'}$$

$$y_{22} = h_{22} - \frac{h_{12}h_{21}}{h_{11}} = j\omega C_c + \alpha \frac{j\omega C_c}{1.2} \qquad (3.26)$$

Choosing the simplest approximation for alpha, $\alpha \simeq \frac{\alpha_0}{1 + j\,\omega/\omega_\alpha}$, y_{22} becomes:

$$y_{22} = j\omega C_c + \frac{1}{\frac{1.2}{j\omega\alpha_0 C_c} + \frac{1.2}{\alpha_0 \omega_\alpha C_c}}$$

The admittance $-y_{12}$ is identified as the feedback branch between output and input, $y_{11} + y_{12} \simeq y_{11}$ is the branch shunting the input terminals, and $y_{22} + y_{12}$ is the admittance across the output terminals. The output current generator is $y_{21} - y_{12} \simeq y_{21}$ times the input voltage, and the resulting equivalent circuit appears in Fig. 3.13b. This circuit has a low-frequency analog in Fig. 3.9c.

The approximate circuits of Fig. 3.13 are remarkably simple, and characterized by only the four quantities r_b', C_c, ω_α and α_0, which are the important transistor parameters at high frequencies. These circuits are valid for a frequency range $\frac{1}{r_c C_c} \ll \omega < 2\omega_\alpha$, very roughly. Since numerous approximations have been used in deriving these circuits, the accuracy to which they represent an actual transistor is uncertain, and it is desirable to obtain experimental evidence regarding the closeness of approximation. A series of measurements designed to provide this information will be given in the next section.

The present section has considered simplifications which may be made in the "exact" common-base equivalent circuit of Fig. 3.6 and corresponding h-parameters of Eq. (3.16). For the low-frequency region, where $\omega \ll \omega_\alpha$, and if the load resistance $R_L \ll r_c$, the equivalent circuits of Fig. 3.9 and h-parameters of Eq. (3.22) were found to provide a good representation. For the medium and high-frequency regions, such that $\frac{1}{r_c C_c} \ll \omega < 2\omega_\alpha$, the equivalent circuit of Fig. 3.10 and h-parameters of Eq. (3.23) are applicable. Further approximations are indicated in the h-parameters of Eq. (3.24). With a particular value of d-c emitter current, the circuit of Fig. 3.12 and approximations of Fig. 3.13 result. It should be noted that the frequency regions considered, $\omega \ll \omega_\alpha$ and $\omega \gg \frac{1}{r_c C_c} = \omega_c$, will generally overlap somewhat, since, typically, f_α is at least several MC and f_c less than a few tens of kc.

Except where indicated, most of the work in this section is believed to be relatively new, particularly the circuits of Figs. 3.9, 3.12 and 3.13. Section C will present measurements on a number of transistors made over a wide frequency range, which indicate that the circuits of Fig. 3.13 are a reasonable approximation to reality. Section D will give a convenient summary of the equivalent circuits and h-parameters developed in Sections A and B.

C. MEASUREMENTS OF COMMON-BASE, SMALL-SIGNAL PARAMETERS

In section B, a number of small-signal approximate equivalent circuits for the common-base configuration have been derived. Two of these, shown in Fig. 3.13, derived for a particular operating point, such that $r_h = 1.21 r_b'$, are of particularly simple form, and it is desirable to undertake measurements on actual transistors which will indicate the validity of these circuits. The results of such measurements will be described in this section, the actual techniques involved being deferred until Chapter V.

The problem is to investigate the validity of the equivalent circuits presented in Fig. 3.13. These circuits are intended to be useful for high-frequency wideband applications, so a number of transistors were chosen which are fairly representative of the medium and high-frequency triodes commercially available at the present date; these are shown, along with identifying numbers, in Table 3.1. Also shown are values of the fundamental high-frequency parameters α_0, r_b', C_c and ω_α as measured by methods described in Chapter V. All these are single frequency measurements, and the task is now to determine if the terminal parameters of the transistor over a wide frequency range are predicted by these parameters according to the equivalent circuits of Fig. 3.13.

TABLE 3.1.--Circuit parameters of measured transistors.

UNIT NO.	TRANSISTOR	MFR	TYPE	High-freq. parameters				Operating point		h_{11}**
				α_0	f_α MC	r'_b † ohms	C_c‡ μμf	V_{cb} volts	I_e ma	ohms
1	222 No. 7	Texas Inst.	npn grown	0.974	5.32	80	22.4	6	-0.29	154
2	222 8	" "	"	0.929	2.71	27	23.0	6	-0.88	37
3	1858 1	West. Elec.	"	0.966	2.35	192	9.0	6	-0.18	224
4	X-23 3	Trans. Prod.	"	0.988	1.37	210	15.6	6	-0.19	228
5	X-22 4	" "	"	0.933	2.95	166	3.5	6	-0.26	219
6	2N43 3	GE	pnp alloy	0.989	1.78	79	31.8	-6	0.22	130
7	XN-2* 9	Motorola	"	0.973	5.34	148	15.8	-6	0.16	195
8	XN-2* 20	"	"	0.995	10.1	144	18.5	-6	0.17	184
9	CK-762 107	Raytheon	"	0.987	19.4	76‡‡	11.1	-5	0.30	97
10	CK-762 108	"	"	0.991	22.3	59‡‡	14.8	-5	0.42	69
11	SB-100 1	Philco	surface barrier	0.954	37.0	136‡‡	4.1	-3	0.18	165

*Experimental units

†Measured at f_c

‡Measured at 100 kc

‡‡Measured at 10 MC

**Measured at 0.5 f_α; I_e adjusted so h_{11} is purely real.

Equipment was available to measure directly the following parameters at any desired frequency up to about 30 MC:

$$y_{11} = 1/h_{11},\ y_{12},\ y_{21},\ y_{22},\ h_{22}$$

These parameters have been measured for each transistor at a number of frequencies covering approximately the range $0.1\omega_\alpha$ to $2\omega_\alpha$.* Of course, only four of these five parameters are independent, the relation between them being:

$$h_{22} = y_{22} - h_{11}y_{12}y_{21}$$

However, it is useful to measure all five and obtain a check on the accuracy of measurement. From such considerations it is estimated that the measurements here presented are accurate to at least 3 per cent.

Since the equivalent circuits to be investigated - those of Fig. 3.13 - are valid for only one operating point, that is, a particular value of d-c emitter current I_e such that $h_{11} = 1.2r_b'$, the emitter current for each transistor must be chosen accordingly. An experimental procedure was adopted, whereby the emitter current of a particular transistor was adjusted so that the measured h_{11} became purely real at a frequency of $0.5\omega_\alpha$ (which is near the geometrical center of the frequency range of interest), and this emitter current was used throughout the series of measurements. The collector-to-base voltage used, V_c, was more or less arbitrarily chosen to be six volts, except for units 9, 10 and 11 which were restricted to lower values. The operating point for each transistor is shown in Table 3.1, as is also the value of h_{11} obtained by the foregoing procedure.

Rather than present curves giving the real and imaginary

---

*At frequencies of five MC and below, all parameters were measured on a Wayne-Kerr B-601 r-f bridge. For frequencies above five MC, h_{11} was measured on a General Radio 916A r-f bridge, and the other parameters on a Wayne-Kerr B-801 VHF admittance bridge. Reference should be made to Chapter V for general considerations relating to measurement techniques.

parts of four parameters as a function of frequency for each of the 11 transistors, which would probably occupy more space than the useful information content of the data warrants, a more compact presentation will be attempted. It is most useful to consider how closely the transistors as a group are approximated by the simple equivalent circuit, rather than focus attention on any particular transistor unless it exhibits unusual behavior. Thus, for example, Fig. 3.14 shows measured values of the real and imaginary parts of h_{11} for the entire group, differentiation being made between n-p-n, p-n-p and surface-barrier types. Curves have been drawn only for the transistors which show the widest deviation from the ideal, the identifying number being indicated on the curve. The data have been normalized, frequency being expressed as a fraction of the alpha cut-off frequency f_α, h_{11_r} (the real part) expressed as a fraction of its ideal value $1.2r_b'$, and h_{11_i} (the imaginary part) given by means of the ratio h_{11_i}/h_{11_r} (ideally zero) which determines whether h_{11_i} is negligible.

Similar treatment is given to measured values of h_{22}, shown in Fig. 3.15 except that h_{22_i} is expressed as a capacitance, since it is ideally a constant capacitance C_c. The real part, h_{22_r}, is supposedly negligible, so the ratio h_{22_r}/h_{22_i} is also shown. An exactly analogous procedure is followed for y_{12} and presented in Fig. 3.16. In the case of y_{21}, both real and imaginary parts are important, and both are normalized with respect to the ideal low-frequency value of the real part, and plotted in Fig. 3.17.

It was decided to make the comparison between predicted and measured values in terms of the measured quantities (that is, h_{11}, h_{22}, y_{12}, y_{21}), rather than convert these to pure h-parameters to agree with the form of Eqs. (3.24) and (3.25). The predicted values of the parameters measured are obtained

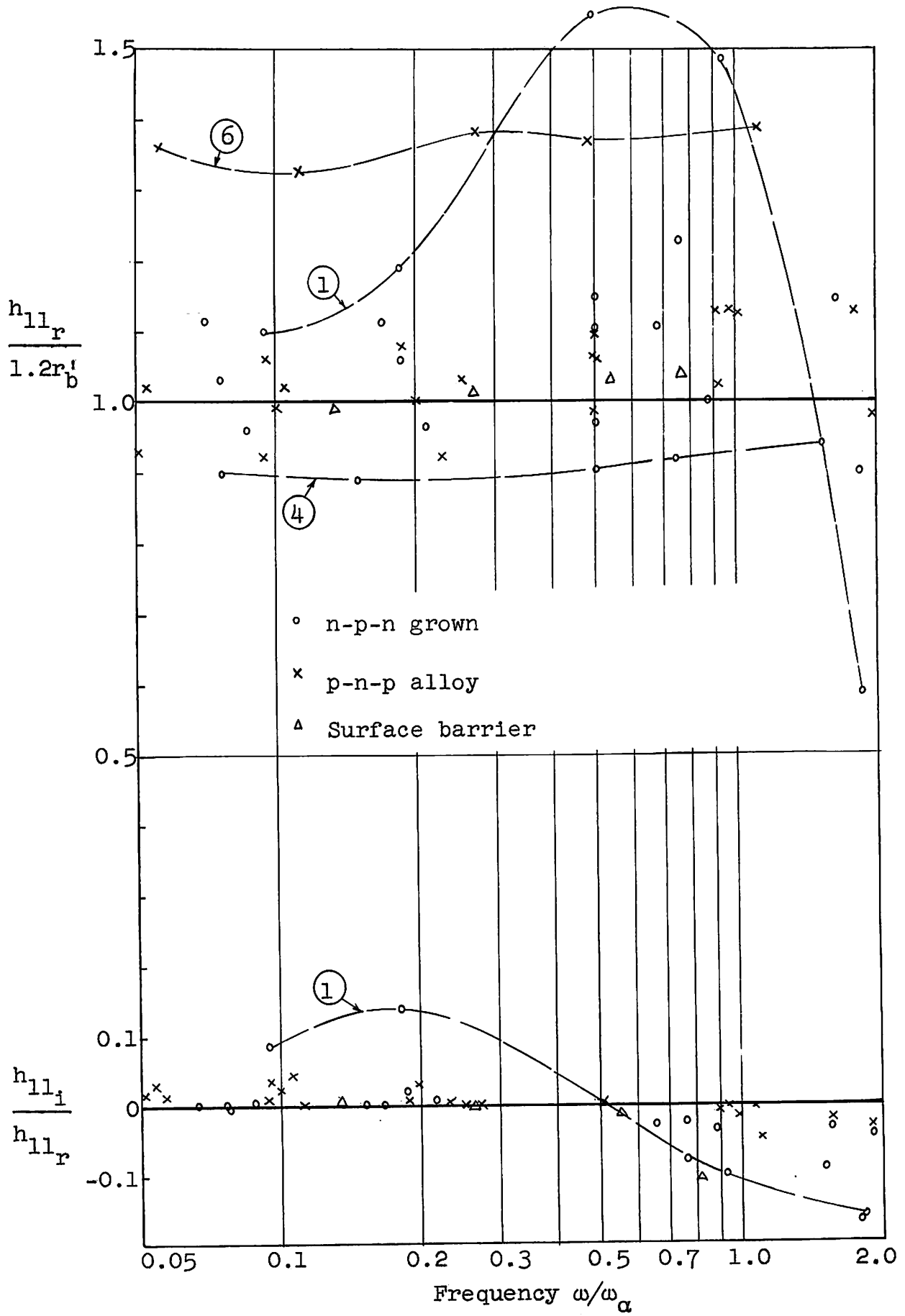

FIG. 3.14.--$h_{11} = h_{11_r} + j\, h_{11_i}$

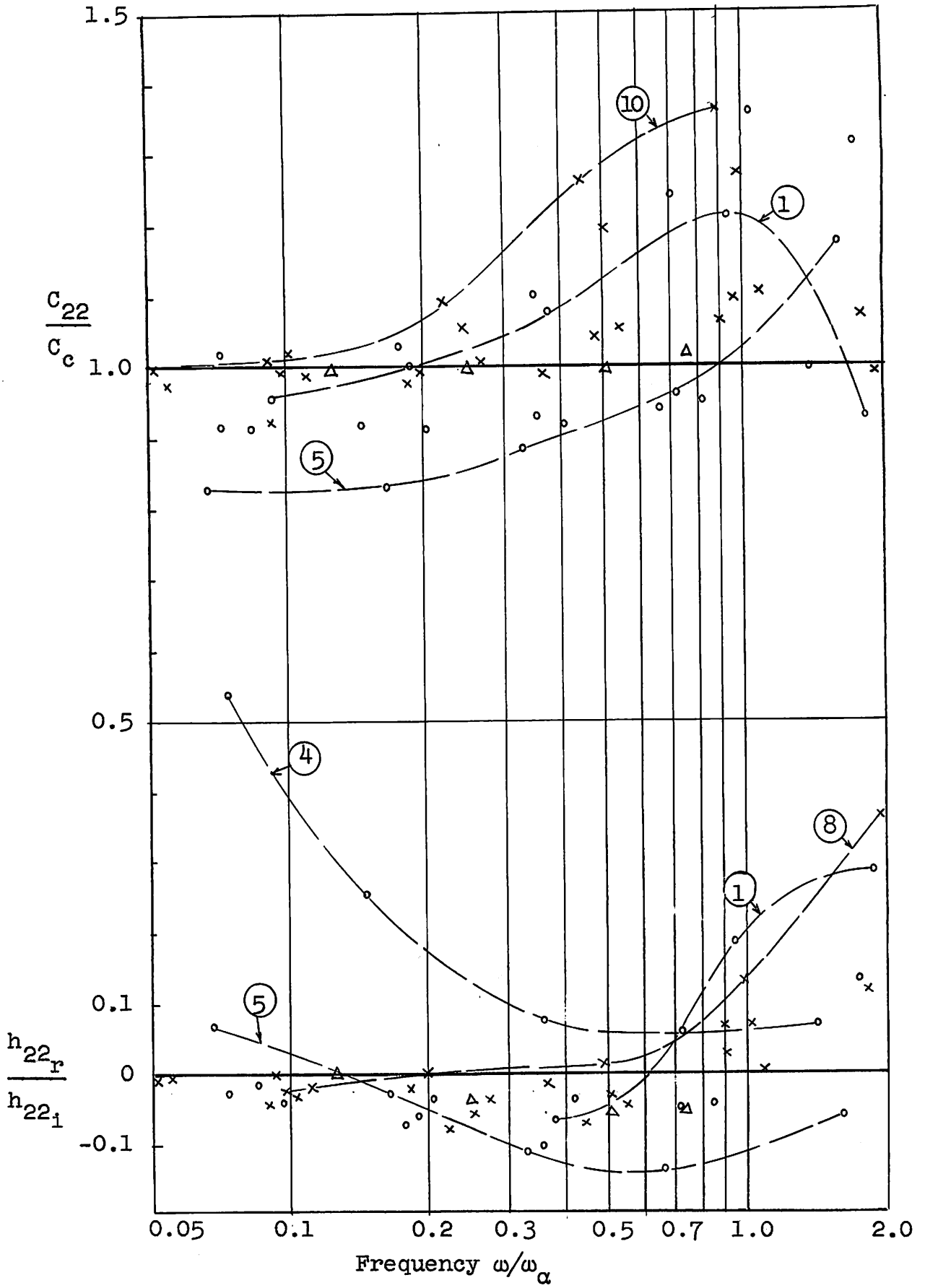

FIG. 3.15.--$h_{22} = h_{22_r} + j\, h_{22_i}$ $\qquad h_{22_i} = \omega\, C_{22}$.

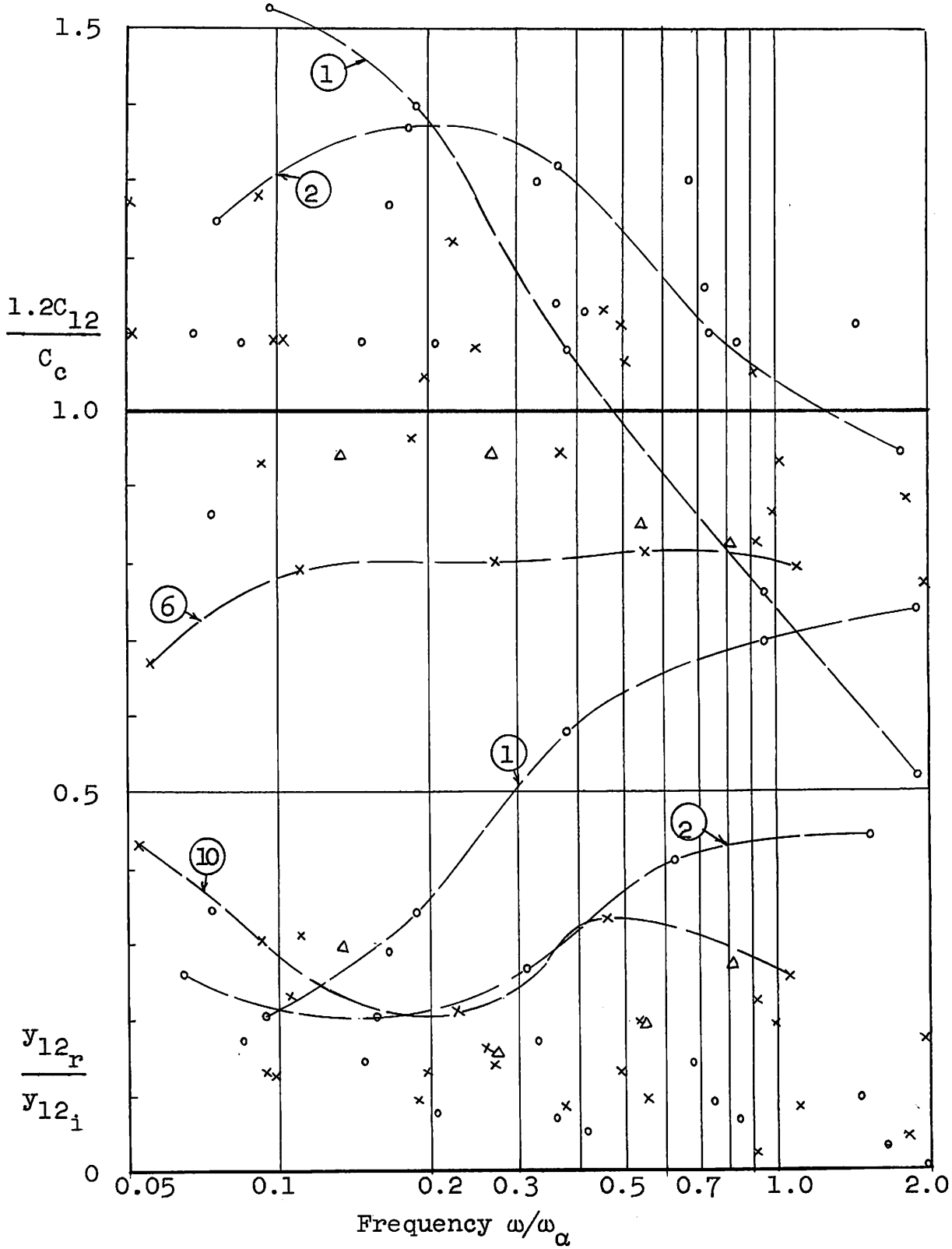

FIG. 3.16.--$y_{12} = y_{12_r} + j\, y_{12_i}$ $\quad - y_{12_i} = \omega\, C_{12}$.

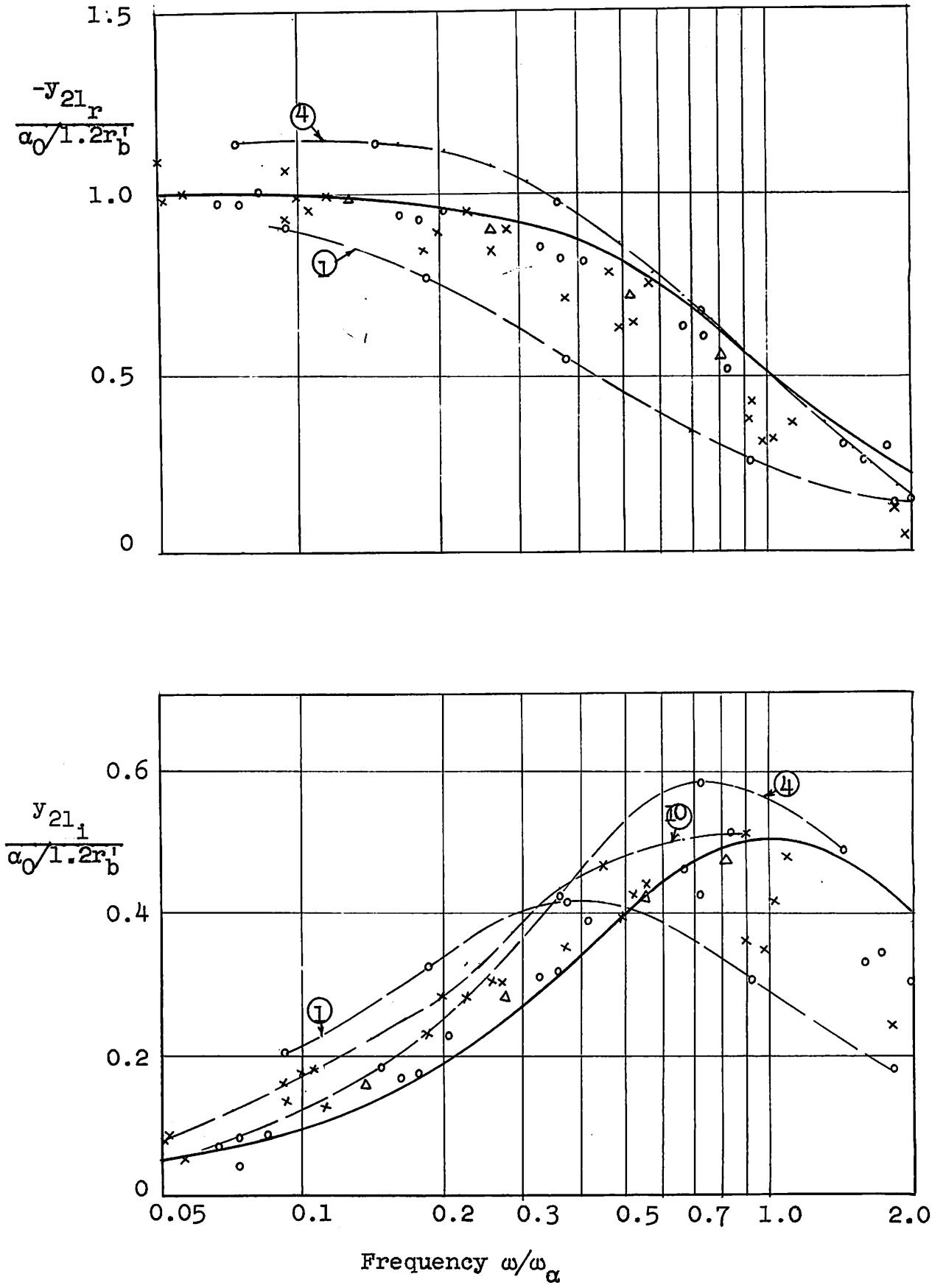

FIG. 3.17.--$y_{21} = y_{21_r} + j\, y_{21_i}$

from Fig. 3.13 and Eq. (3.24), (3.25) and (3.26), and may be written:

$$h_{11} = 1.2r_b'$$

$$h_{22} = j\omega C_c$$

$$-y_{12} = \frac{h_{12}}{h_{11}} = j\omega \frac{C_c}{1.2}$$

$$-y_{21} = \frac{-h_{21}}{h_{11}} \simeq \frac{\alpha_0}{1.2r_b'} \frac{1}{1 + j\,\omega/\omega_\alpha}$$

The normalized quantities which have been plotted are hence ideally (writing $h_{22_i} = \omega C_{22}$ and $-y_{12_i} = \omega C_{12}$):

$$\frac{h_{11_r}}{1.2r_b'} = 1 \qquad \frac{h_{11_i}}{h_{11_r}} = 0$$

$$\frac{C_{22}}{C_c} = 1 \qquad \frac{h_{22_r}}{h_{22_i}} = 0$$

$$\frac{1.2C_{12}}{C_c} = 1 \qquad \frac{y_{12_r}}{y_{12_i}} = 0$$

$$\frac{-y_{21_r}}{\alpha_0/1.2r_b'} = \frac{1}{1 + (\omega/\omega_\alpha)^2} \qquad \frac{y_{21_i}}{\alpha_0/1.2r_b'} = \frac{\omega/\omega_\alpha}{1 + (\omega/\omega_\alpha)^2} \qquad (3.27)$$

These ideal quantities are shown as heavy lines on the corresponding plots of actually measured quantities for comparison.

In general, the agreement is best for h_{11} and y_{21}, these being "low-impedance" parameters less likely to be affected by parasitic capacities. Transistor No. 1 shows wide deviation from constant h_{11_r}; however, this is a grown junction which was found not to possess a constant base spreading resistance. The remaining transistors exhibit relatively constant h_{11_r}, although the value may differ by 10 to 15 per cent from the predicted $1.2r_b'$. The ratio h_{11_i}/h_{11_r} is satisfactorily low over the frequency range.

The values of normalized y_{21} cluster fairly closely together, but it is apparent that an average curve could be drawn falling somewhat lower in frequency than the ideal curve shown. This is the result of the approximation to alpha inherent in y_{21}, which has been employed for simplicity. A better approximation, such as indicated in Eq. (3.24) for the lower frequencies, has the effect of shifting the ideal curve downward in frequency.

Considering now h_{22}, most of the transistors show an output capacitance which increases with frequency by about 15 per cent on the average over the range. This may be due in part to neglect of C_d, but it appears the principal cause is stray capacity from emitter to base, and in particular, emitter space charge layer capacitance which until now has been ignored. As shown in Chapter V, the same cause is probably responsible for negative values of h_{22_r} exhibited by all but one transistor. The magnitude of the ratio h_{22_r}/h_{22_i} is fairly small, being well within 0.1 for the majority of units.

The agreement in the case of y_{12} is not particularly striking. However, except for transistors 1 and 2, which are of grown type, most units show a relatively constant C_{12}, although this value may differ from the ideal $\frac{C_c}{1.2}$ by 25 per cent. The ratio y_{12_r}/y_{12_i} may be about 0.3 (excluding units 1 and 2) which would not ordinarily be regarded as negligible.

This is the principal departure of the measured transistors from the idealized parameters. Nonetheless, this real part will not have a profound effect on circuit performance if the terminating impedances are relatively low, as in wideband situations, and the idealized equivalent circuits are thus useful as first-order approximations for initial circuit design work.

This section has presented measurements of terminal parameters made on a series of medium and high-frequency transistors to investigate the validity of the simple high-frequency equivalent circuits of Fig. 3.13. Agreement between measured and predicted values was generally fair, the principal divergence being in the shunt feedback branch, or y_{12}, of the circuit. It was concluded that the simplified circuits provide useful first-order approximations to the actual situation as represented by the sample of transistors measured.

D. CONCLUSIONS: SUMMARY OF EQUIVALENT CIRCUITS

A number of equivalent circuits for the common-base configuration have been developed in this Chapter. Using the intrinsic h-parameters obtained in Chapter II (Eq. 2.32), h-parameters for the overall transistor as depicted in Fig. 3.1 were derived, (Eq. 3.16) and represented by the equivalent circuits of Figs. 3.3, 3.5 and 3.6, which apply over the entire useful frequency range $0 < \omega < 2\omega_\alpha$. Some approximations valid for certain frequency ranges and operating conditions were then introduced. It was found that the general low-frequency equivalent-T of Fig. 3.7 becomes the much simpler circuit of Fig. 3.9a if terminated in a resistance R_L much smaller than the collector resistance r_c, and restricted to frequencies such that $\omega \ll \frac{1}{R_L C_c}$. For somewhat higher frequencies, but still much smaller than alpha cut-off, the circuits of Fig. 3.9b and 3.9c were derived. For the medium and high-frequency region $\omega \gg \frac{1}{r_c C_c}$, the equivalent-T of Fig. 3.10 was obtained, which

reduced to Fig. 3.12 when a particular operating condition such that $h_{11} = 1.21r_b'$ was chosen. Finally, it was found that Fig. 3.12 could be represented approximately by the simple circuits of Fig. 3.13, and measurements showing fair agreement with these circuits were presented.

It is desirable to give a tabulation of the essential results of this chapter. All the equivalent circuits and their associated h-parameters are expressed in terms of certain assumed fundamental circuit parameters which are given in Table 3.2 and related to fundamental device parameters (refer to Eq. 3.17). As has been observed, six independent quantities are sufficient to characterize the particular model of the junction transistor which has been assumed in this report. Figure 3.18 presents the most important circuits which have been developed, along with their corresponding h-parameters. It is hoped that these results will be of use in designing bandpass circuits, for which the common-base configuration appears to be particularly useful.

TABLE 3.2.--Relations between device and circuit parameters.

Fundamental Device Parameters	Fundamental Circuit Parameters
Intrinsic	
$G = qI_e/kT$ Emitter diffusion conductance	$r'_e = 1/G$ Emitter resistance
w Base width	
τ Effective lifetime of minority carriers in the base	
D Diffusion constant 44 cm^2/sec for holes in Ge	
$L = \sqrt{D\tau}$ Diffusion length	α_0 = sech w/L (see Fig. 2.2) Intrinsic short-circuit current gain
$\tau_d = w^2/D$ Diffusion time constant	$\omega_\alpha = \kappa/\tau_d$ (see Fig. 2.3) Intrinsic current gain cut-off frequency
$1/K = \frac{kT}{q} \frac{1}{w} \frac{\partial w}{\partial V_c}$ Space charge layer widening constant	$r_c = \frac{Kr'_e}{2(1 - \alpha_0)}$ Collector resistance
	$\mu_{ec} = \alpha_0/K$ Intrinsic voltage feedback factor
	$C_d = 1.21/(1 - \alpha_0)\omega_\alpha r_c$ Collector diffusion capacitance
Extrinsic	
r'_b Base spreading resistance	r'_b
C_c Collector space charge layer capacitance	C_c

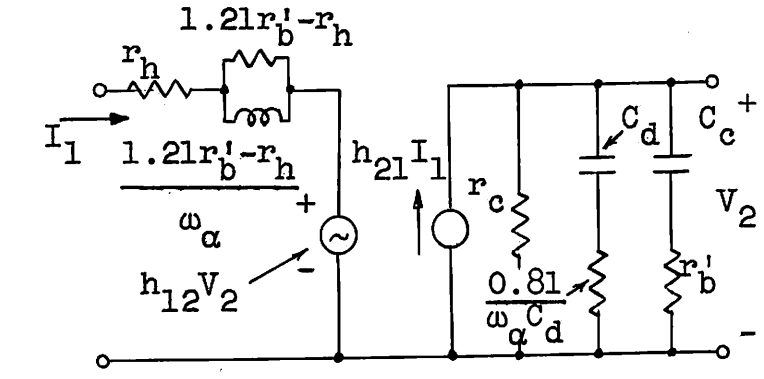

a.

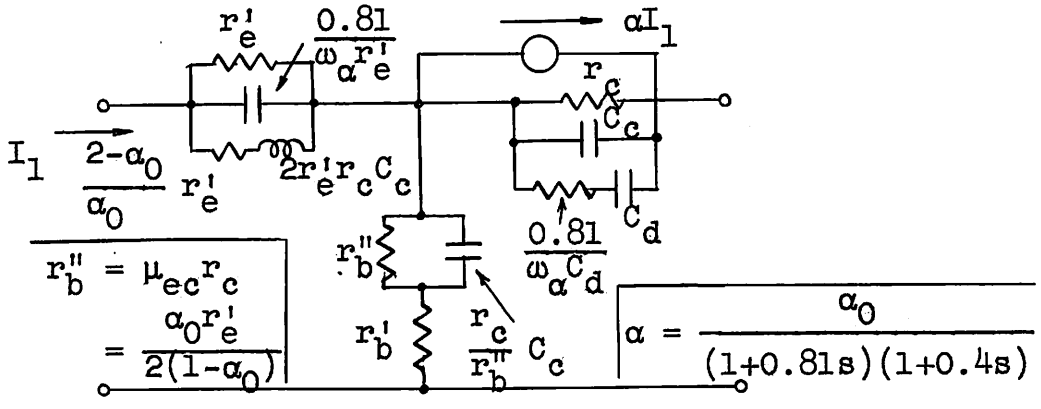

b.

Complete equivalent circuits for the junction triode (common-base).

$$h_{11} = r_h \frac{1 + \frac{1.21 r'_b}{r_h} s}{1 + s} \qquad h_{12} = \mu_b + \frac{\omega_\alpha r'_b C_d s}{1+0.81s} + \frac{\delta s}{1+\delta s}$$

$$h_{21} = \frac{-\alpha_0}{(1+0.81s)(1+0.4s)} - \frac{\delta s}{1+\delta s}; h_{22} = \frac{1}{r_c} + \frac{\omega_\alpha C_d s}{1+0.81s} + \frac{1}{r'_b}\frac{\delta s}{1+\delta s}$$

$$r_h = r'_e + r'_b (1 - \alpha_0); \ \mu_b = \mu_{ec} + \frac{r'_b}{r_c}; \ C_d = 1.21/(1 - \alpha_0)\omega_\alpha r_c;$$

$$\delta = \omega_\alpha r'_b C_c; \text{ for real frequencies, } s = j\omega/\omega_\alpha$$

FIG. 3.18.--Summary of common-base equivalent circuits.

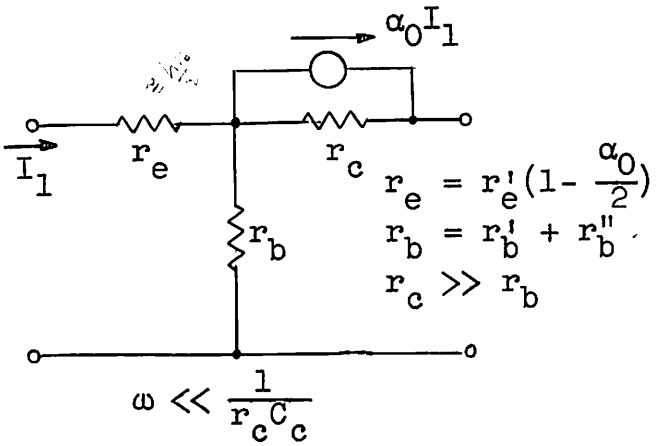

c.

$h_{11} = r_h$ $\quad h_{12} = \mu_b = r_b/r_c$

$h_{21} = -\alpha_0$ $\quad h_{22} = 1/r_c$

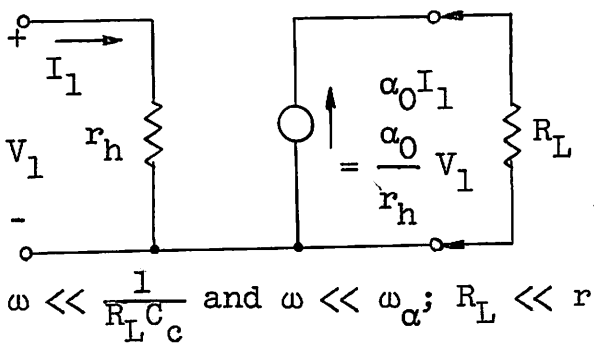

d.

$h_{11} = r_h$ $\quad h_{12} \simeq 0$

$h_{21} = -\alpha_0$ $\quad h_{22} \simeq 0$

Low-frequency equivalent circuits

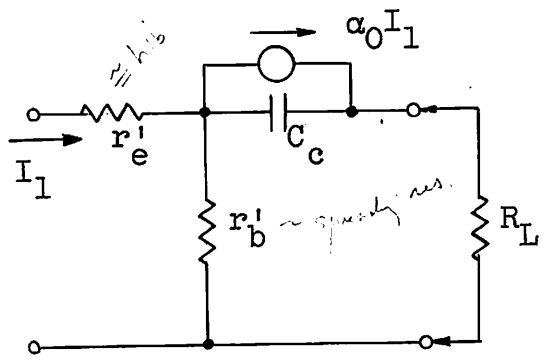

e.

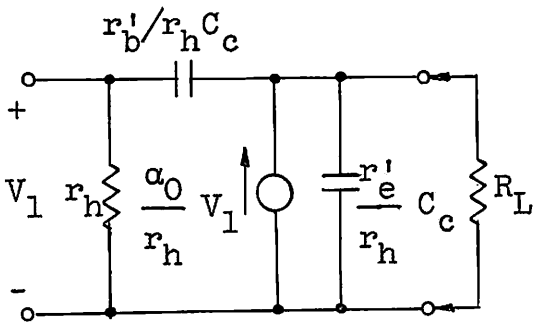

f.

$h_{11} = r_h$ $\quad h_{12} = \delta s$ $\quad h_{21} = -\alpha_0$ $\quad h_{22} = \frac{1}{r_b'} \delta s$

Low-frequency equivalent circuits for $\omega \ll \omega_\alpha$; $R_L \ll r_c$

FIG. 3.18.--Summary of common-base equivalent circuits (cont'd)

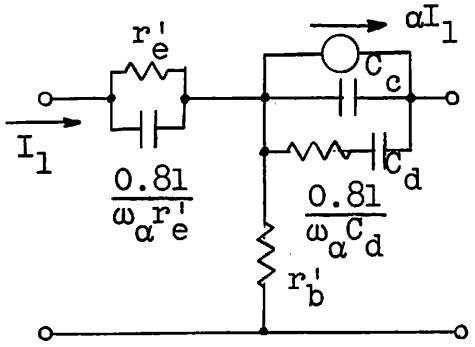

g.

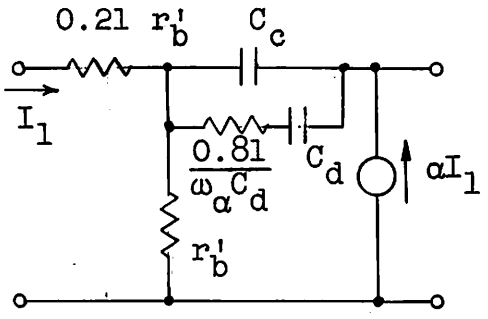

h. Equivalent to g if $h_{11} = r_h = 1.21\ r'_b$

Omit C_d branch as an approximation.

$$h_{11} = r_h \frac{1 + \frac{1.21 r'_b}{r_h} s}{1 + s} \qquad h_{12} = \frac{\omega_\alpha r'_b C_d s}{1 + 0.81s} + \frac{\delta s}{1 + \delta s} \simeq \delta s$$

$$h_{21} = \frac{-\alpha_0}{(1 + 0.81s)(1 + 0.4s)} - \frac{\delta s}{1 + \delta s}; \quad h_{22} = \frac{\omega_\alpha C_d s}{1 + 0.81s} + \frac{\omega_\alpha C_c s}{1 + \delta s}$$

$$\simeq \frac{-\alpha_0}{1 + 1.21s} \text{ for } \omega < \frac{\omega_\alpha}{2} \qquad \simeq \omega_\alpha C_c s$$

High-frequency equivalent circuits for $\omega >> 1/r_c C_c$.

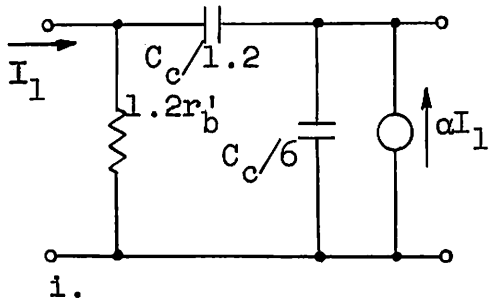

i.

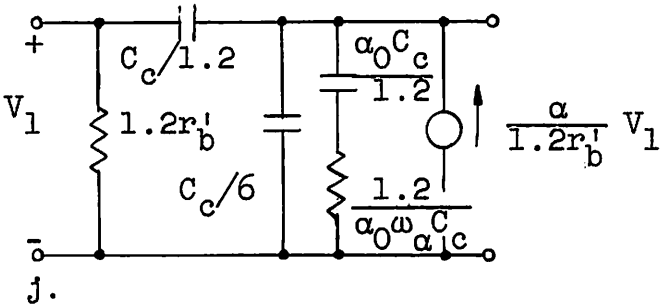

j.

$h_{11} \simeq 1.2r'_b$ $\qquad$ $h_{12} \simeq \delta s$

$h_{21} \simeq \frac{-\alpha_0}{1 + s} - \delta s$ $\qquad$ $h_{22} \simeq \omega_\alpha C_c s$ $\qquad$ $\alpha \simeq \frac{\alpha_0}{1 + s}$

High-frequency approximants to circuit H above.

FIG. 3.18.--Summary of common-base equivalent circuits (cont'd).

IV. COMMON-EMITTER AND COMMON-COLLECTOR EQUIVALENT CIRCUITS

In Chapter III, the common-base configuration of a junction triode was considered in some detail, and equivalent circuits applicable over various frequency ranges were derived. Although these circuits may be drawn in any configuration, for the common-emitter and common-collector connections they become awkward to use, and important circuit properties are obscured. In addition, certain approximations which can be made in the common-base situation become of uncertain validity. It is thus advisable to start with the exact intrinsic parameters in the desired configuration and work entirely in terms of these, absorbing the extrinsic elements in the appropriate place. This chapter gives such a treatment for the common-emitter and common-collector, yielding convenient equivalent circuits and h-parameters in each case.

A. INDEFINITE ADMITTANCE MATRIX FOR THE INTRINSIC TRANSISTOR

The basic equivalent circuit for the junction transistor model considered in this report has been shown in Fig. 2.9, where the intrinsic transistor was described by the y'-parameters of Eq. (2.14). This circuit is redrawn in Fig. 4.1 for the configurations considered in this chapter. Figure 4.1a emphasizes the fact that the intrinsic y-parameters of Eq. (2.14) apply to the connection shown, where terminal b' is common. From Fig. 4.1b and c it is apparent that intrinsic parameters will be needed for the cases of terminals e and c common, respectively. These quantities are readily obtained from the common b' parameters, as will be seen.

Consider any 3-terminal linear network, such as the intrinsic transistor. Let I_i be the current entering terminal i, and V_j be the voltage between terminal j and an arbitrary reference

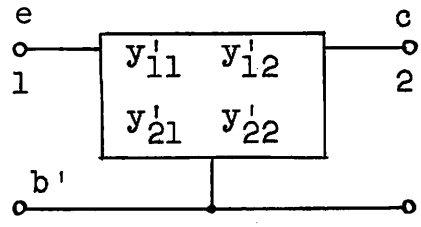

a. Intrinsic transistor.

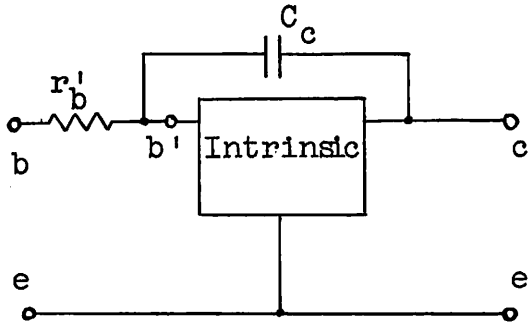

b. Common emitter.

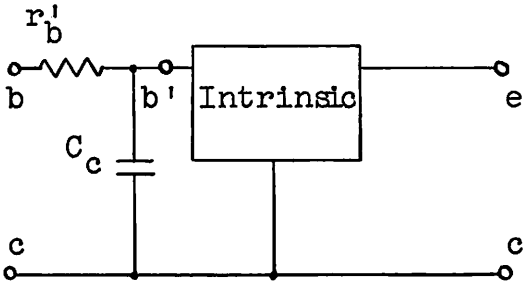

c. Common collector.

FIG. 4.1.--Basic equivalent circuits.

point. The relation between the currents and voltages is a series of linear equations:

$$I_i = \sum_{j=1}^{3} Y_{ij} V_j \qquad i = 1, 2, 3$$

The matrix formed by the Y_{ij} elements is termed the indefinite admittance matrix of the network, because the voltage reference terminal is left undefined.[26] Certain restrictions on the Y_{ij} are present. If all the V's are made equal, there is then no voltage between any terminal pair. Each of the currents is hence zero, and one obtains:

$$\sum_{j=1}^{3} Y_{ij} = 0 \qquad i = 1, 2, 3 \tag{4.1a}$$

Also, the sum of the currents is necessarily zero under all conditions, thus:

$$\sum_{i=1}^{3} \sum_{j=1}^{3} Y_{ij} V_j = \sum_{j=1}^{3} \sum_{i=1}^{3} Y_{ij} V_j = 0$$

where the order of summation has been reversed. Upon letting any two of the V's be zero, one finds:

$$\sum_{i=1}^{3} Y_{ij} = 0 \qquad j = 1, 2, 3 \tag{4.1b}$$

Equations (4.1) above mean that the sum of any row or column of the Y_{ij} matrix is zero. Thus, of the 9 elements for a 3-terminal network, only 4 are independent, and knowledge of any 4 enables the entire indefinite admittance matrix to be constructed by means of the above relation.

The indefinite admittance matrix is convenient to use here, since it allows complete freedom in choosing the voltage reference terminal. The meaning of the elements is readily determined. Suppose the reference terminal be chosen as terminal 3, then $V_3 = 0$. This means terminal 3 is now common for

voltage measurements to terminals 1 and 2. Suppose further that terminals 2 and 3 are short-circuited, so that $V_2 = 0$. Then from Eq. (4.1), $I_1 = Y_{11}V_1$, and $I_2 = Y_{21}V_1$, which means Y_{11} is the admittance looking into terminals 1 and 3 with 2 and 3 short-circuited, and Y_{21} is the transfer admittance from terminals 1 to 2 with terminal 3 common. Similar considerations for terminals 1 and 3 short-circuited lead to the conclusion that the conventional short-circuit admittance matrix for the network with terminal 3 common to input and output is obtained from the indefinite admittance matrix by striking out row and column 3. A similar statement applies for any other terminal.[27]

The indefinite admittance matrix for the intrinsic transistor may now be constructed from the elements known for the case of the b' terminal common. It is convenient to change the notation of these elements; reference to Fig. 4.1a indicates that terminals 1, 2 and 3 should be renumbered e, c and b'. Thus Eq. (2.14) are written:

$$
\begin{aligned}
y'_{ee} &= G\theta \coth \theta \\
y'_{ec} &= -\frac{G}{K}\,\theta \operatorname{cosech} \theta \\
y'_{ce} &= -\,G\theta \operatorname{cosech} \theta \\
y'_{cc} &= \frac{G}{K}\,\theta \coth \theta \\
\theta^2 &= \left(\frac{w}{L}\right)^2 + j\omega\tau_d
\end{aligned}
\qquad (4.2)
$$

The structure of the indefinite admittance matrix is:

$$
\begin{bmatrix}
y'_{ee} & y'_{ec} & y'_{eb'} \\
y'_{ce} & y'_{cc} & y'_{cb'} \\
y'_{b'e} & y'_{b'c} & y'_{b'b'}
\end{bmatrix}
\qquad (4.3)
$$

The elements of (4.3) not given in Eq. (4.2) are obtained by using the fact that the sum of any row or column of (4.3) must be zero. Thus:

$$y'_{eb'} = -(y'_{ee} + y'_{ec}) = G\left(\frac{\theta \operatorname{cosech} \theta}{K} - \theta \coth \theta\right)$$

$$\simeq -G\,\theta \coth \theta$$

$$y'_{cb'} = -(y'_{ce} + y'_{cc}) = G\left(\theta \operatorname{cosech} \theta - \frac{\theta \coth \theta}{K}\right)$$

$$\simeq G\,\theta \operatorname{cosech} \theta$$

$$y_{b'e} = -(y'_{ee} + y'_{ce}) = G(\theta \operatorname{cosech} \theta - \theta \coth \theta)$$

$$y'_{b'c} = -(y'_{ec} + y'_{cc}) = \frac{G}{K}(\theta \operatorname{cosech} \theta - \theta \coth \theta)$$

$$y'_{b'b'} = y'_{ee} + y'_{ec} + y'_{ce} + y'_{cc} = G\left(1 + \frac{1}{K}\right)(\theta \coth \theta - \theta \operatorname{cosech} \theta)$$

$$\simeq G(\theta \coth \theta - \theta \operatorname{cosech} \theta) \qquad (4.4)$$

The approximations indicated above result from the fact that $\theta \coth \theta$ and $\theta \operatorname{cosech} \theta$ are both of order unity, and $K \gg 1$.

The indefinite admittance matrix (4.3) has been obtained for the intrinsic transistor, and the element values given by Eq. (4.2) and (4.4). This matrix provides the basis for the common-emitter and common-collector circuits to be considered.

B. THE COMMON-EMITTER CONFIGURATION

Attention is now directed to the situation of Fig. 4.1b, where terminal "e" is common to input and output. According to the discussion in the previous section, the short-circuit admittance parameters for the intrinsic transistor in this configuration are obtained by striking out row and column "e"

of the indefinite admittance matrix (4.3). It is now desirable to number the input, or b'-terminal, as 1, and the output, or c-terminal, as 2. Referring to Eq. (4.2) and (4.4), one obtains:

$$y'_{11} = G\ (\theta \coth \theta - \theta \operatorname{cosech} \theta)$$

$$y'_{12} = \frac{G}{K}\ (\theta \operatorname{cosech} \theta - \theta \coth \theta)$$

$$y'_{21} = G\ \theta \operatorname{cosech} \theta$$

$$y'_{22} = \frac{G}{K}\ \theta \coth \theta \qquad (4.5)$$

Approximations for the hyperbolic functions involved in y'_{21} and y'_{22} were derived in Chapter II and are given in Eq. (2.26) and (2.27). However, using these approximations in the above expressions for y'_{11} and y'_{12} leads to considerable error, since the difference between two nearly equal quantities is involved. It is more efficient to utilize the basic approximations of Eq. (2.21) and (2.22), which lead to:

$$\theta \coth \theta - \theta \operatorname{cosech} \theta \simeq 1 + \frac{1}{3}\theta^2 - \frac{1}{1 + \frac{1}{6}\theta^2} = \frac{1}{2}\theta^2 \left[\frac{1 + \frac{1}{9}\theta^2}{1 + \frac{1}{6}\theta^2}\right]$$

$$\approx \frac{1}{2}\theta^2 \qquad (4.6)$$

The error involved in replacing the quantity in the square brackets by unity amounts to about 2 per cent (in magnitude) and 4^o at $\omega = 0.5\omega_\alpha$, and 8 per cent and 7^o at $\omega = \omega_\alpha$. This error is considered a satisfactory price to pay for the resulting simplification. Referring to Eq. (2.28) for θ^2, and to Table 3.2 for the change of notation to more convenient circuit parameters, the common-emitter intrinsic y-parameters can be written:

$$y'_{11} = \frac{1 - \alpha_0}{r'_e} + j\omega \frac{1.21}{\omega_\alpha r'_e}$$

$$y'_{12} = -\frac{1}{2r_c} - j\omega \frac{C_d}{2}$$

$$y'_{21} = \frac{\alpha_0}{r'_e} \frac{1}{1 + 0.405\ j\ \omega/\omega_\alpha}$$

$$y'_{22} = \frac{1}{2(1 - \alpha_0)r_c} + j\omega \frac{C_d}{3} \qquad (4.7)$$

Expressions for the overall h-parameters in terms of these intrinsic parameters are obtained by considering Fig. 4.1b. The effect of C_c is to add an admittance $j\omega C_c$ to y'_{11} and y'_{22}, and to subtract the same admittance from y'_{12} and y'_{21}. The resulting parameters are converted to h form, and the effect of r'_b is then simply an addition to h_{11}. The equations obtained are:

$$h_{11} = r'_b + \frac{1}{y'_{11} + j\omega C_c}$$

$$h_{12} = \frac{-y'_{12} + j\omega C_c}{y'_{11} + j\omega C_c}$$

$$h_{21} = \frac{y'_{21} - j\omega C_c}{y'_{11} + j\omega C_c}$$

$$h_{22} = y'_{22} + j\omega C_c - \frac{(y'_{12} - j\omega C_c)(y'_{21} - j\omega C_c)}{y'_{11} + j\omega C_c} \qquad (4.8)$$

Upon substituting Eq. (4.7) in the above, making use of the inequalities $C_c \gg C_d$ and $\omega_\alpha r_e' C_c \ll 1$, and utilizing the notation $s = j\omega/\omega_\alpha$, there results:

$$h_{11} = r_b' + \frac{r_e'/1 - \alpha_0}{1 + \frac{1.21}{1 - \alpha_0} s}$$

$$h_{12} = \frac{r_e'}{2(1 - \alpha_0)r_c} + \frac{\omega_\alpha r_e' C_c}{1 - \alpha_0} \frac{[1 - \frac{0.6}{(1 - \alpha_0)\omega_\alpha r_c C_c}]s}{1 + \frac{1.21}{1 - \alpha_0} s}$$

$$h_{21} = \frac{\alpha_0}{1 - \alpha_0} \frac{1}{1 + \frac{1.21}{1 - \alpha_0} s}$$

$$h_{22} = \frac{1}{(1 - \alpha_0)r_c} + \omega_\alpha C_c s + \frac{\alpha_0}{1 - \alpha_0} \omega_\alpha C_c \frac{[1 - \frac{0.6}{(1 - \alpha_0)\omega_\alpha r_c C_c}]s}{1 + \frac{1.21}{1 - \alpha_0} s}$$

(4.9)

The above is the principal result of this section, and describes the small-signal properties of the common-emitter junction triode from zero-frequency to somewhat above alpha cut-off.

Synthesis of an equivalent circuit representing these h-parameters is most readily accomplished by separating r_b' and the remainder of the circuit, the remainder being most conveniently realized in terms of a π. Figure 4.2a shows the relationships involved, obtained by calculating the h-parameters for the structure assumed, and then solving for the unknown elements. Reference to Eq. (4.9) yields expressions for these elements, which are readily recognized as RC circuits. The resulting equivalent circuit is shown in Fig. 4.2b.

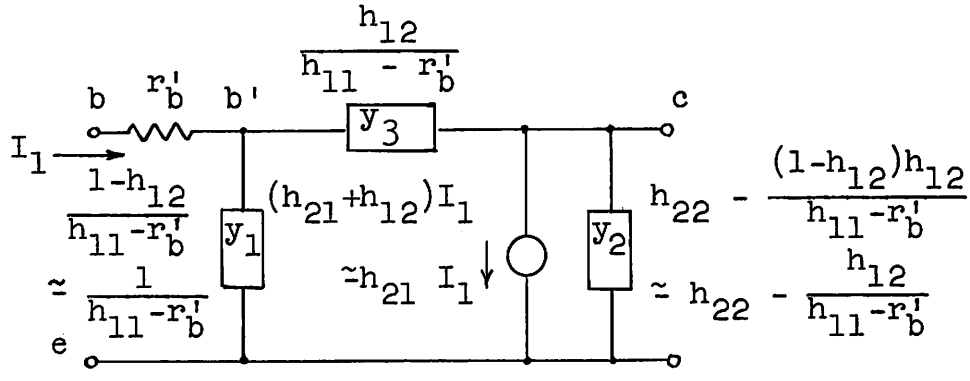

a.

NB $r_e' \simeq h_{11b}$

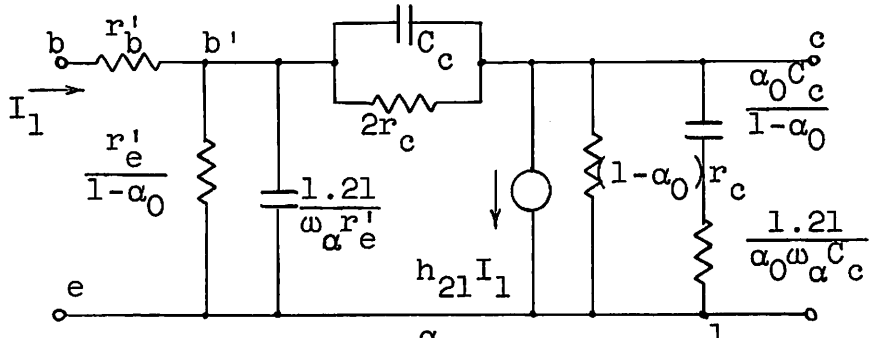

b. $h_{21} \simeq \dfrac{\alpha_0}{1 - \alpha_0} \dfrac{}{1 + \dfrac{1.21}{1 - \alpha_0} j\, \omega/\omega_\alpha}$

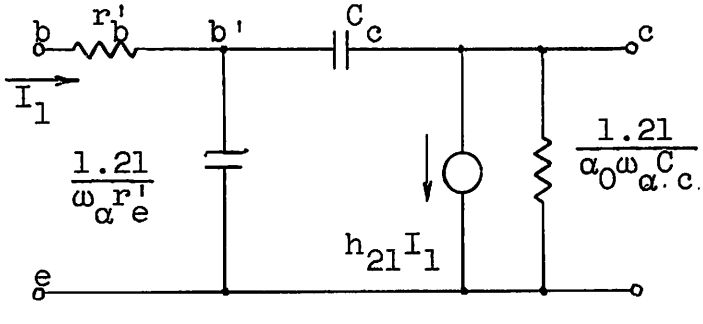

c.

Valid for
$\omega >> (1 - \alpha_0)\omega_\alpha$

$h_{21} \approx - \dfrac{\alpha_0}{1.21} j\, \omega_\alpha/\omega$

FIG. 4.2.--Common-emitter equivalent circuit and high-frequency equivalent.

For frequencies such that $\omega >> \frac{1}{2r_c C_c}$, the resistance $2r_c$ may be omitted in the feedback branch. For frequencies such that $\omega >> (1 - \alpha_0)\omega_\alpha$, the circuit can be simplified, approximately, to that of Fig. 4.2c,* which is useful in determining the limiting high-frequency performance of the common-emitter configuration. At these frequencies the h-parameters may be approximately written:**

$$h_{11} \simeq r_b' + \frac{r_e'}{1.21s}$$

$$h_{12} \simeq \frac{\omega_\alpha r_e' C_c}{1.21}$$

$$h_{21} \simeq \frac{\alpha_0}{1.21s}$$

$$h_{22} \simeq \omega_\alpha C_c \left(\frac{\alpha_0}{1.21} + s\right) \qquad (4.10)$$

Another common-emitter circuit in which the output current generator is controlled by the input voltage can be obtained from the intrinsic y-parameters of Eq. (4.7), according to the scheme of Fig. 4.3a. (see also Fig. 4.1b) This procedure yields the circuit of Fig. 4.3b,*** which for purposes of circuit analysis is often more convenient than that of Fig. 4.2b. Once again, the shunt resistance $2r_c$ may be ignored except possibly at very low frequencies. Also, where $\omega < 0.5\omega_\alpha$, the current generator can be regarded

---

*A circuit essentially similar to Fig. 4.2c, except that the output current generator is arranged to be frequency independent, has been given by R. L. Pritchard; see footnote on page 51.

**For common-emitter h-parameters derived by using somewhat different approximations, see footnote on page 51, p. 1084. See also reference 25, p. 842.

***A circuit having similar form has previously been obtained by L. J. Giacoletto, "Study of p-n-p alloy junction-transistor from d-c through medium frequencies," RCA Rev., vol. 15, December 1954, p. 555.

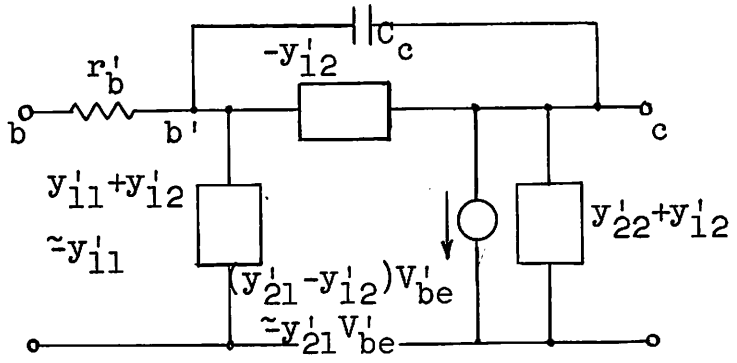

a.

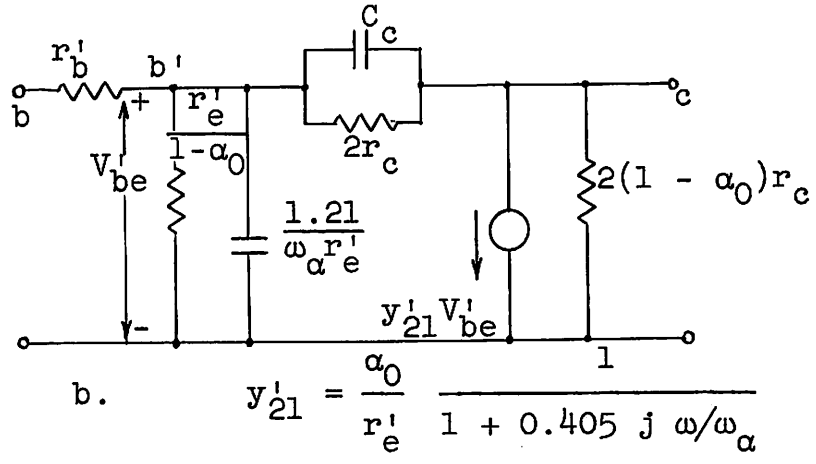

b. $$y'_{21} = \frac{\alpha_0}{r'_e} \frac{}{1 + 0.405\ j\ \omega/\omega_\alpha}$$

FIG. 4.3.--Alternative common-emitter equivalent circuit.

as frequency independent. An analysis of a video amplifier on the basis of this circuit will be given in Chapter VI. The convenience of the circuit lies in the fact that it is well adapted to nodal analysis (as distinct from loop or mesh analysis) even though the voltage controlling the output generator, $V_{b'e}$, appears at an "internal" node not accessible in practice. It is interesting to note that aside from the feedback capacitance C_c, substantially the entire frequency dependence of the circuit is contained in the capacitance $1.21/\omega_\alpha r'_e$.

In this section equivalent circuits and corresponding h-parameters have been derived representing the small-signal properties of the common-emitter connection of a junction triode. The circuits obtained are not entirely new, but it is hoped the derivation is more systematic than any presented to date.

C. THE COMMON-COLLECTOR CONFIGURATION

The procedure for deriving an equivalent circuit for the common-collector case is entirely analogous to that presented above for the common-emitter. The basic circuit is shown in Fig. 4.1. Terminal "c" is common, so the intrinsic y-parameters are obtained from the indefinite admittance matrix (4.3) by striking out row and column "c". The remaining elements are then renumbered so that the input (b') terminal is denoted by 1, and the output (e) terminal by 2. There results:

$$\begin{aligned} y'_{11} &= G(1 + \tfrac{1}{K})(\theta \coth \theta - \theta \operatorname{cosech} \theta) \\ y'_{12} &= G\,(\theta \operatorname{cosech} \theta - \theta \coth \theta) \\ y'_{21} &= -\,G\,\theta \coth \theta \\ y'_{22} &= G\,\theta \coth \theta \end{aligned} \qquad (4.11)$$

The factor $1 + \frac{1}{K}$ has been retained in $y'_{b'b'} = y'_{11}$, since the quantity $y'_{11}\, y'_{22} - y'_{12}\, y'_{21}$ which occurs later, would otherwise be zero.

Approximations to the above functions have been covered in the previous section. In terms of the fundamental circuit parameters they may be written:

$$y'_{11} = \frac{1 - \alpha_0}{r'_e} + \frac{1}{2r_c} + j\omega\left(\frac{1.21}{\omega_\alpha r'_e} + \frac{C_d}{2}\right)$$

$$y'_{12} = -\frac{1 - \alpha_0}{r'_e} - j\omega\,\frac{1.21}{\omega_\alpha r'_e}$$

$$-y'_{21} = y'_{22} = \frac{1}{r'_e}\,(1 + 0.81\ j\ \omega/\omega_\alpha) \qquad (4.12)$$

Reference to Fig. 4.1c indicates that the overall h-parameters may be obtained by adding the term $j\omega C_c$ to y'_{11}, converting to the h form, and then adding r'_b to h_{11}. Using the approximations $\omega_\alpha r'_e C_c \ll 1$, and $C_d \ll C_c$, this procedure yields the expressions:

$$h_{11} = r'_b + \frac{r'_e/1 - \alpha_0}{1 + \frac{1.21}{1 - \alpha_0}\,s}$$

$$h_{12} = 1 - \frac{r'_e}{2(1 - \alpha_0)r_c}\,\frac{1 + 2\omega_\alpha r_c C_c s}{1 + \frac{1.21}{1 - \alpha_0}\,s} \approx 1$$

$$h_{21} = -\frac{1}{1 - \alpha_0}\,\frac{1 + 0.81s}{1 + \frac{1.21}{1 - \alpha_0}\,s}$$

$$h_{22} = \frac{1}{2(1 - \alpha_0)r_c}\,\frac{1 + 2\omega_\alpha r_c C_c s}{1 + \frac{1.21}{1 - \alpha_0}\,s}$$

$$s = j\ \omega/\omega_\alpha \text{ for real frequencies} \qquad (4.13)$$

These equations constitute a complete description of the small-signal properties of a junction triode in the common-collector configuration. Note that h_{12} can usually be sufficiently well approximated by unity, the maximum departure from unity being $\omega_\alpha r_e' C_c/1.21$ at high frequencies. [$\omega >> \omega_\alpha(1 - \alpha_0)$]

An equivalent circuit which clearly brings out the important properties of this configuration is derived from the scheme of Fig. 4.4a using the y'-parameters of Eq. (4.11). It is convenient to use a voltage generator in the output branch, since this turns out to be not only independent of frequency, but equal to the voltage $V_{b'c}$ at the internal base node. Otherwise the circuit is similar in form to the common-emitter version shown in Fig. 4.3. Figure 4.4b gives the final result. It is seen that the circuit can be expected to show a ratio of output to input voltage of very nearly unity at low frequencies, if the load resistance is large compared with r_e'. Under the same conditions, the input impedance is high (compared with that of the other two configurations) although it drops rapidly with frequency above, roughly, $\omega_\alpha(1 - \alpha_0)$.

Other equivalent circuits can be derived, corresponding, for example, to the situation of Fig. 4.2a, where the internal generator is dependent on the input current. In this case, however, the impedance in the output branch turns out to have negative elements, which is not particularly desirable.

Some further approximation is possible in the equivalent circuit of Fig. 4.4b. The element $2r_c$ of the parallel branch comprising C_c and $2r_c$ across terminals b' and c may be omitted, as may the inductance in the output branch. At frequencies such that $\omega >> (1 - \alpha_0)\omega_\alpha$, only the capacitance in the feedback branch is of importance. Making these alterations, the circuit of Fig. 4.5a results, and the corresponding approximate h-parameters are:

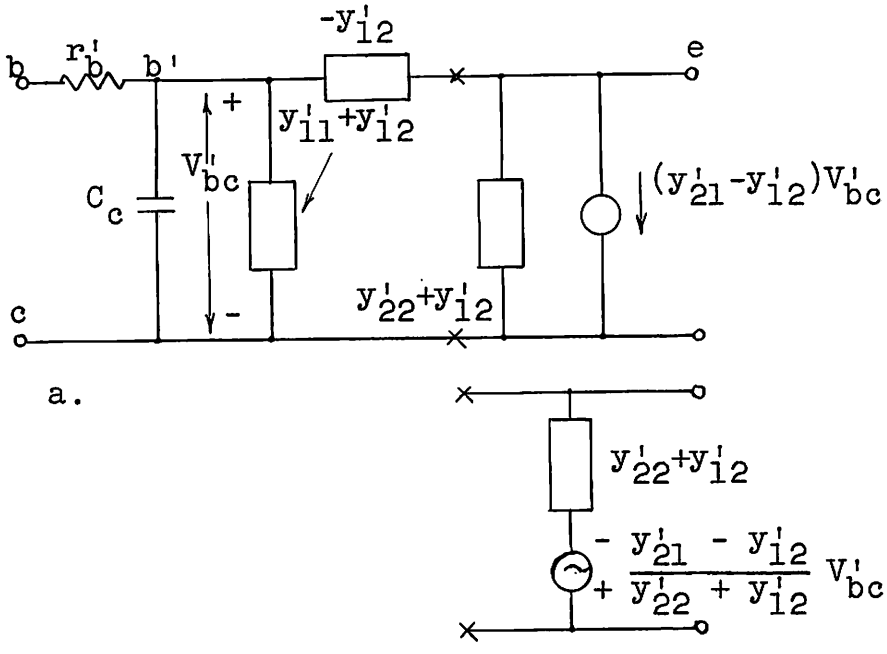

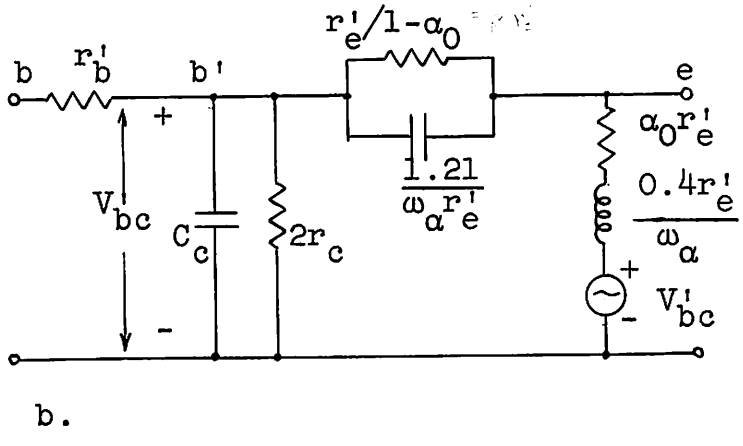

b.

FIG. 4.4.--Common-collector equivalent circuit.

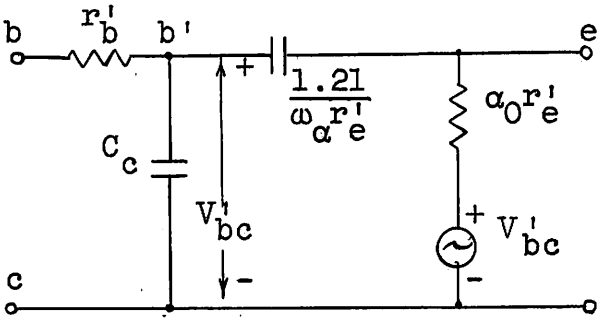

a.

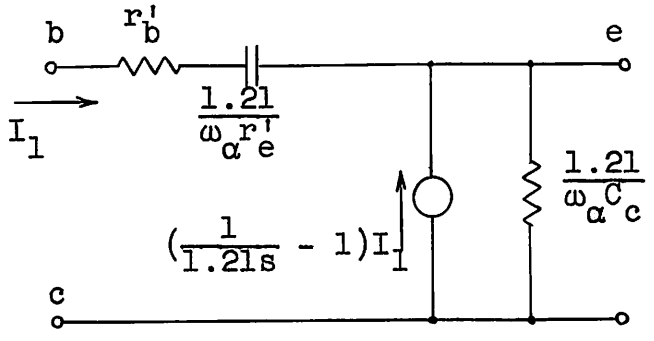

b.

Both circuits valid for $(1 - \alpha_0)\omega_\alpha << \omega < \omega_\alpha$

FIG. 4.5.--Common-collector high-frequency equivalent circuits.

$$h_{11} \simeq r_b' + \frac{r_e'}{1.21s}$$

$$h_{12} \simeq 1$$

$$h_{21} \simeq -\frac{1}{1.21s}$$

$$h_{22} \simeq \frac{\omega_\alpha C_c}{1.21} \qquad (4.14)$$

From these relations an alternative approximate circuit immediately follows which is shown in Fig. 4.5b.

In this section the common-collector configuration of a conventional junction transistor triode has been briefly considered. Starting from the intrinsic parameters obtained from the indefinite admittance matrix of Section A, equivalent circuits and h-parameters have been derived. The common-collector at high frequencies has received little consideration in the literature, and the results presented here are believed to be new.* An application of this configuration will be given in Chapter VI.

D. CONCLUSIONS

The purpose of this chapter has been to derive, on a reasonably simple and approximate basis, small-signal equivalent circuits and four-pole parameters representing junction transistor common-emitter and common-collector configurations. The initial model assumed for the transistor, and the method of treatment, was the same as for the common-base connection treated in Chapter III. Making use of approximations to the hyperbolic functions developed in Chapter II, the y-parameters for the intrinsic transistor in each connection were obtained from the intrinsic indefinite admittance matrix introduced in

---

*See, however, F. R. Stansel, "The common-collector transistor amplifier at carrier frequencies," Proc. IRE, vol. 41, Sept. 1953, pp. 1096-1103. Input and output impedances as a function of frequency are derived on the basis of a somewhat less accurate equivalent circuit.

Section A. These parameters were used to synthesize equivalent circuits, the extrinsic elements being added to complete the circuit for the overall transistor. Complete h-parameters were then derived, and used to synthesize alternative equivalent circuits. In each case, approximations useful at high frequencies were indicated. It is hoped that the results are simple enough to facilitate the task of designing transistor amplifiers with acceptable accuracy. A simple example of a video amplifier design will be given in Chapter VI as an illustration. The measurements made on this amplifier constitute, to some extent, an experimental verification of the equivalent circuits which have been derived herein.

V. MEASUREMENT OF TRANSISTOR SMALL-SIGNAL PARAMETERS

In the present chapter the attempt is made to present the basic philosophy and techniques of small-signal transistor measurements which have been developed in support of concurrent theoretical equivalent-circuit work. This theoretical work has been presented by R. D. Middlebrook in TR-No. 83,* and simplifying extensions of it were given in the present report.

The discussion will have two aspects. First, one must decide which parameters to attempt to measure. This decision depends upon consideration of the parameters that are actually significant and useful for a particular application, and also upon the relative ease and simplicity of measurement (which may be conditioned by the equipment available). In general, as simple and direct a measurement as possible is preferable, and it may be worthwhile to design special equipment with this end in mind for measurement of certain quantities. Secondly, the actual technique of measuring the proposed parameter must be considered, and as noted above, may have a considerable bearing on the initial choice of the parameter. Thus, the two parts indicated are interdependent, and discussion of each will not be sharply separated.**

The work which resulted in the measurement techniques reported here has been a rather general study of junction transistor equivalent circuits, principally in the common-base configuration. Starting from physical principles, it was shown in TR-No. 83 how the small-signal terminal properties depend on the geometry and physical properties of the transistor materials,

---

*See reference 7. A brief outline of some of the measurement methods reported here has also appeared in TR-No. 83.

**A general discussion along these lines has been given by D. A. Alsberg, "Transistor metrology," Convention Record of the IRE, Part 9, 1953, pp. 39-44.

i.e. fundamental device parameters, as outlined in Table 3.2 of this report. It was further shown that the short-circuit admittance parameters of the overall device are determined as a function of frequency by six quantities corresponding to the fundamental circuit parameters of Table 3.2. In order to investigate this conclusion experimentally, it was thus necessary to make two types of measurements: a) general four-pole parameter measurements at a number of frequencies covering a fairly wide range, where the transistor is regarded as a "black box" containing a linear active network and four measurements are necessary to describe it at a given frequency; b) measurements intended to single out the six parameters in terms of which it is desired to specify the entire transistor. From the measurements of b) one can predict the four-pole parameters as functions of frequency for comparison with the measurements of a), which is done for a series of transistors in TR-No. 83. This procedure indicates to what degree of accuracy the complete transistor can be characterized by the six fundamental circuit parameters. In other words, the measurements show how closely an actual transistor is approximated by the theoretical model assumed for purposes of analysis.

A. MEASUREMENT OF THE FOUR-POLE PARAMETERS

A linear active network is specified by a set or matrix of four independent parameters, of which the most commonly used are the z- (open-circuit impedance), y- (short-circuit admittance), and h- (hybrid) parameters.* Each of these sets involves two immittances measured at input and output terminal pairs (the opposite terminal pair being either open- or short-circuited), and two transfer parameters. The two driving-point immittances may be measured on a conventional bridge, if one can be found to operate at the desired frequency and immittance level. The

*The y- and h-parameters have been defined in 1st footnote on page 12 and Fig. 2.6, respectively. The z-parameters are defined implicitly in Fig. 3.4. Also, see the references in the footnote on p. 22.

transfer parameters are generally more difficult to measure, particularly the transfer h's which are dimensionless ratios of current or voltage observed at one end of the network to current or voltage applied at the other end. Such a ratio would ordinarily be measured in terms of magnitude and phase, and requires rather complex equipment for accurate results at high frequencies. The other transfer parameters, being in the nature of immittances, can be handled more readily, and bridges have been devised to measure directly the transfer y- and z-parameters at high frequencies.* As a practical matter, it is usually much more convenient to measure the transfer y-parameters because of difficulty in realizing the open-circuit condition required for the z-parameters.

It should be pointed out that it is possible to measure transfer parameters indirectly by measuring only driving-point immittances on a network and then resorting to calculations. Four independent measurements are required; as an example, if the h-parameters of a network are desired, one can measure h_{11} and h_{22} directly (refer to Fig. 5.1). A third independent measurement is y_{22}, which yields the product $h_{12}h_{21}$ as shown. A fourth measurement giving the sum or difference of h_{12} and h_{21} is required (note that $z_{11} = h_{11} - h_{12}h_{21}/h_{22}$ does not give this); this may be obtained from the quantity h_{11_e}, which in the example shown represents h_{11} of the common-emitter connection.

The above procedure is always possible, but the calculations required are somewhat cumbersome and may compound the errors of the individual measurements, leading to inaccurate results. It is thus preferable to measure the transfer parameters directly, and as previously mentioned, the transfer y-parameters are the most readily obtained. At least two methods are available, one of which is useful at relatively low frequencies where the transfer admittances are substantially real, the other being of

---

*A discussion of such bridges is given by H. A. M. Clarke and P. B. Vanderlyn, "Double-ratio a-c bridges with inductively-coupled ratio arms," Proc. IEE, vol. 96, pt. III, May 1949, p. 189. See also H. L. Kirke, "Radio frequency bridges," JIEE, vol. 92, pt. III, March, 1945, p. 2.

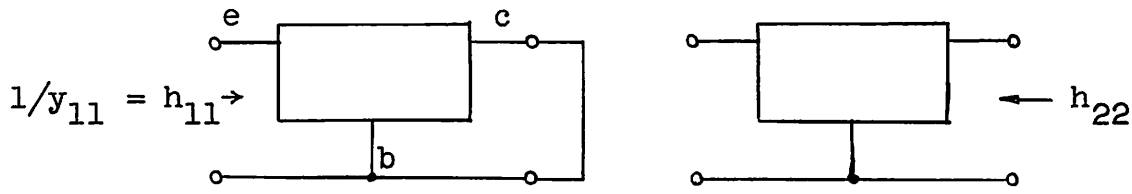

Common-base configuration shown as an example.

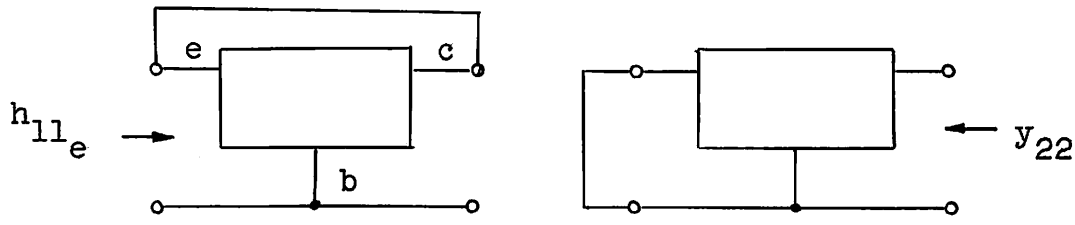

$$y_{22} = h_{22} - \frac{h_{12}h_{21}}{h_{11}}$$

$$1/h_{11_e} = y_{22} + \frac{1 + h_{21} - h_{12}}{h_{11}}$$

FIG. 5.1.--Illustrating the determination of four-pole parameters by driving-point immittance measurements.

use principally at higher frequencies. The high-frequency method makes use of a transformer ratio-arm bridge such as shown in essential form in Fig. 5.2.* An input transformer with closely coupled secondary windings applies equal and opposite potentials between the neutral point and the unknown and standard admittances Y_x and Y_s. When Y_s is adjusted to be equal to Y_x, equal and opposite currents flow through them, hence the current in the detector transformer is zero, and a null is observed. An advantage of this arrangement is that any impedance, stray or otherwise, appearing between either side of the input transformer secondary and neutral has no effect on the balance, since an equal impedance is reflected into the other half of the transformer provided that the impedance is large compared with the small leakage impedance between secondary halves.

The above property makes possible the measurement of the transfer admittances of four-terminal networks (more properly, three-terminal networks). Referring to Fig. 5.2b, the transfer admittance is defined as $Y_{21} = I_2/V_1$ with $V_2 = 0$. This last condition is met at balance, since the voltage across the detector transformer is necessarily zero. Since $V_1 = V_s$, despite the impedance presented by the network to V_1, and, at balance, $I_d = 0$, or $I_2 = - I_s$, there results:

$$Y_{21} = \frac{I_2}{V_1} = \frac{I_s}{V_s} = - Y_s$$

Upon interchanging ends 1 and 2 of the network, the transfer admittance Y_{12} can be measured. In practice, Y_s is essentially a parallel resistance and capacitance, both of which can be varied over a considerable range, and the zero-point values of

---

*See F. E. Terman and J. M. Pettit, Electronic Measurements, 2nd ed., McGraw-Hill Book Co., Inc., 1952, pp. 116-117. Refer also to footnote on page 95. A commercial embodiment of the bridge of Fig. 5.2 is the Wayne-Kerr r-f Bridge Type B 601, which is useful from 15 kc to 5 MC. A similar bridge is the Wayne-Kerr VHF Admittance Bridge Type B 801 which extends the frequency range to 100 MC.

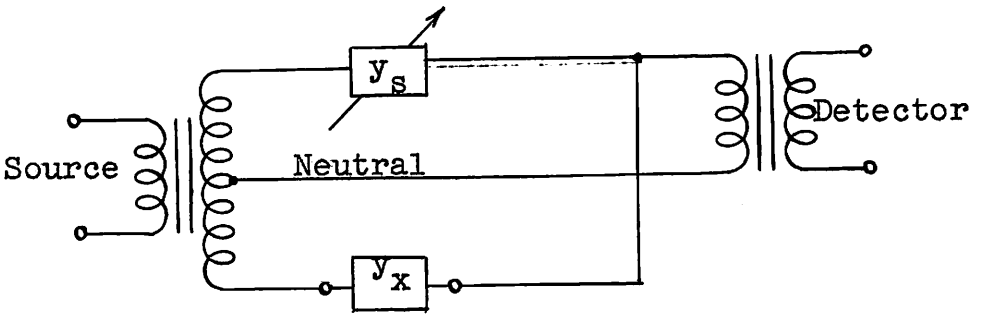

a. Measurement of driving-point admittance.

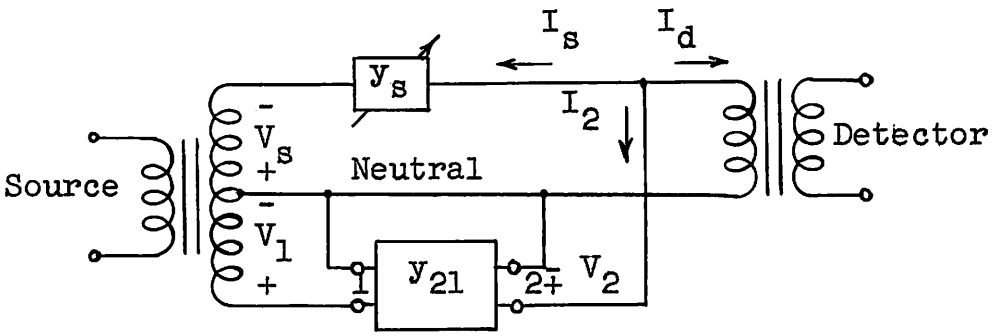

b. Measurement of transfer admittance.

FIG. 5.2.--Measurement of four-pole admittance parameters with a transformer ratio-arm bridge.

which are compensated for by adding fixed elements to the unknown side of the bridge. A negative real part of $-Y_{21}$ is handled in effect by switching the variable resistance branch of Y_s to the opposite side of the bridge. The variable capacitance is similarly switched if $-Y_{21}$ is inductive.

Using the particular bridges mentioned in footnote on page 97, the y-parameters of any linear network may be investigated at any frequency from 15 kc to 100 MC, and at admittance levels appropriate to junction triodes in any of the three configurations. (Other driving-point immittances may of course be measured, such as h_{22}.) Practical problems arising from the necessity of supplying d-c bias to the transistor will be considered in Section B.

Another method of directly measuring transfer parameters (and driving-point quantities) which is particularly convenient and accurate at low frequencies where the parameters are substantially resistive, involves the use of low-impedance voltage sources whose relative magnitudes are accurately known and controlled.* Thus in Fig. 5.3a, the current I_2 flowing from voltage source V_2 through the unknown driving-point resistance can be adjusted to equal the current I_1, flowing from voltage source V_1 through the standard resistance R_s, at which point a null balance is observed, and one obtains:

$$\frac{V_2}{R_x} = \frac{V_1}{R_s} \quad \text{or} \quad R_x = R_s \frac{V_2}{V_1}$$

---

*Terman and Pettit, footnote on page 97, pp. 299-301, 304. This voltage-ratio method is used in the General Radio Type 561-D Vacuum-Tube Bridge. Reference may be made to the operating instructions for this bridge; also see A. G. Bousquet, "Transistor measurements with the vacuum-tube bridge," General Radio Experimenter, vol. 27, no. 10, March, 1953; and L. J. Giacoletto, "Transistor characteristics at low and medium frequencies," Tele-Tech., vol. 12, March, 1953, p. 157.

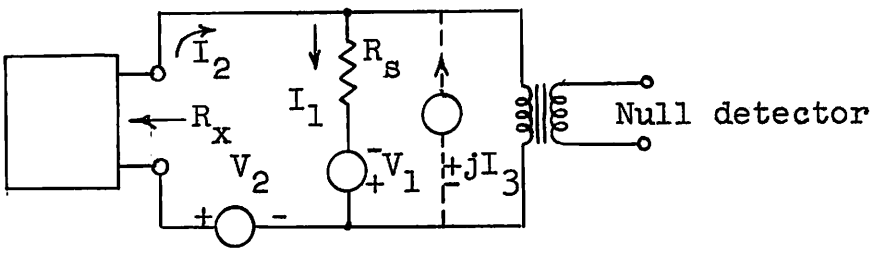

a. Driving-point resistance.

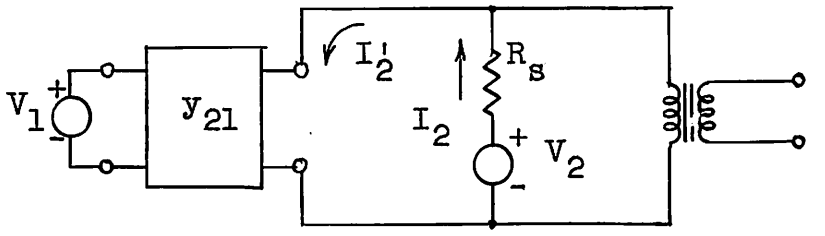

b. Transfer conductance.

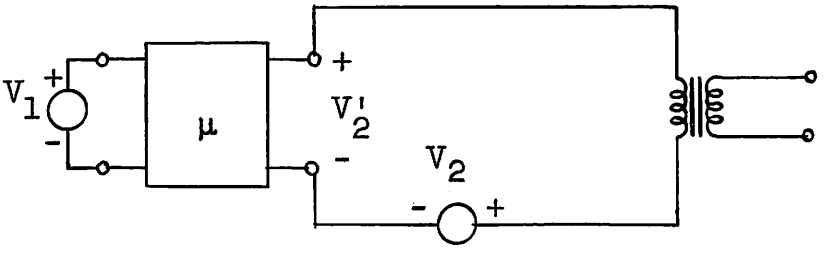

c. Voltage transfer ratio.

FIG. 5.3.--Measurement of four-pole parameters by the voltage-ratio method.

since, at balance, no voltage exists across the transformer. The voltages V_1 and V_2 are normally obtained from identical windings of a transformer, and their magnitudes adjusted by means of low-impedance attenuators.* A variable quadrature current I_3 is provided to balance out any existing small reactive component. Transfer conductance is measured as shown in Fig. 5.3b; voltage V_1 is applied to the input terminals of the network (the input impedance of which must be much greater than the source impedance of V_1) resulting in an output current I_2'. If current I_2 is adjusted to equal I_2', a null exists, and, since the network output terminals are effectively short-circuited at this point, the following relation results:

$$I_2' = y_{21}V_1 = \frac{V_2}{R_s} \text{ or } y_{21} = \frac{1}{R_s}\,\frac{V_2}{V_1}$$

Figure 5.3c illustrates the measurement of a voltage transfer ratio (such as h_{12}), defined as the ratio of output to input voltage when zero output current flows. This occurs at the null point, when $V_2 = V_2'$, thus $\mu = \frac{V_2}{V_1}$. The voltage ratio method as illustrated here is hence suitable for measurement of transfer conductances and transfer voltage ratios, as well as driving-point quantities.** Under certain circumstances, as explained later, current transfer ratios, such as h_{21}, can be measured.

For low-frequency measurements there have been devised straight-forward voltmeter-ammeter techniques, which are somewhat less accurate than null methods, but have the advantage of

---

*Except for the fact that the voltages are controlled by attenuators and the standard impedance normally left fixed, the voltage-ratio method in essence is the same as the transformer ratio-arm method. Thus compare Figs. 5.2a and 5.3a.

**A modification of this method to allow transfer impedances to be measured is given by B. F. C. Cooper, "A bridge for measuring audio-frequency transistor parameters," Proc. IRE, vol. 43, July 1955, pp. 796-805.

being direct-reading and relatively rapid. From the standpoint of convenience and minimization of the errors involved, it is generally desirable to measure the h-parameters.[28] This approach is noted here because of its practical importance, but will not be further discussed.

By means of the methods described, one can investigate the four-pole parameters of a transistor over the entire useful frequency range.* The remaining problems occur because of the necessity to supply d-c bias to the transistor, and will now be briefly discussed.

B. BIAS AND TERMINATION PROBLEMS

Since the emitter-base circuit of a junction transistor is of low impedance and the collector-base circuit of high impedance, the d-c operating point is customarily specified in terms of emitter current and collector-base voltage. As seen from Table 3.2, the fundamental device parameters G and K depend on d-c emitter current and collector voltage, respectively. It is thus desirable to measure and control these quantities directly. To obtain stability of operating point, emitter current is usually supplied to the transistor through a resistance large compared to the transistor input resistance, and collector voltage applied from a low-resistance source as illustrated in Fig. 5.4a. (In all cases, polarity is shown for a p-n-p transistor.) In this manner, the operating point is independent of the particular transistor, and I_e and V_{cb} may be varied independently. The particular bridges previously mentioned (see footnotes on pages 97 and 99) have

---

*An arrangement for measuring admittance parameters rapidly over a wide bandwidth is described by L. J. Giacoletto, "Equipments for measuring junction transistor admittance parameters for a wide range of frequencies," RCA Review, vol. 13, June 1953, p. 269. Here, the transistor is balanced against a passive network which is adjusted to have the same frequency dependence, so that the form of the admittance must be known in advance.

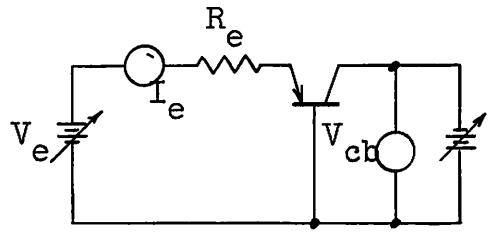

a.

$$I_e \simeq \frac{V_e}{R_e}$$

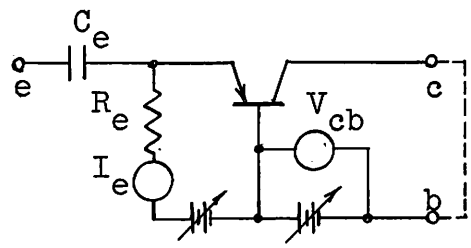

b.

Common-base bias

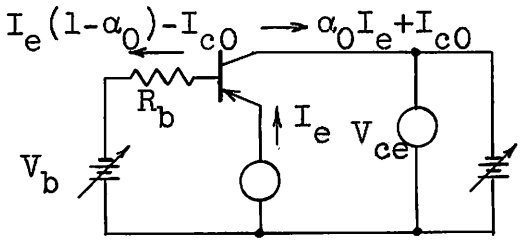

$$I_e \simeq \frac{V_b + I_{c0}R_b}{(1 - \alpha_0)R_b}$$

c.

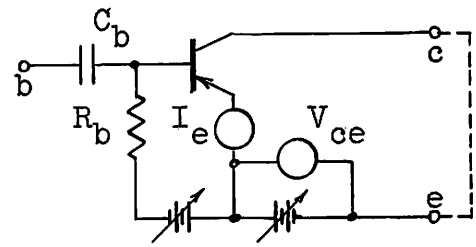

$$V_{cb} \simeq V_{ce}$$

d.

Common-emitter bias

FIG. 5.4.--Bias arrangements for bridge measurements.

low-resistance d-c paths between terminals; thus the preferred bias arrangement may generally be used, as in Fig. 5.4b. Here, collector current is supplied through the bridge, the emitter is isolated for d-c by the capacitor C_e, and receives current through R_e which can readily be made large enough compared with the emitter-base impedance so that its effect becomes negligible. In this arrangement, the a-c ground of the system must ordinarily coincide with terminal b, which is not always convenient, or possible. In such a case, the method of Fig. 5.4c may be used, where, since emitter-to-base voltage is rarely greater than 0.1 v, $V_{ce} \simeq V_{cb}$. However, as shown, the emitter current I_e depends strongly on the current gain α_0 of the transistor, and less strongly on I_{c0}, the collector saturation current. (R_b is assumed large compared with the resistance seen at the base). In the arrangement of Fig. 5.4d, the emitter-to-collector d-c path is completed through the bridge, while the base is isolated by the capacitor C_b. Once again, R_b can be made large enough to have an insignificant effect on small-signal measurements.

The circuits given here are of use in the general situation where all three of the device terminals are connected to the bridge, as occurs when transfer parameters are measured. If only two terminals are to be connected, simplifications are possible; for example the blocking capacitors C_e and C_b are not needed. If the particular bridge used does not possess a d-c path for collector current, the collector must be shunt-fed through a resistance, as is the emitter in Fig. 5.4a, for example. However, it is generally impractical to make this resistance large compared with the collector impedance, so that a calculation must be made to take its effect into account. In addition, the d-c collector voltage cannot be directly read on a meter external to the a-c bridge circuit, but must be obtained by temporarily connecting a meter to the collector terminal.

The various four-pole parameters are defined under the condition that one end of the network is open- or short-circuited. This condition cannot be exactly realized in practice because of the necessity of supplying d-c bias to the terminals from power supplies of finite impedance; however, a good approximation may be achieved by making the supply impedance sufficiently large, or small. The requirements on this impedance will be obtained for the common-base situation; the analysis for other configurations is exactly similar.*

Consider the measurement of h_{11}. Ideally, the collector is short-circuited to the base, but the bias supply is supposed to possess an admittance Y_2 which is large but not infinite, so that the input impedance actually measured is:**

$$Z_{in} = h_{11} - \frac{h_{12}\, h_{21}}{h_{22} + Y_2}$$

At low frequencies, using the parameters given in Fig. 3.18c:

$$Z_{in} = r_h + \frac{\alpha_0 r_b}{1 + r_c Y_2}$$

The necessary condition for the second term to be negligible is hence

$$1 + r_c Y_2 \gg \frac{\alpha_0 r_b}{r_h} \quad \text{or, approximately,} \quad Y_2 \gg \frac{1}{r_c} \quad \frac{\alpha_0 r_b}{r_h}$$

---

*The errors in four-pole parameter measurements, caused by finite terminating impedances, have been considered for the low-frequency case, and with emphasis on sweep measurement techniques, by H. G. Follingstad, "An analytical study of z, y, and h-parameter accuracies in transistor sweep measurements," Convention Record of the IRE, Part 3, 1954, pp. 104-116.

**See footnote on page 22, p. 336, for general formulas of this nature.

which is very easily satisfied.* At high frequencies, no essential loss of generality results from using the approximate parameters given in Fig. 3.18j:

$$Z_{in} = 1.2\, r_b' + \frac{j\omega r_b' C_c \alpha_0}{(j\omega C_c + Y_2)(1 + j\frac{\omega}{\omega_\alpha})} \qquad (5.1)$$

The magnitude of the second term is, within a factor of $\sqrt{2}$ up to ω_α:

$$\left| \frac{\alpha_0 r_b'}{1 + \frac{Y_2}{j\omega C_c}} \right|$$

Hence Z_{in} is very nearly h_{11} if $|Y_2| \gg \omega C_c$ which can be achieved by a suitable resistance, or, if this is not possible, by a by-pass capacitor $C_2 \gg C_c$.

For the measurement of y_{22}, the input terminals are assumed to be terminated by an admittance Y_1. The output admittance actually measured is then:

$$Y_{out} = y_{22} - \frac{y_{12}\, y_{21}}{y_{11} + Y_1}$$

At high frequencies, by use of the y-parameters of Eq. (3.26), this admittance becomes:

$$Y_{out} = j\omega C_c + \alpha \frac{j\omega C_c}{1.2} - \frac{\frac{\alpha j\omega C_c}{1.2}}{1 + 1.2\, r_b' Y_1} \qquad (5.2)$$

---

*If it is desired to measure z_{11}, a terminating impedance $Z_2 \gg r_c$ must be used, which is not generally practical. See, however, second footnote on page 101, where an active circuit is used to establish zero current in the output loop.

The last term will be negligibly small if $r_b' Y_1 \gg 1$, which is usually realized by means of a by-pass capacitor C_1 chosen such that $\omega C_1 r_b' \gg 1$. (It is desirable to maintain a high resistance, corresponding to R_e in Fig. 5.4a, to control d-c emitter current.) For low frequencies, the criterion is $\omega C_1 r_h \gg 1$, which implies a rather large capacitor.

Consider now the measurement of h_{22}. The admittance observed at the output with a terminating impedance Z_1 at the input is:

$$Y_{out} = h_{22} - \frac{h_{12}\, h_{21}}{h_{11} + Z_1} \tag{5.3}$$

which is, using the approximate high-frequency h-parameters:

$$Y_{out} = j\omega C_c + \frac{j\omega C_c\, \alpha_0/1.2}{(1 + \dfrac{Z_1}{1.2 r_b'})(1 + j\, \omega/\omega_\alpha)} \tag{5.4}$$

The second term is small compared with the desired first term if $Z_1 \gg r_b'$, which is readily achieved by the resistance R_e in Fig. 5.4a, for example. One aspect of this measurement is deserving of more detailed analysis. The impedance Z_1 will always possess some shunt capacitance C_1 owing to stray lead and socket capacitance, and additional parasitic capacitance may be caused by the transistor structure,* as well as the emitter space charge layer capacitance which, until now, has been ignored. Supposing Z_1 to consist only of this capacitance C_1, there is obtained for the measured output admittance:

$$Y_{out} = j\omega C_c - \alpha_0 \frac{\omega^2 r_b'\, C_c C_1}{(1 + j\omega r_b'\, C_1)(1 + j\, \omega/\omega_\alpha)} \tag{5.5}$$

---

*See reference 23.

Thus, Y_{out} may possess a negative conductive component if the real part of the second term above is greater in magnitude than the real part of h_{22}, which has been ignored in the passage from Eqs. (5.3) to (5.4). It appears that this situation is often realized, since apparent negative real parts of h_{22} have been observed on the majority of transistors measured. If the frequency is sufficiently below alpha cut-off, and $\omega r_b' C_1$ is small, the ratio of real to imaginary parts of Eq. (5.5) is approximately $-\alpha_0 \omega r_b' C_1$. This behavior is in qualitative agreement with the measurements reported in Chapter III. Referring to Fig. 3.15, the quantity $-h_{22r}/h_{22i}$ tends to increase with frequency up to about 0.5 ω_α, and a rough estimate of the quantity $\omega_\alpha r_b' C_1$ is 0.2. Since the quantity $\omega_\alpha r_b' C_c$ is generally of the order of 0.02 to 0.1, C_1 may be 2 to 10 times as great as C_c, which is somewhat larger than expected for stray capacity. However, C_1 may be partially accounted for by capacitances inherent in the transistor structure; in particular, the emitter space charge layer capacitance C_e may contribute.*

No attempt at completeness has been made in this section, the intent being a discussion of the most important practical problems arising in the measurement of transistor four-pole parameters.

C. MEASUREMENT OF THE CIRCUIT PARAMETERS

Attention is now directed to the measurement, in as direct a manner as possible, of the six basic quantities in terms of which it is possible to characterize a junction triode. Some choice exists as to which six of a number of interdependent quantities are to be considered as basic; this section will

---

*In this theory two difficulties which have not been fully resolved are that C_e is usually much larger than the value predicted above for C_1, and that, strictly speaking, C_e appears from the emitter terminal to the internal base terminal where it does not produce the effect of a negative conductance at the collector-base terminals.

deal with the fundamental circuit parameters defined in Eq. (3.17) and Table 3.2. These are believed to be the most convenient parameters for equivalent circuit representations, and still are quite closely related to the underlying physical situation. From Table 3.2 the intrinsic transistor is described by four quantities, which can be identified as follows: (refer to Eq. 2.32)

r_e' Low-frequency value of h_{11}'

α_0 Low-frequency value of $-h_{21}'$

ω_α (Radian) frequency at which $|h_{21}'| = 0.707\ \alpha_0$

r_c Low-frequency value of $1/h_{22}'$

In addition, the extrinsic quantities are:

r_b' Base spreading resistance

C_c Collector space charge layer capacitance

Not all of these quantities can be easily measured directly;*

---

*R. D. Middlebrook (refer to p. 115 of TR-No. 83) chooses substantially the same set of basic parameters, except that in place of r_c, g_c is used (the low-frequency value of the intrinsic collector admittance y_{22}'), and $g_{ee} = 1/r_h$ (low-frequency value of the overall emitter admittance y_{11}) is chosen in place of r_e'. From Eqs. (3.15) and (C.4).

$$g_c = \frac{1}{2(1 - \alpha_0)r_c}, \quad \frac{1}{g_{ee}} = r_e' + r_b' (1 - \alpha_0)$$

As directly measurable parameters, Middlebrook chooses, in addition to α_0, g_{ee}, and $r = r_b'$, the low-frequency conductance and capacitance of the overall collector admittance y_{22}. Reference to Eq. (3.19) yields for these quantities:

$$G_{cc} = \frac{1}{r_c}\left(1 + \alpha_0 \frac{r_b' + r_b''}{r_h}\right), \quad C_{cc} = C_c\left(1 + \alpha_0 \frac{r_b'}{r_h}\right)$$

$$\text{where } r_b'' = \frac{\alpha_0 r_e'}{2(1 - \alpha_0)}$$

The sixth measured parameter chosen is the 3-db cut-off frequency of the overall current gain h_{21}, which is denoted in TR-No. 83 by ω_α. This frequency will be indicated here by ω_c, the symbol ω_α being reserved for the intrinsic current gain (h_{21}') cut-off frequency. The relation between ω_c and ω_α will be developed shortly.

in particular, r_e' and ω_α are most conveniently obtained by calculations on measurements of related quantities, as will be seen. Consider now the parameters which can be measured at low frequency. Upon reference to Eq. (3.15), one has for the common-base configuration,

$$r_c = 1/h_{22}$$

$$\alpha_0 = -h_{21}$$

$$r_h = h_{11} = r_e' + r_b' (1 - \alpha_0)$$

The parameters h_{11} and h_{22} can be measured as described in the previous section,* and r_e' calculated from r_h when r_b' is determined. The measurement of h_{21} is made possible by the fact that the input resistance r_h is normally rather small. If a resistance R_e much larger than r_h is placed in series with the input, the input signal current will be fixed by the known external resistance, and not depend on the transistor parameters. Thus $I_1 = V_1/R_e$ and $I_2 = h_{21}I_1$, so that the transfer conductance of the circuit is $y_{21} = I_2/V_1 = h_{21}/R_e = -\alpha_0/R_e$. This quantity may be measured on a voltage-ratio bridge or by observing the voltage drop caused by I_2 flowing through a small resistance in the collector circuit, and comparing this drop with V_1. Somewhat greater accuracy is possible in the determination of α_0, particularly if it is near unity, by measurement of h_{21} in the common-emitter configuration, which is

$$h_{21_e} = \frac{\alpha_0}{1 - \alpha_0}$$

from which

$$\alpha_0 = \frac{h_{21_e}}{1 + h_{21_e}}$$

---

*The General Radio vacuum-tube bridge will accurately measure these parameters, or, one of a number of commercial test sets designed to measure low-frequency h-parameters may be used -- see, for example, reference 28.

According to the theoretical discussion of Chapter III, the transistor is completely characterized at low frequencies by the above three measurements, plus measurement of r_b'. However, at low frequencies, the significant base resistance is $r_b = r_b' + r_b''$ (refer to Fig. 3.18c) which is conveniently obtained by measurement of $h_{12} = r_b/r_c$, using the method of Fig. 5.3c, for example. Although, in theory, r_b'' is known from measurement of r_e' and α_0, (see Fig. 3.18b) surface recombination effects, as considered in Appendix B, can destroy this relationship so that the above method is always preferable.

The remaining three parameters C_c, r_b' and ω_α, are most conveniently measured at frequencies above the audio range. The capacity C_c is easily obtained by measurement of the reactive component of h_{22}, which (from Fig. 3.18) at frequencies somewhat below ω_α, is $j\omega(C_c + C_d) \simeq j\omega C_c$.* A bridge measuring in terms of parallel resistance and capacitance is desirable.** In some cases, it is possible to measure C_c with fair accuracy in the audio range, since here $h_{22} \simeq \frac{1}{r_c}(1 + j\omega r_c C_c)$, and $\omega r_c C_c$ may be read directly from the capacitive balance dial (if this is previously calibrated) of the GR vacuum tube bridge at the same time r_c is being measured. An exactly similar method is shown in the second footnote on page 101. If $\omega r_c C_c$ is much smaller than 0.1, however, a sharp balance is difficult to obtain for the capacitance.

A number of methods exist for determining the high-frequency base resistance r_b'. The first one to be described is not direct-reading, but can be carried out at a low frequency.***

---

*It is assumed here that C_d is considerably smaller than C_c, which may not always be the case. Pritchard (see reference 19, p. 799) shows that C_d is proportional to d-c emitter current; thus by measuring the output capacitance at zero emitter current, one obtains C_c alone.

**The bridges mentioned in footnote on page 97 are useful here, or, alternatively, the General Radio Type 821A Twin-T Impedance Measuring Circuit is convenient to use.

***See second footnote on page 101.

The voltage ratio method of Fig. 5.3c is used to measure h_{12}, where the voltage V_2 is arranged to have an adjustable phase angle, so that real and imaginary parts of h_{12} may be determined. Referring to Fig. 3.18 and the notation of Eq. (3.20), h_{12} can be written at frequencies much below ω_α:

$$h_{12} = \frac{r_b}{r_c} + j\omega r_b' C_c \qquad \text{if} \quad C_d \ll C_c$$

Thus, measurement of the imaginary part $\omega r_b' C_c$ yields r_b', if the operating frequency and C_c are known. In many cases, this measurement may be performed at 1 kc.

A second method of measuring r_b' is by the measurement of h_{11} in the common-emitter connection. From Eq. (4.9), if the frequency of measurement is such that $\omega \gg (1 - \alpha_0)\omega_\alpha$:

$$h_{11_e} \simeq r_b' + \frac{r_e'\omega_\alpha}{1.21\ j\ \omega}$$

Thus, if a bridge measuring series resistance and reactance components is used,* the resistance measured is r_b' directly.

Possibly the simplest and most direct determination of r_b' involves measurement of the reverse transfer impedance z_{12} in the common-base connection. This impedance appears explicitly in Fig. 3.6 as the portion of the T common to input and output. At frequencies such that $\omega r_c C_c \gg 1$, $z_{12} \simeq r_b'$. Thus, if a current I_c is injected into the collector, the open-circuit emitter-to-base voltage observed is $I_c r_b'$. In practice, the current I_c may be measured by noting the drop across a known resistor in the collector-base loop, as shown in the scheme of Fig. 5.5. Here, the VTVM compares the drop across the 100-ohm resistance with the drop across r_b', care being taken to insure that I_c remains constant. Since I_c must be small for linear

*For example, the General Radio 916-A (or 1606 A) r-f bridge, whose range is appropriate to this measurement.

operation, the VTVM must have high sensitivity, and, since the open-circuit emitter voltage is desired, it must also have low input capacitance. If the input impedance of the voltmeter is Z_1, the requirement for a true open-circuit voltage measurement, since the collector is actually driven from a relatively low impedance source, is:

$$|Z_1| \gg |h_{11}|$$

At high frequencies, Z_1 will be predominantly capacitive, and for a given capacitance, the above restriction puts an upper limit on the frequency at which an accurate measurement may be made.

The circuit of Fig. 5.5 may be used for a rough determination of C_c, by comparison of the emitter voltage with the voltage on the collector, the ratio of these at high frequencies being:

$$|h_{12}| \simeq \omega r_b' C_c$$

Thus, C_c may be determined from a previous measurement of r_b' and knowledge of the operating frequency.

It remains to discuss the measurement of the alpha cut-off frequency ω_α. Like r_e', this is a property of the intrinsic transistor, and does not appear isolated in the characteristics of the overall transistor. As shown in Chapter III, however, the short-circuit current gain h_{21} of the overall transistor (common-base) is very nearly alpha; from Eq. (3.12):

$$-h_{21} = \alpha + \frac{\partial s}{1 + \partial s} \qquad (5.6)$$

where $s = j\,\omega/\omega_\alpha$ and $\partial = \omega_\alpha r_b' C_c$. The second term is due to the extrinsic elements r_b' and C_c. It is a relatively simple matter to measure the cut-off frequency of h_{21}, defined as the frequency at which h_{21} is 3 db down from its low-frequency value of α_0, and denoted by ω_c. Using a simple approximation to

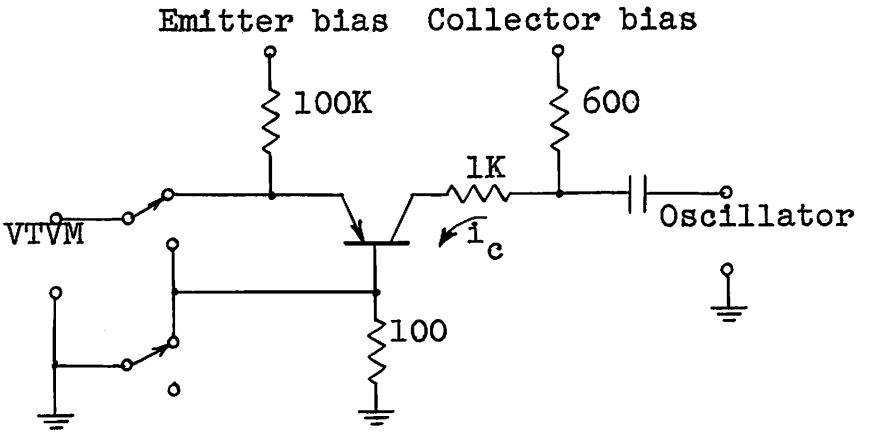

FIG. 5.5.--Circuit for measurement of r_b'.

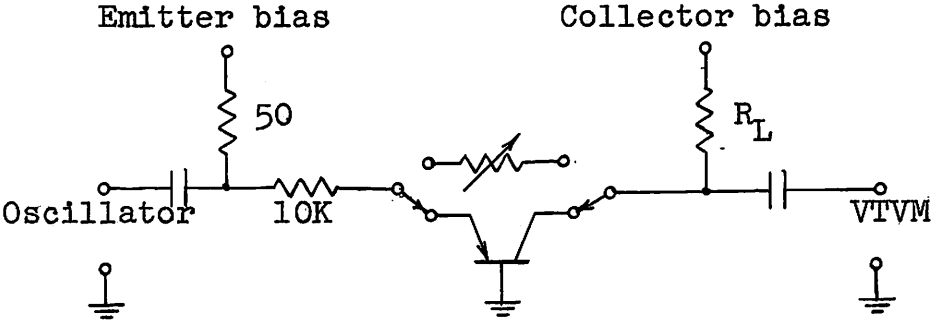

FIG. 5.6.--Circuit for measurement of ω_α.

alpha, and letting $\lambda = \omega/\omega_\alpha$, one has:

$$-h_{21} \simeq \frac{\alpha_0}{1 + j\lambda} + j\partial\lambda$$

if $\partial \ll 1$. The quantity h_{21} is 3 db down at a normalized frequency $\lambda_c = \omega_c/\omega_\alpha$, such that:

$$|h_{21}|^2 = \frac{\alpha_0^2}{2} = \left| \frac{\alpha_0 - \partial\lambda_c^2 + j\partial\lambda_c}{1 + j\lambda_c} \right|^2$$

$$\simeq \frac{\alpha_0^2 - 2\alpha_0\partial\lambda_c^2}{1 + \lambda_c^2} \qquad (5.7)$$

ignoring terms in ∂^2. Solving (5.7) for λ_c:

$$\lambda_c = \frac{\omega_c}{\omega_\alpha} = \frac{1}{[1 + 4\frac{\partial}{\alpha_0}]^{1/2}} \simeq \frac{1}{1 + 2\frac{\partial}{\alpha_0}}$$

Expressing ω_α in terms of the measured quantities ω_c, r_b', C_c, and letting $\partial_c = \omega_c r_b' C_c$, there results:

$$\omega_\alpha = \frac{\omega_c}{1 - 2\frac{\partial_c}{\alpha_0}} \simeq \omega_c \left(1 + 2\frac{\partial_c}{\alpha_0}\right) \qquad (5.8)$$

Equation (5.8) is a crude, but nonetheless useful, approximation relating the alpha, or "internal," cut-off frequency to the h_{21}, or "external," cut-off frequency. It is observed that the effect of the extrinsic elements, as expressed by ∂_c in Eq. (5.8), is to lower the apparent cut-off ω_c with respect to ω_α.

Alpha cut-off may thus be measured indirectly through measurement of ω_c, which may be accomplished by means of a scheme such as shown in Fig. 5.6.* A relatively large resistance in series with the input to the emitter simulates a current source. One then compares the transmission through the transistor with the transmission through a frequency insensitive path adjusted to have the same response at a low frequency, and observes the frequency at which the transistor response is 3 db less. The output current is measured by the drop across a small load resistance R_L, the actual current gain in this situation being:**

$$\frac{I_2}{I_1} = \frac{h_{21}}{1 + R_L h_{22}}$$

Since $h_{22} \simeq j\omega C_c$, the above quantity is very nearly h_{21} at ω_c, if $\omega_c R_L C_c \ll 1$. This puts an upper limit on R_L which is commonly of the order of 100 ohms, or less.

The arrangement of Fig. 5.6 may also be used with the transistor in the common-emitter configuration, in which case the h_{21} cut-off frequency is, from Eq. (4.9):

$$\omega_e = \frac{1 - \alpha_0}{1.21} \omega_\alpha$$

If $1 - \alpha_0$ is known, ω_α may thus be calculated. Since ω_e is considerably lower than ω_α, this measurement is often more convenient to perform. It may be done at even lower frequencies,

---

*A similar scheme incorporating a neutralizing network to balance out the forward transmission caused by r_b' and C_c, is given by R. J. Turner, "Surface-barrier transistor measurements and applications," Tele-Tech., vol. 13, August, 1954, pp. 78-79. In this manner, the second term of Eq. (5.6) is effectively eliminated, and one measures ω_α directly. However, a transformer is required, if, as is usually the case, the oscillator and VTVM both have one side grounded.

**See footnote on page 22, p. 336.

by the voltage-ratio method of Fig. 5.3b, for example, if provision is made for determining in-phase and quadrature components. The transfer admittance of the transistor with a large resistance R_b in series with the input (base) is $\frac{1}{R_b} h_{21}$. From Eq. (4.9), if $\omega << \frac{1 - \alpha_0}{1.21} \omega_\alpha$, this may be written:

$$\frac{1}{R_b} \frac{\alpha_0}{1 - \alpha_0} \left[1 - \frac{1.21}{1 - \alpha_0} j \frac{\omega}{\omega_\alpha}\right]$$

If the ratio of real and imaginary parts can be determined, and the operating frequency is known, ω_α may be calculated. This method has been successfully employed at 1 kc for audio-frequency transistors having alpha cut-offs in the vicinity of 1 MC.*

In this section, various methods have been considered which were developed, or adapted, for measurement of fundamental circuit parameters of conventional junction triodes. The work was originally done with transistors having alpha cut-off frequencies of less than 2 MC, and was later extended to the 20-MC region.

D. CONCLUSIONS

This chapter has presented the results of a program intended to develop measurement methods for the small-signal high-frequency properties of junction transistors. Measurement of the general four-pole parameters was discussed first; this work applies to any active network, and in particular to transistor types such as the tetrode which are not well represented by the equivalent circuits of this report. It was shown that the transfer admittance parameters, as well as driving-point parameters, may be measured by a transformer

*See second footnote on page 101.

ratio-arm bridge. Bridges exist for performing these measurements up to 100 MC; it is apparent that measurements to still higher frequencies will be necessary with transistors presently in development, and much work remains to be done in this region.

Measurement of the quantities in terms of which the equivalent circuits of this report are expressed, the so-called fundamental circuit parameters, was discussed. The techniques described were designed principally for junction triodes in the low radio-frequency region, and have been used successfully to about 20 MC. It is expected that some modification of the methods shown would be required for use at higher frequencies.

The work reported in this chapter is largely original and constitutes one of the contributions of this report. Some duplication with the work of other authors has occured; this has been indicated in the references.

VI. TRANSISTOR AMPLIFIER PERFORMANCE AND DESIGN

In Chapters I to IV, a number of equivalent circuits and corresponding four-pole parameters were developed which characterized the junction transistor triode in each of the three useful configurations. This work forms the principal contribution of this report and is a necessary prelude to the discussion of the behavior of the device in an external circuit environment and its properties regarding gain, bandwidth and stability, about which nothing has yet been said. In the first portion of this chapter some of these topics are treated briefly, using work which generally has been developed elsewhere, the intention being to obtain explicit results in terms of fundamental transistor circuit parameters by application of the four-pole parameters previously derived in this report. The maximum power gain obtainable from the device (at a given frequency) is considered, which leads to the possibility of instability over a certain frequency region owing to internal feedback. A useful figure of merit for some situations is the frequency at which the maximum obtainable power gain falls to unity; this point denotes the maximum oscillation frequency. For wideband, rather than single-frequency applications, no solution has yet been obtained to the problem of determining the maximum gain obtainable over a specified bandwidth. A much simplified version of this problem is considered for the case of a single stage with purely resistive terminations, which at least gives an understanding of the principal factors limiting the bandwidth. In the latter part of the chapter, two new amplifier designs are presented, bandpass and lowpass, and measurements made on experimental models are compared with the predicted results.

A. MAXIMUM AVAILABLE POWER GAIN: POTENTIAL INSTABILITY

A measure of the usefulness of any active four-terminal device intended for high-frequency amplification is the maximum power gain obtainable at a particular frequency. It is generally appropriate to consider power gain when dealing with transistors, since in contrast to pentode vacuum tubes, for example, their input impedance is relatively small and may absorb an appreciable amount of power. The available power gain is the ratio of the power available at the load terminals to the power available from the source. When the load is conjugate-matched to the output impedance (as observed with the source impedance connected at the input), and the source impedance is conjugate-matched to the input impedance (as observed with the load impedance connected), one obtains the maximum power gain possible from the device. The source and load impedances required for this condition are known as the conjugate image impedances,[29] by analogy to the concept of ordinary image impedances. It may frequently happen that, for an active network, the conjugate image impedances possess negative real parts. The implication of this is that the device has sufficient internal reverse transmission to allow it to sustain oscillations when certain passive terminations are chosen. The device is then said to be potentially unstable, and the maximum available gain becomes meaningless, since, theoretically, any desired gain may be realized.

It is interesting to determine the maximum available gain as a function of frequency for the various transistor configurations, or, where this is meaningless, determine the frequency range over which potential instability may be expected. Expressions for the maximum gain have been given by Roberts,[29] and in somewhat more convenient form, for present purposes, by Linvill.[30] The criterion for potential instability has, in addition, been stated by Stern, Aldridge and Chow.*

---

*See page 839 of reference 24.

Linvill has shown that the expression:

$$\frac{P_{00}}{P_{i0}} = \frac{|h_{21}|^2}{4h_{11_r} h_{22_r} - 2[h_{12} h_{21}]_r} \tag{6.1}$$

where h_{11_r} is the real part of h_{11}, etc., is within 3 db of the maximum available power gain, provided that:

$$C = 2 \left|\frac{h_{12}}{h_{21}}\right| \frac{P_{00}}{P_{i0}} < 1 \tag{6.2}$$

If the above inequality is not satisfied, the device is potentially unstable. Substitution of the exact h-parameters for various configurations into (6.1) and (6.2) leads to algebraically complicated expressions which are not particularly illuminating. If one chooses simplified versions of the parameters, much simpler results are achieved which do not obscure the essential behavior.

Consider the approximate common-base high-frequency parameters given in Fig. 3.18. In terms of the dimensionless quantities:

$$\partial = \omega_\alpha r_b' C_c$$

$$\lambda = \frac{\omega}{\omega_\alpha}$$

the expressions for power gain and stability factor are:

$$\frac{P_{00}}{P_{i0}} = \frac{\alpha_0}{2\partial\lambda^2} \qquad C = \frac{(1 + \lambda^2)^{1.2}}{\lambda} \tag{6.3}$$

Since $C > 1$ for any λ, the common-base configuration can be expected to be <u>potentially</u> unstable over the range for which the parameters are valid (roughly $\frac{1}{r_c C_c} \ll \omega < 2\omega_\alpha$).

For the common-emitter connection, use of the parameters of Eq. (4.10) yields the results:

$$\frac{P_{00}}{P_{i0}} = \frac{\alpha_0}{4.8\,\partial\lambda^2} \qquad C = \frac{1}{2.4}\,\frac{r_e'}{r_b'}\,\frac{1}{\lambda} \tag{6.4}$$

Unconditional stability is thus obtained when $\lambda > \frac{r_e'}{2.4 r_b'}$, which, for typical values, is about 0.1. Since the parameters used are not valid much below $\lambda = 0.1$, stability in this region should be investigated by using the more complete parameters of Eq. (4.9).

In the common-collector situation (see Eq. 4.14) the gain and stability factors are:

$$\frac{P_{00}}{P_{i0}} = \frac{1}{4.8\,\partial\,\lambda^2} \qquad C = \frac{1}{2\partial\lambda} \tag{6.5}$$

Since ∂ is typically of the order of 0.1, potential instability exists over the entire useful high-frequency region. It should be noted that the instability referred to simply implies that it is possible to find passive terminations which will make the device oscillate; its operation in typical amplifier circuits, particularly in the wideband case, may be perfectly stable.

Since the common-base and common-collector configurations are potentially unstable in the high-frequency region, the expressions derived above for power gain are not particularly meaningful. Pritchard* has given an equation for the maximum available power gain which results when the source impedance is constrained to be purely resistive. Under this condition, all configurations are stable (for the particular transistor model considered in this report), and the resulting gain expressions are:

---

*See p. 1076 of the reference given in the second footnote on page 51.

Common-base:

$$G_{av} = \frac{\alpha_0}{\partial\lambda^2 \left(1 + 2.4 \left[1 + \lambda^2\right]^{1/2}\right)} \tag{6.6}$$

Common-emitter:

$$G_{av} = \frac{\alpha_0}{2.4\ \partial\lambda^2 \left\{1 + \left[1 + \left(\frac{r_e'}{1.2 r_b' \lambda}\right)^2\right]^{1/2}\right\}} \tag{6.7}$$

Common-collector:

$$G_{av} = \frac{1}{2.4\ \partial\lambda^2 \left\{1 + \left[1 + \left(\frac{r_e'}{1.2 r_b' \lambda}\right)^2\right]^{1/2}\right\}} \tag{6.8}$$

If r_e'/r_b' is small, and λ of order unity, the common-emitter gain above becomes approximately equal to the maximum gain of Eq. (6.4), and, in terms of f_α, r_b' and C_c, is:

$$G \simeq \frac{\alpha_0}{30 f^2} \frac{f_\alpha}{r_b' C_c} \tag{6.9}$$

which is essentially the same expression which has been derived elsewhere.*

Another figure of merit pertaining to high-frequency power gain has been developed by Mason.[32] If the device is made unilateral (neutralized) by means of a lossless passive external network, which can always be done at a particular frequency, the available power gain of the resulting structure is shown to be:

$$U = \frac{\left|y_{21} - y_{12}\right|^2}{4\left(y_{11_r} y_{22_r} - y_{12_r} y_{21_r}\right)} \tag{6.10}$$

---

*R. L. Pritchard, "High-frequency power gain of junction transistors," Proc. IRE, vol. 43, p. 1078. See also J. M. Early, reference 4, p. 519. See also reference 31.

where the y's are the short-circuit admittance parameters of the device alone. The quantity U has the interesting property of being independent of the choice of the (lossless) neutralizing network, and is invariant under permutations of the three device terminals. Thus, in the transistor case, U is identical for the three configurations being considered, and need only be calculated for one. Further, the frequency at which U becomes unity (supposing U to decrease with increasing frequency) is the frequency above which a power gain greater than unity cannot be obtained from the device in any external (passive) environment. This critical frequency has been termed the maximum oscillation frequency f_{max}, since it is apparent that the transistor cannot be made to oscillate above f_{max}. Since this frequency may be measured fairly readily, it is useful to have an expression relating it to the transistor parameters.[33] A simple and sufficiently accurate result is achieved by use of the approximate common-base y-parameters of Eq. (3.26). Substitution in (6.10) yields:

$$U = \frac{\alpha_0}{4\,\partial\lambda^2} \simeq \frac{\alpha_0}{25\,f^2}\,\frac{f_\alpha}{r_b' C_c} \tag{6.11}$$

and, setting $U = 1$, $f = f_{max}$, results in

$$f_{max} = f_\alpha \left(\frac{\alpha_0}{4\partial}\right)^{1/2} = \left(\frac{\alpha_0 f_\alpha}{25\, r_b' C_c}\right)^{1/2} \tag{6.12}$$

If $\partial = 0.1$, as is typical, $f_{max} \simeq 1.55\, f_\alpha$, which means that useful power gain can not generally be achieved much beyond the alpha cut-off frequency. These relations do not, of course, apply down to very low frequencies; here U is limited by the low-frequency parameters, which have been largely ignored in the above calculation.

The expression for U given above is essentially the same as that derived by Guillemin, Statz and Pucel.* (Note that it has a form similar to the maximum available gain expressions previously derived, and increases with decreasing frequency at the rate of 6 db per octave.) It is to be emphasized, however, that these formulas represent single-frequency gain, where driving point reactances may be tuned out as desired. If a particular transistor is found to have 10 db available gain at 10 MC, it does not necessarily follow that 10 db gain can be obtained over a band with this frequency as its upper limit, say from 5 to 10 MC. For example, a large capacitance shunting the output terminals has no effect on the single-frequency gain, but can be expected to limit bandwidth considerably. The problem of determining the maximum gain obtainable uniformly over a specified bandwidth is an exceedingly complex one, and cannot be considered within the scope of this report. In the next section, however, the gain-vs-frequency characteristics of simple single-stage resistance-terminated amplifiers are derived, which give a preliminary understanding of the problem and some insight into transistor gain-bandwidth relationships.

B. SINGLE-STAGE RESISTANCE-TERMINATED AMPLIFIERS

It is desired to calculate the gain-vs-frequency characteristic of the simple configuration shown in Fig. 6.1, where the network H represents a transistor in any configuration. The definition of gain chosen is the ratio of actual power in the load $\frac{I_2^2}{G_L}$ to available power from the generator $\frac{V_g^2}{4R_G}$. This definition, known as transducer gain G_t, takes into account the efficiency of the transistor input circuit in making use of the power available at the source. Straightforward manipulation yields G_t in

*See reference 15, p. 1626.

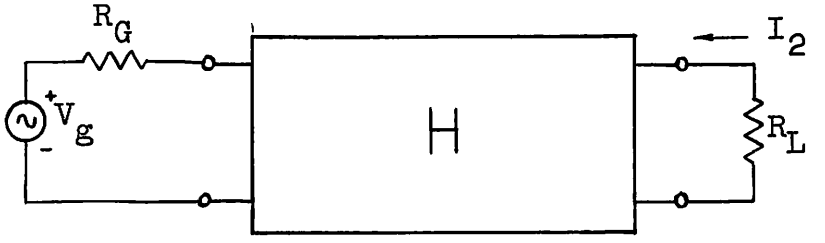

FIG. 6.1.--Resistance-terminated amplifier.

terms of the h-parameters of the network H:

$$G_t = 4R_G G_L \left| \frac{h_{21}}{(h_{11} + R_G)(h_{22} + G_L) - h_{12}h_{21}} \right|^2 \qquad (6.13)$$

For the common-base configuration, use of the h-parameters of Eq. (3.24) results in:*

$$G_t = G_0 \, |A(p)|^2$$

where:

$$G_0 = \frac{4 \, \alpha_0^2 \, R_L \, R_G}{(R_g + r_h)^2}$$

$$A(p) = \frac{1}{1 + \left[\frac{1}{F_1 \omega_\alpha} + \frac{R_L C_c}{F_2}\right] p + \frac{R_L C_c}{F_1 \omega_\alpha} p^2}$$

$$F_1 = \frac{R_G + r_h}{R_G + 1.21 r_b'} \qquad F_2 = \frac{R_G + r_h}{R_G + r_e' + r_b'}$$

$$p = j\omega \text{ (in the steady-state case)} \qquad (6.14)$$

*A similar expression has been given by J. M. Mathias, "Common-base transistor equivalent circuits for wideband amplification," TR-No. 94, Contract N6onr 251(07), Stanford University (Electronics Research Laboratory), December 12, 1955.

The expression above is valid for $R_L \ll r_c$ and $\omega \gg \frac{1}{r_c C_c}$.

The low-frequency gain G_0 can be made large by making R_L large (provided $R_L \ll r_c$), and is maximized by making $R_g = r_h$. This situation corresponds to the equivalent circuit of Fig. 3.9a. For large R_L, $R_L C_c \gg \frac{1}{\omega_\alpha}$, and from the expression for A(p), the 3-db bandwidth is seen to be $B = \frac{F_2}{R_L C_c}$, approximately. Here, the frequency cutoff is caused almost entirely by the collector capacitance C_c, modified by the factor F_2, which can be identified as the low-frequency return difference of the circuit of Fig. 3.9b.* If this bandwidth is specified in advance, then R_L is determined by $R_L = \frac{F_2}{BC_c}$, and the gain G_0 becomes:

$$G_0 = \frac{4\alpha_0{}^2 F_2 R_G}{(R_G + r_h)^2 BC_c} = \frac{4\alpha_0{}^2 R_G}{(R_G + r_h)(R_G + r_e' + r_b')BC_c}$$

In this situation, G_0 is maximized by choosing $R_G = [r_h(r_e' + r_b')]^{1/2}$, and the resulting maximum gain-times-bandwidth product can be written:

$$G_{0\,\max} B = \frac{4\alpha_0{}^2}{(r_e' + r_b')C_c} \frac{1}{[1 + (\frac{r_h}{r_e' + r_b'})^{1/2}]^2} \qquad (6.15)$$

The corresponding value of F_2 is:

$$F_2 = (\frac{r_h}{r_e' + r_b'})^{1/2} \qquad (6.16)$$

---

*See D. E. Thomas, footnote on page 54.

If r_e' is made small, then the following approximate expression results:

$$G_{0\ max}\, B \simeq \frac{4\alpha_0^2}{r_b' C_c} \tag{6.17}$$

It should be noted that this product, which is a constant depending only on the transistor parameters, applies only to the low-pass case,* and for bandwidths somewhat less than $F_2\omega_\alpha$. Also, it represents a power gain times bandwidth in distinction to the usual voltage gain-bandwidth product which is defined for conventional vacuum tube pentodes.

For small load resistances such that $R_L C_c \ll \frac{1}{\omega_\alpha}$, the bandwidth given by Eq. (6.14) approaches $F_1\omega_\alpha$, which is attained as $R_L \to 0$. A good approximation for small R_L is:

$$B = \frac{F_1\omega_\alpha}{1 + \frac{F_1}{F_2}\omega_\alpha R_L C_c}$$

To attain maximum bandwidths, F_1 can be made unity by letting $r_h = 1.21\, r_b'$. The maximum gain which can be achieved for bandwidths close to ω_α then becomes:

$$G_{0\ max} \simeq \frac{1.6\ \alpha_0^2}{\omega_\alpha r_b'\ C_c}\ \left(\frac{\omega_\alpha}{B} - 1\right) \tag{6.18}$$

For typical values of α_0 and $\omega_\alpha r_b' C_c$, $G_{0\ max}$ falls to unity when $B \simeq 0.95\ \omega_\alpha$. The pure-resistance-loaded circuit is very inefficient in this region, and considerable improvement can be effected by the use of reactive elements.

---

*For the neutralized common-base bandpass amplifier described later, a similar power gain-bandwidth product exists.

In the common-emitter configuration, attention will be confined to the frequency range above $(1 - \alpha_0)\omega_\alpha$, where the approximate h-parameters of Eq. (3.10) may be used. Substitution in Eq. (6.13) yields for the transducer gain:

$$G_t = G_0 \, |A(p)|^2$$

$$G_0 = \frac{4\alpha_0^2 R_G R_L}{r_e'^2}$$

$$A(p) = \frac{1}{1 + \left[\frac{1}{F_3\omega_\alpha} + \frac{R_L C_c}{F_4}\right] p + \frac{R_L C_c}{F_3\omega_\alpha} p^2}$$

$$F_3 = \frac{r_e'}{1.21\ (r_b' + R_G)} \qquad F_4 = \frac{r_e'}{r_e' + \alpha_0(r_b' + R_G)} \tag{6.19}$$

It is interesting to note the similarity to the common-base circuit in the form of A(p). (cf Eq. 6.14) Consider the situation for large R_L, where $\omega_\alpha R_L C_c >> 1$. (Note that F_3 and F_4 are generally quite closely equal.) The 3-db bandwidth is $B = \frac{F_4}{R_L C_c}$. Substituting for R_L in G_0, one is tempted to conclude that for maximum gain at a specified bandwidth, $R_G >> r_b'$. This is misleading, however, since F_4 then becomes small, and, to maintain B, R_L must be small rather than large, as originally assumed. A point is soon reached where the bandwidth is controlled by the $F_3\omega_\alpha$-term. It seems most efficient to choose $R_L = \frac{1}{\omega_\alpha C_c}$, so that alpha cut-off and collector capacitance play an approximately equal part in limiting the bandwidth. Assuming for simplicity that $F_4 \simeq F_3$, the bandwidth is then nearly $B = \frac{F_3\omega_\alpha}{2}$. Substitution in the expression for G_0 yields:

$$G_0 \simeq \frac{\alpha_0^2 R_G \omega_\alpha}{1.46 (r_b' + R_G)^2 C_c B^2}$$

For a given B, G_0 is maximized when $R_G = r_b'$:

$$G_{0\,max} \simeq \frac{\alpha_0^2}{5.8 \omega_\alpha r_b' C_c} \left(\frac{\omega_\alpha}{B}\right)^2 \qquad (6.20)$$

The relation above applies only up to $B = \frac{\omega_\alpha}{2}$ at most.

In this section equations have been developed for the power gain of simple common-base and common-emitter amplifiers. The frequency dependence has been brought out explicitly in order to examine the factors influencing the bandwidth. In each case, the controlling time constants are essentially $\frac{1}{\omega_\alpha}$ and $R_L C_c$, modified by factors (depending upon the source resistance) which express the effect of internal reverse transmission in the transistor.

C. BANDPASS AMPLIFIER DESIGN EXAMPLE

To illustrate the use of the approximate equivalent circuits and h-parameters developed earlier in this report, consider the design of a bandpass (IF) type of amplifier, with simplicity being an important requirement. The shape of the passband is controlled largely by the external coupling circuits, and, to keep design and alignment problems at a minimum, it is convenient to neutralize the transistor, thus avoiding interaction between stages.* One of the simplest procedures, which also results in an overall equivalent circuit of easily handled form, is due to Angell and Keiper.[34] The circuit, which provides neutralization over a wide band of frequencies, is shown in Fig. 6.2, together

*A wide variety of neutralizing procedures are possible by associating external networks with the transistor in various ways. A discussion of these procedures has been given by Stern, Aldridge, and Chow, reference 24. See also G. Y. Chu, "Unilateralization of junction-transistor amplifiers at high frequencies," Proc. IRE, vol. 43, August 1955, pp. 1001-1006; and C. C. Cheng, "Neutralization and unilateralization," Trans. IRE, PGCT, June, 1955, pp. 138-145.

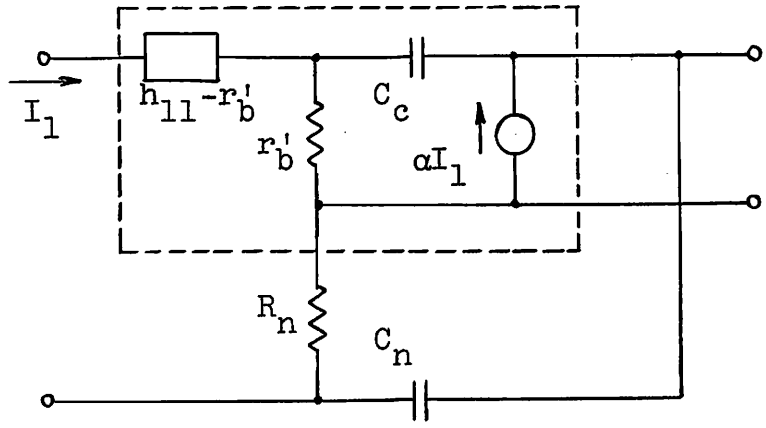

$$R_n C_n = r'_b C_c$$

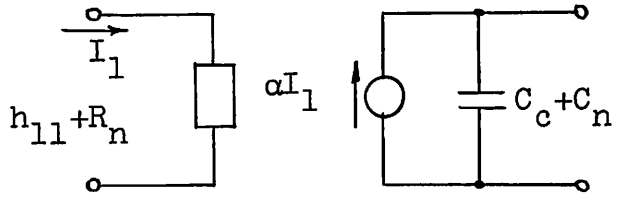

FIG. 6.2.--Neutralized common-base configuration, and approximate equivalent circuit.

with the resultant equivalent circuit in approximate form. The common-base representation of Fig. 3.11 has been employed for convenience.

If the frequency range of interest lies somewhat below the alpha cut-off frequency, the magnitude of alpha is nearly α_0, and, if one can ignore the small phase shift, α may be replaced by α_0. Further, the transistor may be biased so that h_{11} appears to be approximately a constant resistance r_{11}. With these simplifications, a suitable coupling circuit immediately suggests itself. A transformer is required to obtain gain, and for isolation, since input and output terminals no longer have one terminal in common. Referring to Fig. 6.3, and assuming a transformer with unity coupling, one chooses the primary inductance L_m to resonate with $C_c + C_n$ at band center. Damping of this tuned circuit to provide the required bandwidth is provided entirely by the reflected input resistance of the next stage.

The properties of this particular configuration are readily determined. The insertion power gain of one stage, at band center, is simply:

$$G = \left(\frac{I_1'}{I_1}\right)^2 = \alpha_0^2 \, n^2 \qquad (6.21)$$

The shape of the response is that of a single tuned circuit, the bandwidth (in radians) between 3-db points being:[35]

$$B = \frac{1}{RC} = \frac{1}{n^2 \, (r_{11} + R_n)(C_c + C_n)}$$

It is apparent that, for maximum B, the product $(r_{11} + R_n)$ $(C_c + C_n)$ should be as small as possible. By using the constraint that $R_n C_n = r_b' C_c$ for neutralization, one finds that, for maximum B, R_n should be chosen to be $(r_{11} r_b')^{1/2}$, and the resultant

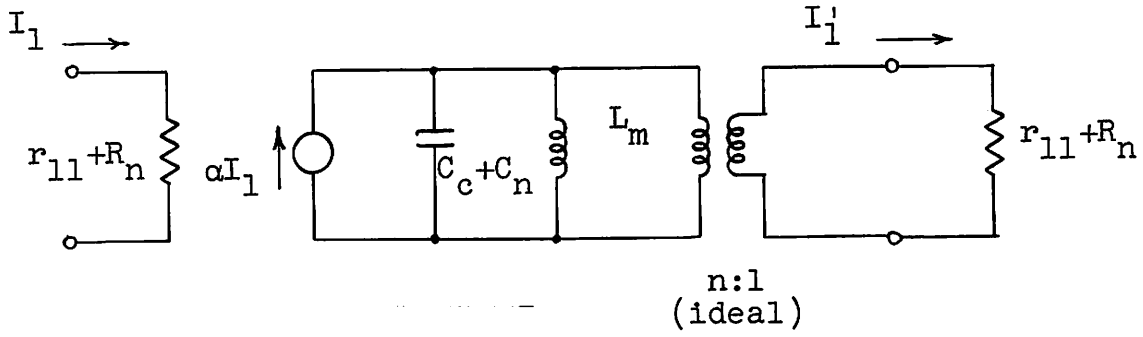

FIG. 6.3.--Single-tuned transformer-coupled interstage.

maximum B is:

$$B = \frac{1}{n^2 \left[r_{11}^{1/2} + r_b'^{1/2}\right]^2 C_c} \tag{6.22}$$

From (6.21) and (6.22), a power gain-bandwidth product exists which is independent of n:

$$GB = \frac{\alpha_0^2}{\left[r_{11}^{1/2} + r_b'^{1/2}\right]^2 C_c} \tag{6.23}$$

This expression holds also for the low-pass situation, where $L_m \to \infty$, and may be compared with the gain-bandwidth product of a common-base stage without neutralization, as given by Eq. (6.17) (which holds only for bandwidths considerably less than ω_α). If r_{11} is somewhat smaller than r_b', the price paid for neutralization is approximately a factor of four in power gain-bandwidth product. This is jointly caused by loss of power in R_n and restriction of bandwidth because of the addition of C_n.

As a practical matter, it is not possible to build a transformer with unity coupling. Some leakage inductance L_e is always present, shown in Fig. 6.4, which may be used to improve the gain-bandwidth product, as consideration of Fig. 6.5 will show. Here, a capacitance C_2 is placed in series with the transformer secondary and chosen so that its reflected equivalent capacitance in the primary resonates with L_e at band center; thus:

$$\omega_0^2 = \frac{1}{L_m C_1} = \frac{1}{L_e C_2'} \tag{6.24}$$

Under this condition, a lowpass equivalent circuit[36] exists, shown in Fig. 6.5b, and the bandwidth, as calculated from this circuit, is the same as the bandwidth of the original circuit. Straightforward calculation yields for the transfer function of the circuit of Fig. 6.5b:

$$\frac{I_{out}}{I_{in}} = n \frac{1}{L_e C_1 p^2 + R_2' C_1 p + 1} \tag{6.25}$$

The capacitance C_1 depends on the transistor, and, once the gain n has been selected, R_2' is fixed. The inductance L_e may be chosen almost arbitrarily, depending upon the desired shape of the response. Attention will be restricted here to the "maximally flat" case,[37] where the transfer function in terms of the bandwidth B has the form:

$$\frac{1}{\frac{p^2}{B^2} + \sqrt{2}\,\frac{p}{B} + 1}$$

Comparing coefficients with Eq. (6.25), one finds:

$$L_e C_1 = \frac{1}{B^2}$$

$$B = \frac{\sqrt{2}}{R_2' C_1} \tag{6.26}$$

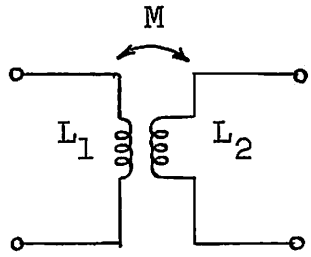

$$k = \frac{M}{\sqrt{L_1 L_2}}$$

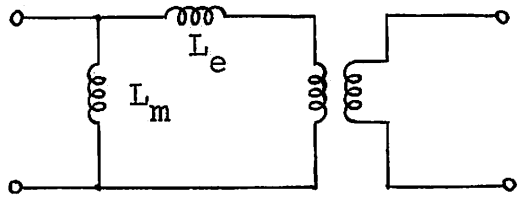

n:1
ideal

$$L_1 = L_m$$

$$L_2 = \frac{L_m + L_e}{n^2}$$

$$k^2 = \frac{L_m}{L_m + L_e}$$

$$L_m = L_1$$

$$L_e = L_1 \frac{1 - k^2}{k^2}$$

$$n = \frac{1}{k}\sqrt{\frac{L_1}{L_2}}$$

FIG. 6.4.--Actual transformer and equivalent circuit.

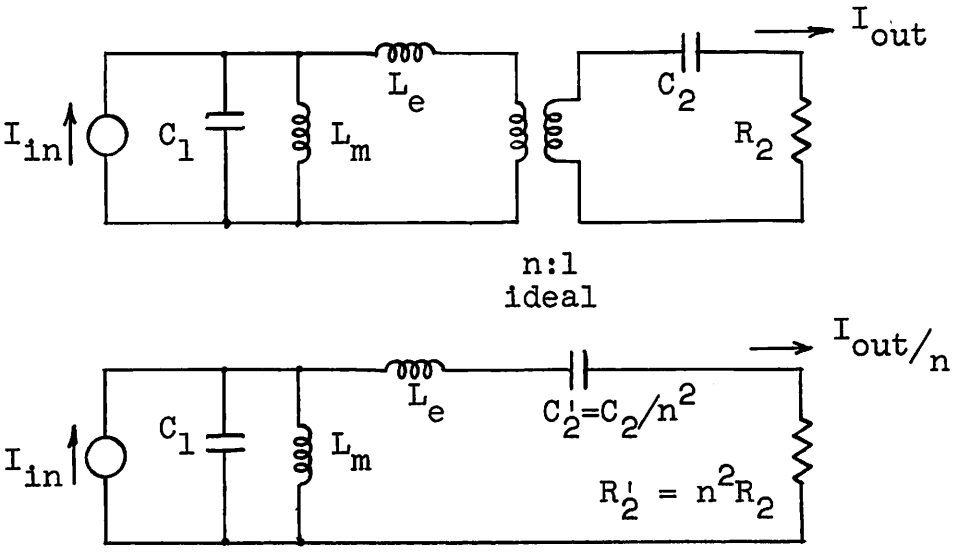

a. Equivalent circuits.

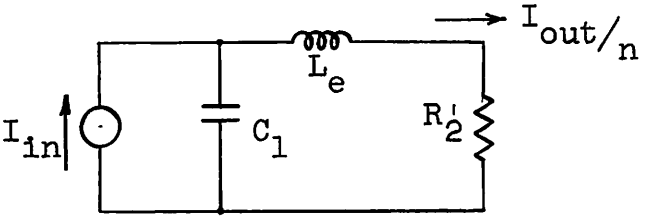

b. Lowpass equivalent, if $L_mC_1=L_eC_2'$.

FIG. 6.5.--Double-tuned transformer-coupled interstage.

The bandwidth here, and the power gain-bandwidth product, is $\sqrt{2}$ times as large as that of the single-tuned circuit previously considered. See Eqs. (6.22) and (6.23).

Using Eqs. (6.24), (6.26), and the transformer relations given in Fig. 6.4, the transformer constants L_1, L_2, and k can be expressed in terms of the bandwidth B, center frequency ω_0, capacitance $C_1 = C_c + C_n$ and resistance $R_2 = r_{11} + R_n$:

$$L_1 = \frac{1}{\omega_0^2 C_1}$$

$$k = \frac{B/\omega_0}{(1 + B^2/\omega_0^2)^{1/2}}$$

$$L_2 = R_2 \frac{1 + B^2/\omega_0^2}{\sqrt{2}\, B} \qquad (6.27)$$

The effective turns ratio of the transformer, giving its current gain at center frequency, is:

$$n = \frac{2^{1/4}}{(R_2 C_1 B)^{1/2}} \qquad (6.28)$$

Finally, the capacitance C_2 to be placed in series with the transformer secondary, is given by using (6.24), (6.26) and (6.28):

$$C_2 = n^2 C_1 \frac{B^2}{\omega_0^2} = \frac{\sqrt{2}}{R_2} \frac{B}{\omega_0^2} \qquad (6.29)$$

Equations (6.27), (6.28) and (6.29) give design information for the interstage in terms of the center frequency and bandwidth, and the transistor parameters (including the neutralizing network).

An example of a specific design will now be given. The Philco SB-100 surface-barrier transistor was chosen because of its large gain-bandwidth product (as given by Eq. 6.23), and its relatively high alpha cut-off frequency of about 50 MC. In order to stay reasonably well below this frequency, the center frequency of the amplifier was selected to be 20 MC. By biasing the transistor to approximately 1.5 ma emitter current, it was found possible to maintain the real part of h_{11} (which is r_{11}) at a nearly constant value of 50Ω for a considerable range around this frequency. (The imaginary part of h_{11} is much smaller than the reactance of C_2 in a typical case.) The important transistor parameters are:

$$\alpha_0 = 0.95$$

$$r_{11} = 50\Omega$$

$$r_b' = 150\Omega$$

$$C_c = 5\ \mu\mu f \qquad (6.30)$$

Application of the gain-bandwidth formula (6.23), multiplied by $\sqrt{2}$ for the double tuned interstage, results in a figure of 109 MC, if B is expressed in MC. Thus, if a bandwidth of 6 MC is desired, for example, the power gain realized will be about 18, or 12.6 db. This figure refers to one stage. More gain may be obtained by cascading stages at the expense of some bandwidth shrinkage. Each stage (for the maximally flat design considered) provides a selectivity curve identical with that of a "flat-staggered pair" of conventional single-tuned vacuum tube stages, and the bandwidth shrinkage entailed by cascading has been given by Valley and Wallman.*

---

*See page 187 of reference 35.

A design of three stages with an overall bandwidth of 6 MC was decided upon. Assuming identical stages,* the bandwidth shrinkage factor is 0.71, so that each stage must have a bandwidth of 8.45 MC. Accordingly, a power gain of 109/8.45 = 12.9, or about 11 db per stage, can be expected. From the transistor parameters of Eq. (6.30), the most efficient neutralizing network is $R_n = 87\Omega$ and $C_n = 8.6$ μμf. The important design parameters are thus (using the nearest standard resistance value of 82Ω for R_n):

$$R_2 = r_{11} + R_n = 132\Omega$$

$$C_1 = C_c + C_n = 14.2 \text{ μμf}$$

$$\omega_0 = 2\pi \times 20 \times 10^6$$

$$B = 2\pi \times 6 \times 10^6$$

Substitution of these quantities in Eqs. (6.27) and (6.29) yields for the interstage parameters:

$$L_1 = 4.47 \text{ μhy}$$

$$L_2 = 2.08 \text{ μhy}$$

$$k = 0.389$$

$$C_2 = 36 \text{ μμf} \qquad (6.31)$$

A two-winding air-core transformer having the above specifications is easily realized by making both windings a single layer of wire

---

*Although not immediately apparent, calculation shows that, in this case, conventional "stagger-tuning" techniques lead to a lower overall gain-bandwidth product than can be achieved by simply making the stages identical.

of a single winding pitch on a common cylindrical form. For this situation, convenient design curves exist,[38] and the resulting transformer configuration is shown in Fig. 6.6, along with the amplifier schematic diagram.

The interstage parameters of Eq. (6.31) were selected by measurement to be close to the design values, no provision for adjustment being made. The neutralizing capacitor C_n was made adjustable so that nearly exact neutralization could be obtained. The neutralizing procedure consisted simply of applying a signal generator to the amplifier output, and observing the reverse transmission by means of a sensitive receiver at the input terminals. The neutralizing capacitors were then adjusted for minimum transmission, which resulted in a nearly complete null. It was observed that neutralization was substantially complete at any frequency within the band of interest.

The collector capacitance C_c of the transistors is actually somewhat less than the assumed value of 5 μμf; hence both the neutralizing capacitance C_n and $C_1 = C_c + C_n$ are less than their design values. In order to bring C_1 up to the required amount, a small trimming capacitor was added across the transformer primary, and adjusted to tune to band center with the primary inductance L_1. No other tuning was done on the amplifier, the resonance of L_2 and C_2 being dependent on the accuracy of their measured values.

The measured amplitude response vs frequency is shown in Fig. 6.7, along with the theoretical response. The measured 3-db bandwidth was 5.8 MC, and the gain realized at center frequency was 30 db, which is 3 db less than the predicted value. In view of the approximate nature of the transistor equivalent circuit, and the lack of complete tuning adjustments, this agreement is considered quite satisfactory. In fact, it is believed that the results justify the use of the approximate equivalent circuit, and that the design shown is useful for practical amplifiers.

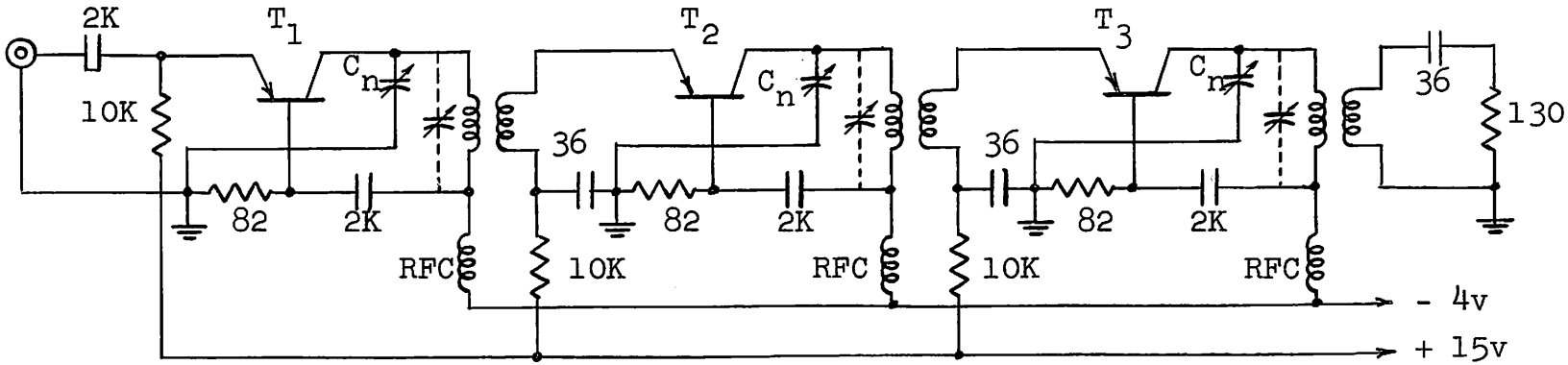

Values in ohms, μμf

C_n = 5-12 μμf

RFC = 10 μhy

T_1, T_2, T_3 SB-100 transistors

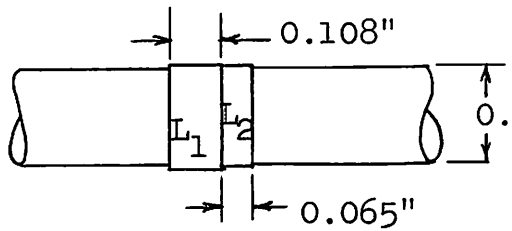

L_1 = 4.47 μhy

L_2 = 2.08 μhy

k = 0.389

No. 38 close wound

Transformer detail

FIG. 6.6.--Bandpass amplifier schematic.

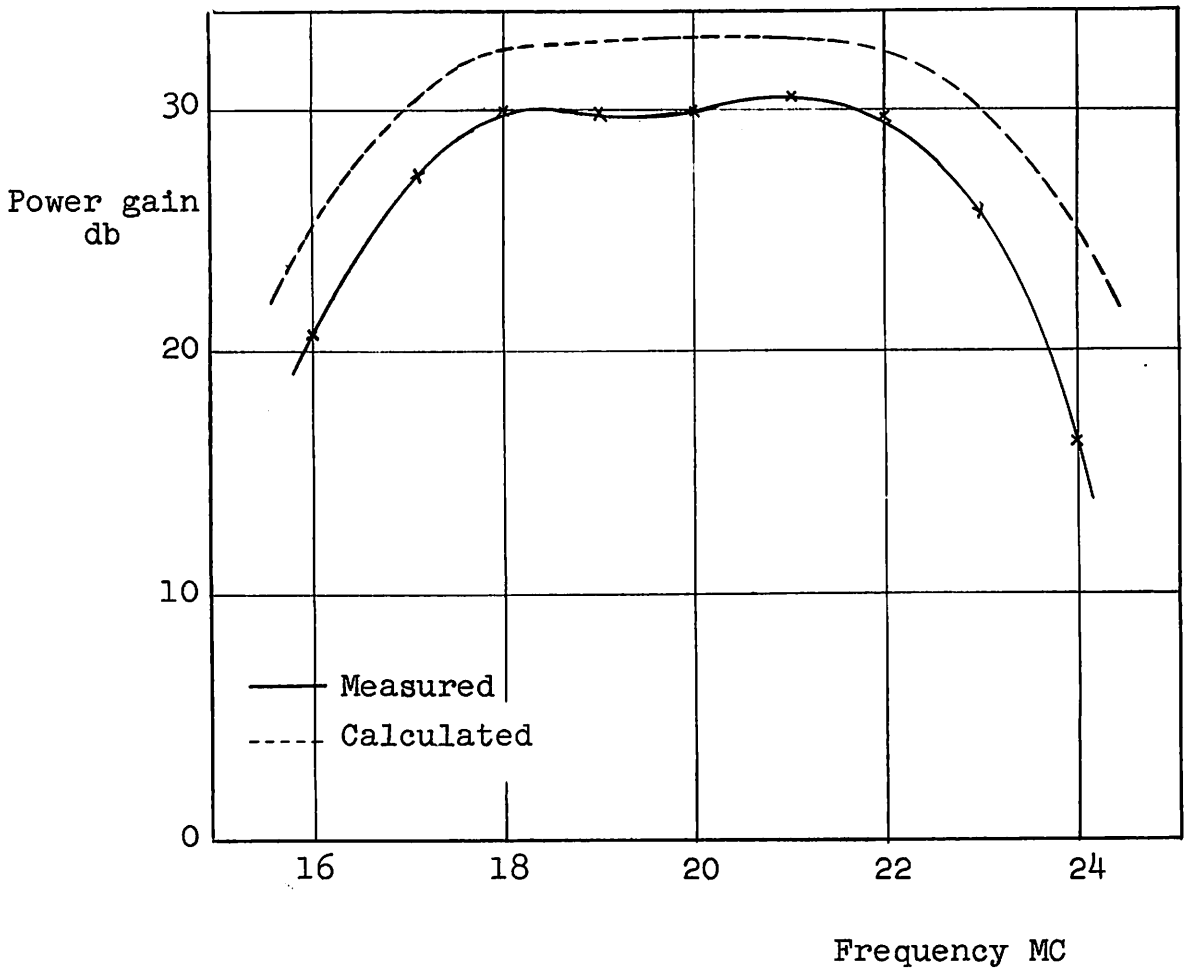

FIG. 6.7.--Bandpass amplifier frequency response.

D. LOWPASS AMPLIFIER DESIGN EXAMPLE

In the design of a video amplifier, where response essentially down to d-c is required, thereby excluding transformer coupling, one is constrained to use the common-emitter configuration if more gain is required than can be obtained in one stage. This situation prevails because no other arrangement gives an increase in gain when several stages are directly cascaded. It may be desirable, however, to use other configurations in conjunction with the common-emitter. For example, it will be shown that a common-collector stage driving a common-emitter stage gives a greater gain-bandwidth product than a pair of common-emitter stages.

Consider a series of identical cascaded common-emitter stages, as shown in Fig. 6.8.* The analysis will make use of the equivalent circuit of Fig. 4.3b, redrawn in Fig. 6.9a, where the feedback resistance $2r_c$ and the output resistance $2(1 - \alpha_0)r_c$ have been neglected because of the small load resistance R_L necessary for wideband operation. The frequency range is sufficiently below ω_α that y'_{21} can be written as a real constant α_0/r'_e. The remaining feedback element C_c can be taken into account in an approximate manner analogous to the treatment of the "Miller effect" in vacuum tubes. Figure 6.9b shows an approximate equivalent to Fig. 6.9a, the principal effect being the addition of a "Miller" capacitance at the input.

Relations for gain and bandwidth may now be obtained for one stage of the iterated structure of Fig. 6.8. The stage is driven from a current generator in parallel with R_L, and the capacitance C_c across R_L may be ignored to a good approximation. If $R_L \ll r'_b + \frac{r'_e}{1 - \alpha_0}$ (which is generally a fair approximation at optimum R_L for most transistors), the equivalent circuit for

---

*For the ideas leading to the analysis of this situation, the author is indebted to Georg Bruun, "Common-emitter transistor video amplifiers," a report issued by Stanford Research Institute, Menlo Park, California.

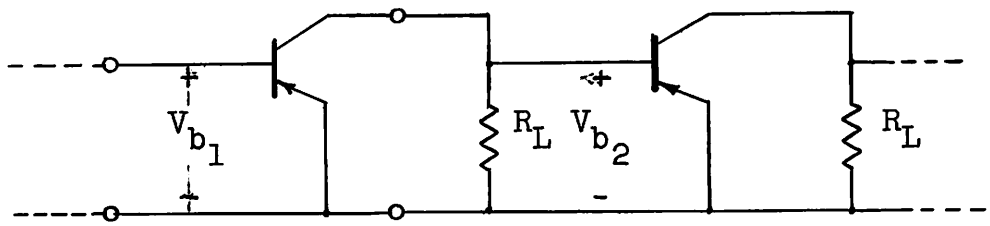

FIG. 6.8.--Cascaded common-emitter amplifier.

the output of one stage and input to the next reduces to that of Fig. 6.10. For purposes of calculating the "Miller" capacitance, the load on the transistor is assumed to be purely R_L, which is not strictly true but still yields useful results.

Referring to Fig. 6.10, consider the voltage ratio $V_{b_2'}/V_{b_1'}$, which in the iterative structure is equal to the ratio V_{b_2}/V_{b_1}. The magnitude of this ratio, which will be referred to as the stage gain, is (at low frequencies):

$$A = \alpha_0 R_L / r_e' \tag{6.32}$$

The 3-db bandwidth (in radians) is readily obtained as:

$$B = \frac{\omega_\alpha r_e'}{(R_L + r_b')(1.21 + \alpha_0 \omega_\alpha R_L C_c)} \tag{6.33}$$

The product of the two quantities above is independent of r_e', and is maximized by choosing:

$$R_L = \left[\frac{1.21 r_b'}{\alpha_0 \omega_\alpha C_c}\right]^{1/2} \tag{6.34}$$

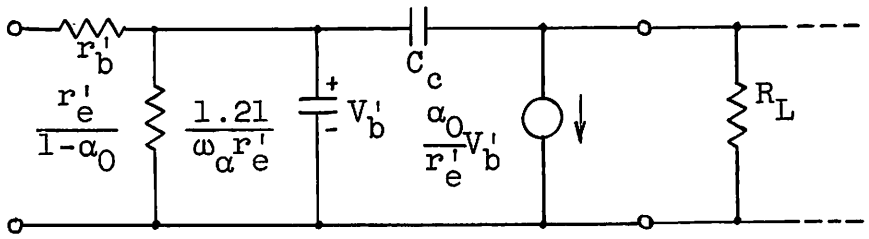

a.

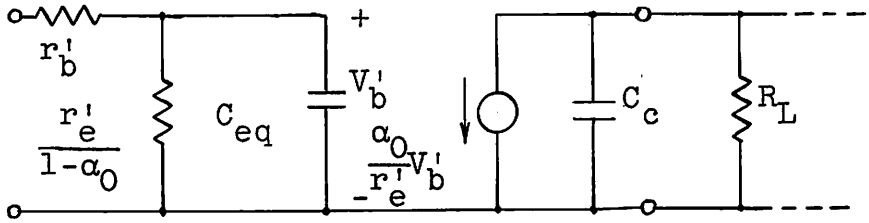

$$C_{eq} = \frac{1.21 + \alpha_0 \omega_\alpha R_L C_c}{\omega_\alpha r'_e}$$

b.

FIG. 6.9.--Common-emitter equivalent circuits.

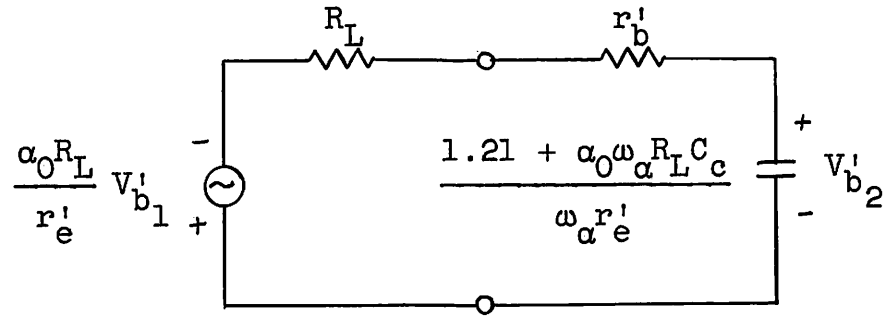

FIG. 6.10.--Equivalent circuit for one interstage of Fig. 6.8.

in which event:

$$AB_{max} = \frac{\alpha_0 \omega_\alpha}{1.21 \left[1 + \left(\frac{\alpha_0 \omega_\alpha r_b' C_c}{1.21} \right)^{1/2} \right]^2} \qquad (6.35)$$

It is to be noted that the optimum value of R_L, given by (6.34) above, is a function solely of the fixed transistor parameters ω_α, r_b' and C_c. The desired gain is obtained by adjusting r_e' in accordance with Eq. (6.32), which may be done by varying the d-c emitter current.

It is interesting to compare the figure of merit of Eq. (6.35) with one obtained when ideal transformer coupling is used between stages. The analysis given in section B of this chapter suggests that for maximum transducer gain at a given bandwidth, the source resistance should be r_b' and the load resistance $1/\omega_\alpha C_c$. This situation can be realized approximately as shown in Fig. 6.11, where an ideal transformer with appropriate turns ratio is assumed. Rewriting the expression for power gain (Eq. 6.20) in terms of the voltage gain per stage in an iterative structure, one finds:

$$AB = \frac{\alpha_0 \omega_\alpha}{4.8 \, (\omega_\alpha r_b' C_c)^{1/2}} \qquad (6.36)$$

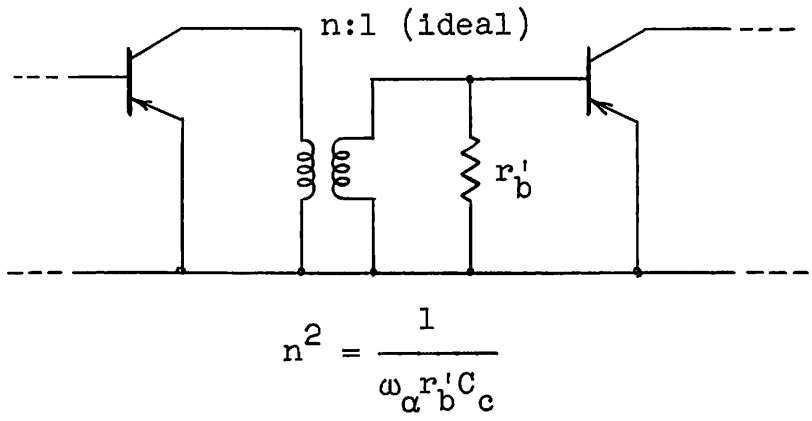

FIG. 6.11.--Transformer-coupled common-emitter stage.

Equations (6.35) and (6.36) have been plotted as a function of $\delta = \omega_\alpha r_b' C_c$ in Fig. 6.12 (for α_0 nearly unity), where it is seen that the advantage resulting from the use of a transformer is considerable for small values of δ. In a practical case, however, transformer coupling would generally be excluded because of inadequate low-frequency response.

Consider now the situation shown in Fig. 6.13, where a common-collector (CC) stage drives a common-emitter (CE) stage, a complete amplifier being built up by cascading such pairs of stages. This procedure is suggested by examining the CE equivalent circuit of Fig. 6.9b. It is apparent that to achieve a large bandwidth, a low source impedance is required, which is provided by the CC stage. A brief analysis will be made of the CC-CE pair, and its performance compared tothat of a pair of CE stages. Considering the pair to be a unit in an iterated structure, and combining Figs. 6.9b and 4.5a, one may draw the equivalent circuit of Fig. 6.14. The transistors are assumed to have identical characteristics, except for r_e' which can be controlled by the d-c emitter current. Upon analysis of this

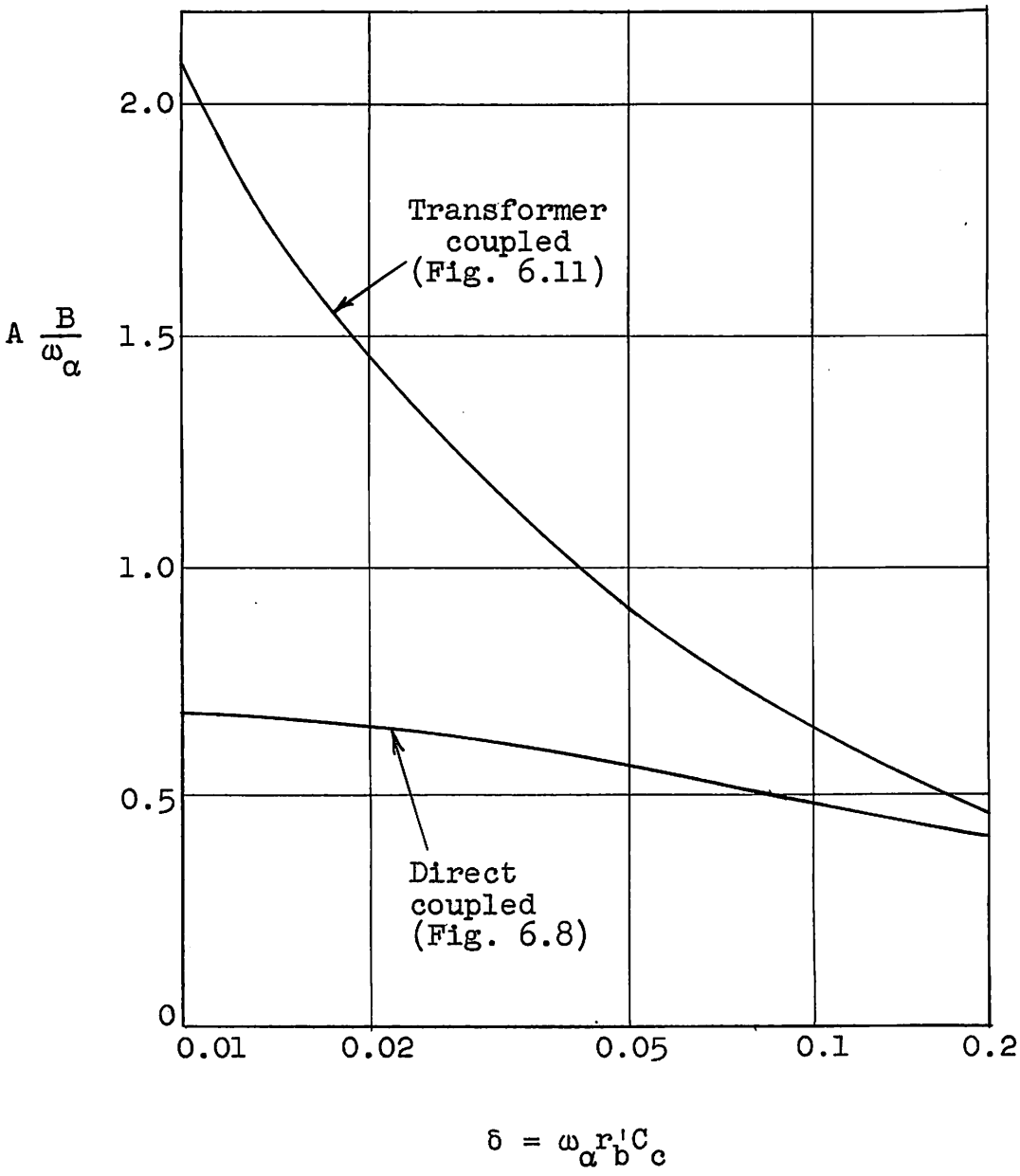

FIG. 6.12.--Voltage gain times normalized bandwidth (per stage) for cascaded common-emitter stages.

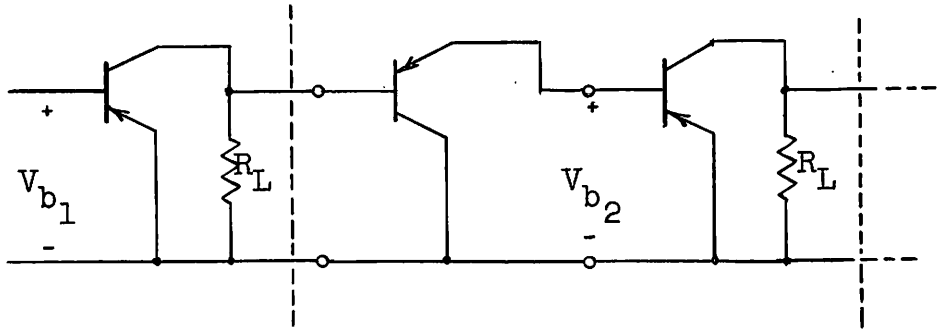

FIG. 6.13.--Common-collector/common-emitter pair.

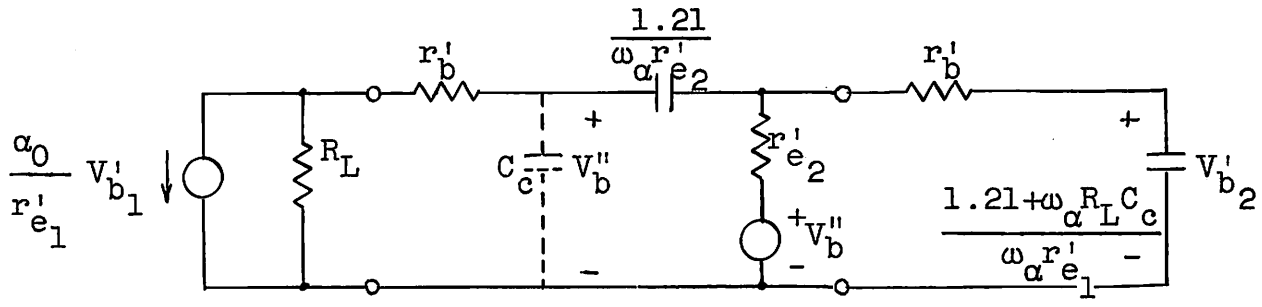

FIG. 6.14.--Equivalent circuit for CC-CE pair.

circuit, the voltage transfer function is found to be:

$$V'_{b2}/V'_{b1} = -\frac{\alpha_0 R_L}{r'_{e1}} \frac{1 + 1.21p/\omega_\alpha}{1 + a_1 p/\omega_\alpha + a_2(p/\omega_\alpha)^2}$$

where

$$a_1 = \frac{\alpha_0 r'_{e2} + r'_b}{r'_{e1}} (1.21 + \omega_\alpha R_L C_c) + 1.21\ \alpha_0$$

$$a_2 = 1.21\ \alpha_0 \frac{R_L + 2r'_b}{r'_{e1}} (1.21 + \omega_\alpha R_L C_c) \qquad (6.37)$$

The three quantities R_L, r'_{e1} and r'_{e2} may be varied independently. For a given gain, the ratio $\alpha_0 R_L/r'_{e1}$ is fixed, leaving two quantities independently variable. Both the bandwidth and, to some extent, the shape of the response may be controlled. The bandwidth will generally be sufficiently less than ω_α that the numerator term $1.21p/\omega_\alpha$ may be ignored. It seems reasonable to specify a maximally flat amplitude response; for bandwidth B the denominator polynomial must then have the form:

$$1 + \sqrt{2}\ p/B + (p/B)^2$$

The relation between the coefficients a_1 and a_2 of Eq. (6.37) must therefore be:

$$a_1 = \sqrt{2a}_2 \qquad (6.38)$$

and the bandwidth of the pair, denoted by B_2, is:

$$B_2 = \frac{\omega_\alpha}{1.21} \left[\frac{R_L}{A_2(R_L + 2r'_b)(1 + \frac{\omega_\alpha R_L C_c}{1.21})} \right]^{1/2}$$

where the gain of the pair, A_2, has been written for $\alpha_0 R_L / r'_{e_1}$. If A_2 is fixed, the maximum bandwidth occurs when:

$$R_L = \left[\frac{2.42 r'_b}{\omega_\alpha C_c} \right]^{1/2} \tag{6.39}$$

The resulting relation between gain and bandwidth for the CC-CE pair is:

$$A_2^{1/2} B_2 / \omega_\alpha = \frac{1}{1.21 \left[1 + \left(\frac{2\omega_\alpha r'_b C_c}{1.21} \right)^{1/2} \right]} \tag{6.40}$$

For purposes of comparison with the CC-CE pair, consider a pair of identical CE stages. If each stage has gain A and bandwidth B, the overall gain and bandwidth are:

$$A_2 = A^2 \qquad\qquad B_2 = 0.64B$$

From Eq. (6.35), one obtains for the CE pair:

$$A_2^{1/2} B_2 / \omega_\alpha = \frac{\alpha_0}{1.89 \left[1 + \left(\frac{\alpha_0 \omega_\alpha r'_b C_c}{1.21} \right)^{1/2} \right]^2} \tag{6.41}$$

which is less than Eq. (6.40) by a factor of at least 0.64. This means that the CC-CE pair will give at least 1.56 times the bandwidth for the same gain, or 2.44 times the gain for the same bandwidth, in comparison with the CE pair. The advantage is even greater for cascaded pairs, since the maximally flat shape of the CC-CE pair leads to less bandwidth shrinkage. Equations (6.40) and (6.41) are shown plotted against $\delta = \omega_\alpha r'_b C_c$ in Fig. 6.15.

In order to test the foregoing theory experimentally, a CE pair and a CC-CE pair were designed for the same gain, and measurements were made of their frequency responses. Two

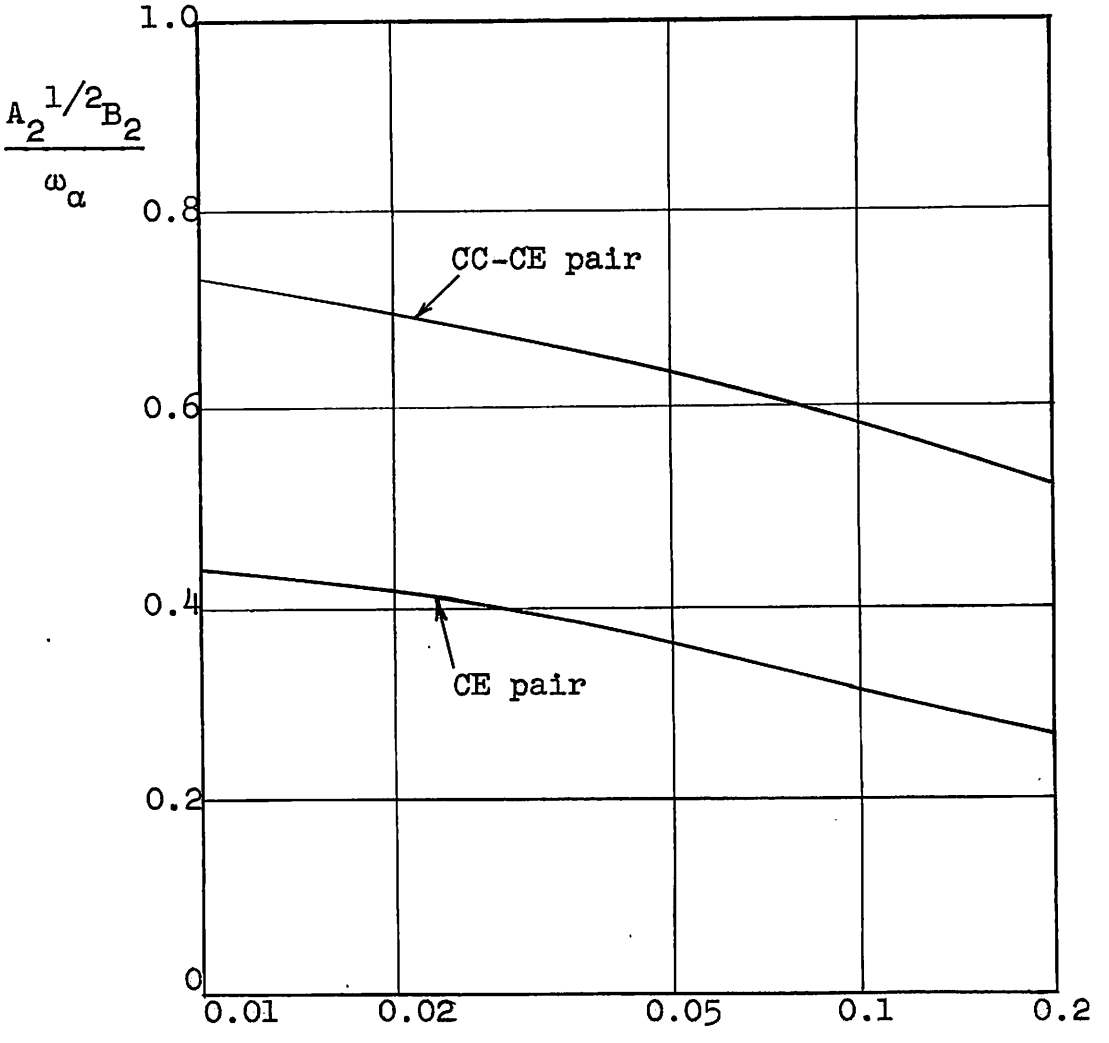

FIG. 6.15.--Gain-bandwidth of the CE pair and the CC-CE pair.

transistors (type 2N136) with virtually identical characteristics were chosen, their important parameters being (as measured by the techniques given in Chapter V):

$$r_b' = 87\Omega \qquad f_\alpha = 4.2 \text{ MC}$$
$$C_c = 14\ \mu\mu f \qquad \alpha_0 = 0.99 \simeq 1$$

An overall gain of $A_2 = 10$ was chosen. For the CE pair, the optimum load resistance, from Eq. (6.34), is $R_L = 500\Omega$. The stage gain is $\sqrt{10} = 3.16$; thus $r_e' = 500/3.16 = 158\Omega$ which corresponds to a d-c emitter current of approximately $25/158 \simeq 0.16$ ma. For the CC-CE pair, Eq. (6.39) yields $R_L = 720\Omega$, which means $r_{e1}' = 72\Omega$. Once R_L and r_{e1}' are known, use of Eqs. (6.37) and (6.38) enables r_{e2}' to be determined. In this case, $r_{e2}' = 170\Omega$.

The simple circuitry involved is shown in Fig. 6.16. Each pair was driven from a source resistance of R_L to simulate iterative conditions, and the d-c emitter current of each transistor was adjusted to the appropriate value shown. In each case it was found that the gain (ratio of output to input voltage) was within 0.5 db of the design value of 20 db. The measured amplitude response of the two circuits is shown in Fig. 6.17, as well as the theoretical response obtained by considering two cascaded circuits of Fig. 6.10 for the CE pair case, and from Eq. (6.37) for the CC-CE pair situation. The agreement is excellent in both cases, and indicates that the simple equivalent circuits used appear to be adequate. However, the experiment is illustrative of one fixed circuit condition only, and does not test all the aspects of the theory.

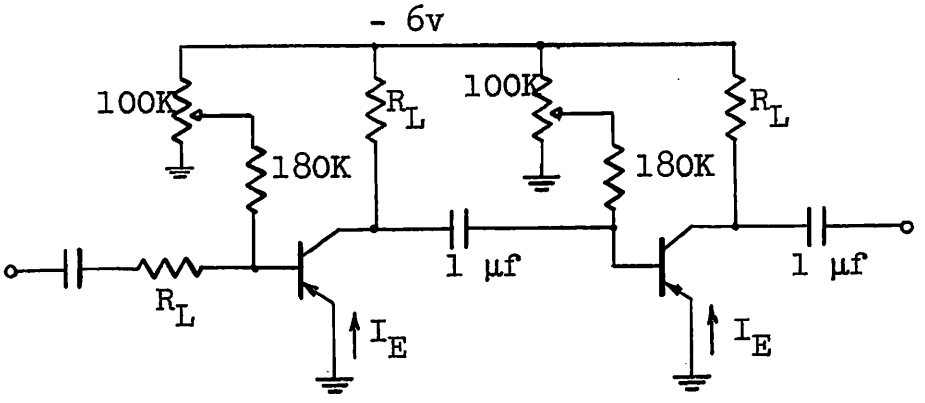

a. CE pair R_L = 500 Ω I_E = 0.16 ma

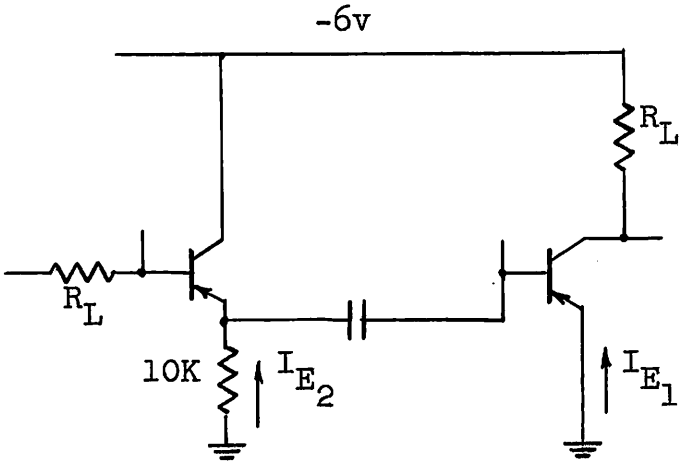

b. CC-CE pair R_L = 720 Ω I_{E_1} = 0.35 ma

I_{E_2} = 0.14 ma

2N136 Transistors

FIG. 6.16.--Lowpass amplifier schematic diagrams.

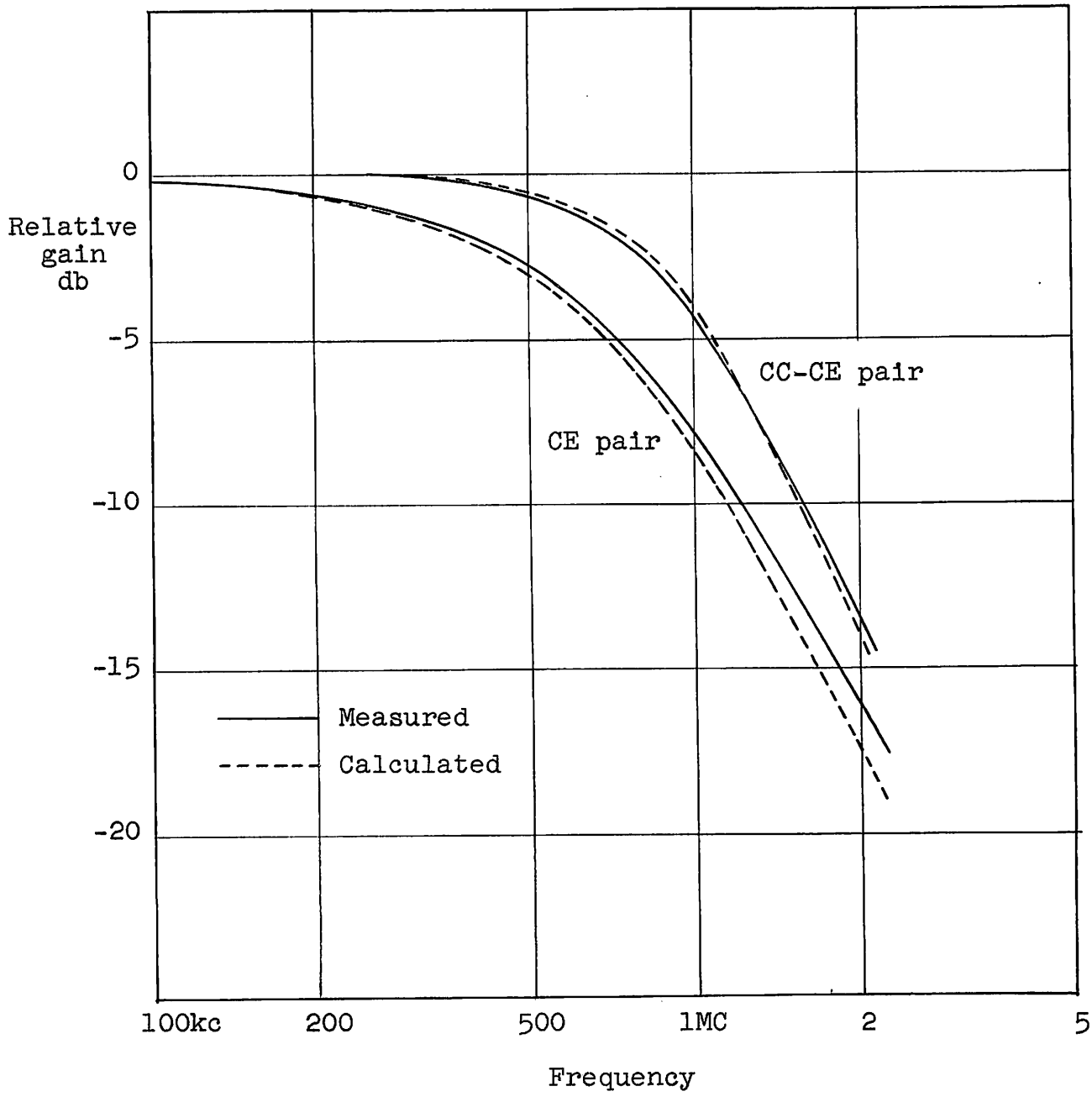

FIG. 6.17.--Relative frequency response of lowpass amplifiers.

E. CONCLUSIONS

To illustrate the application of the equivalent circuits and four-pole parameters derived in Chapters III and IV, a number of fundamental properties involving maximum single-frequency gain and potential instability were obtained for the three transistor configurations. These relations are of principal use in predicting the maximum performance of a small-signal transistor amplifier from the measured parameters of the transistor. The problem of obtaining gain over large bandwidths was considered for simple resistance-terminated amplifiers, and expressions which are believed to be new were obtained for the gain-bandwidth product in terms of fundamental transistor parameters.

Design theory for bandpass and lowpass amplifiers has been presented. In the bandpass case, neutralized transformer-coupled common-base stages were used, the bandwidth being limited principally by the $r_b'C_c$ product of the transistor. The lowpass design employed common-collector/common-emitter pairs, and it was shown that the bandwidth, which is limited principally by the alpha cut-off frequency, is greater than that obtainable from the use of common-emitter stages alone. Measurements made on actual amplifiers showed excellent agreement with the theory. The above two designs are believed to represent an original contribution.

VII. CONCLUSIONS

The work reported here has been undertaken as a step toward the design of high-frequency linear amplifiers employing junction transistor triodes. This report is concerned principally with the characterization of the transistor by means of equivalent circuits and associated four-pole parameters, the requirement of relative simplicity being considered as important as accuracy. An attempt has been made to realize three objectives: 1) of primary importance is to develop, from a firm theoretical base, simple equivalent circuits for the three useful transistor configurations; 2) to develop useful measurement methods for the four-pole parameters and equivalent circuit element values of an actual transistor; 3) to derive some limitations existing on gain and bandwidth, and to design simple bandpass and lowpass amplifiers.

It is perhaps appropriate to summarize the work, to indicate how the objectives have been met and to point out contributions which are thought to be new. The theoretical model assumed for the transistor (Fig. 2.9) consists of the collector space-charge layer capacitance C_c and the base spreading resistance r_b' added to the ideal one-dimensional "intrinsic" transistor, whose properties arise because of minority carrier diffusion in the base region. The intrinsic transistor has been studied in considerable detail in TR-No. 83,* and the results of that study are made use of here in the form of four short-circuit admittance (or y-) parameters. It is found that these parameters can be expressed in terms of four quantities characteristic of the transistor; these quantities, together with the "extrinsic" elements C_c and r_b' are denoted as the fundamental device parameters (Table 3.2). Specification

*See reference 7.

of the six device parameters thus constitutes a complete description of the transistor. The intrinsic four-pole parameters are non-rational functions of frequency, and simple rational function approximations to these are developed which are the key to later equivalent circuit representations (Eqs. (2.26) to 2.28). These approximations are useful to somewhat above the alpha cut-off frequency, and in the form given are thought to be new.

The common-base configuration is studied by means of the h-parameters, obtained for the complete transistor by absorbing the extrinsic elements into equations developed for the intrinsic h-parameters. The resultant new expressions (Eq. 3.16) are susceptible of simple physical interpretation and lend themselves easily to further approximation. It is found that these overall h-parameters (and, in fact, the four-pole parameters for the transistor in any configuration) are conveniently expressed in terms of six quantities which are related to, but different from, the device parameters mentioned above. These quantities, which are easily measurable (but not necessarily directly measurable), are denoted as the fundamental circuit parameters* (Table 3.2). The common-base h-parameters lead to a number of equivalent circuit representations which are similar to earlier circuits derived on a semi-empirical basis; for example, the equivalent T. For certain frequency ranges, approximations result in some new equivalent circuits of considerably

---

*A somewhat different use of the terms "device parameters" and "circuit parameters" has been made by R. L. Pritchard in the excellent review paper "Electric-network representation of transistors -- a survey," scheduled for publication in the Trans. IRE, PGCT, March 1956. Circuit parameters are considered to be those which are directly measurable, i.e., four-pole parameters, while device parameters are those characteristic of the device per se, independent of the circuit configuration. According to this viewpoint, the "circuit parameters" of this report would be considered as device parameters, as would also the "device parameters," the latter being phrased more in the language of the device designer.

simplified form (Fig. 3.18); for a particular d-c operating point an especially simple high-frequency equivalent is obtained. Measurements of the four-pole parameters are made on a number of high-frequency junction triodes, which show that this simple circuit is justified for approximate calculations.

For consideration of the common-emitter and common-collector, the intrinsic y-parameters form the starting point. These parameters are obtained from the common-base intrinsic y-parameters by a simple transformation. Absorption of the extrinsic elements in the appropriate place yields the over-all four-pole parameters which are expressed in h-form (Eqs. (4.9), 4.13). Approximations which are useful at high frequencies are given (Eqs. (4.10), 4.14). A number of equivalent circuits are obtained, the element values of which are expressed in terms of the fundamental circuit parameters. The common-emitter circuits are similar to those previously published, but the common-collector circuits (Figs. 4.4, 4.5) are thought to be new.

The work which has been summarized to this point completes the first objective, that of developing simple equivalent circuits for the three principal transistor triode configurations. It is believed that the characterizations achieved are adequate for exploratory circuit design and development work. However, there appears to be a need for further work of this nature on transistor devices which do not conform to the theoretical model assumed here initially. For example, the present equivalent circuits are not necessarily applicable to many grown-junction transistors,* or to junction tetrodes [5] and diffused-base transistors[39] which appear extremely promising for high-frequency applications.

---

*See reference 21, and also footnote on page 51.

The second problem treated in this report is that of the measurement of transistor small-signal properties. It is first shown how the general four-pole parameters (in particular, the short-circuit admittance parameters) may be measured at various frequencies. A new contribution here is believed to be the use of a transformer ratio-arm bridge for direct measurement of the transfer y-parameters (Fig. 5.2). Problems arising because of the necessity to supply bias to the transistor are briefly discussed. It is then shown how the six fundamental circuit parameters may be conveniently measured, these parameters determining the element values in all the equivalent circuits of this report. The techniques discussed for the measurement of four-pole parameters are applicable to any transistor device, and are useful to at least 100 MC (depending on the particular bridge used). It seems likely that new methods will be required for the UHF region. The circuit parameter measurement techniques are believed to be adequate for present day conventional junction triodes. However, a different set of circuit parameters may be preferable for other transistor types, and measurement methods appropriate to these will need to be devised.

The final portion of this report deals with transistor amplifiers and makes use of the characterizations developed in the first four chapters. A number of previously published figures of merit are evaluated, which indicate essentially the maximum power gain available from a transistor in various configurations. The factors limiting the bandwidth obtainable are examined for the special case of a single resistance-terminated stage. New designs are presented for cascaded bandpass and lowpass amplifiers, involving, respectively, transformer-coupled common-base stages, and common-collector/common-emitter pairs (Figs. 6.6, 6.16). Measurements made on these amplifiers show good agreement with the calculated response based on the simple equivalent circuits. It is concluded that

the third objective of this report, that of developing transistor gain-bandwidth relationships and amplifier design methods, is realized only to a very limited extent. A completely satisfactory analysis of the gain-bandwidth problem has not yet appeared, and much work remains to be done on efficient amplifier design methods. The work reported here emphasizes simplicity, and utilizes approximate equivalent circuits directly. Another approach, particularly valuable where there may be doubt regarding the applicability of an equivalent circuit, employs measured values of the four-pole parameters independently of any equivalent circuit, and has been termed by Pritchard the quadripole approach.*

It is hoped that the equivalent circuits and measurement methods presented here will be of use in further developing the theory of high-frequency amplifiers. An attempt has been made throughout to reach a useful compromise between accuracy and simplicity, so that the circuit designer may be provided with representations which are neither forbiddingly complex, nor unduly inaccurate.

---

*This approach has been emphasized, for example, by Linvill, reference 30. See also J. F. Gibbons, "Transistor amplifier performance," presented at the IRE/AIEE University of Pennsylvania Conference on Transistor Circuits, Philadelphia, Pa., February 16-17, 1956.

APPENDIX A: ELECTRIC CIRCUIT ANALOGY FOR MINORITY CARRIER FLOW IN THE BASE REGION

There exists a mathematical analogy between the flow of minority carriers in the base region of the transistor caused by a concentration gradient, and the flow of current in a conducting medium caused by a potential gradient.* Thus, considering an n-type base, from Eq. (2.3) the hole current density is:

$$\underline{i} = -qD \nabla p = - qD \nabla p_e \tag{A.1}$$

where the excess density $p_e = p - p_n$. For a medium of conductivity σ, and potential gradient ∇V, the current density is:

$$\underline{i} = -\sigma \nabla V \tag{A.2}$$

The quantities qD and σ are thus analogous, as are p_e and V.

Considering an element of volume a^3, the continuity Eq. (2.5) gives the net current entering this volume from the surrounding medium:

$$I_v = -a^3 \nabla . \underline{i} = qa^3 \frac{p_e}{\tau} + qa^3 \frac{\partial p_e}{\partial t} \tag{A.3}$$

The corresponding equation for the analogue must have the form:

$$I_v = g_v V + c \frac{\partial V}{\partial t} \tag{A.4}$$

which may be interpreted as a conductance g_v (analogous to $\frac{qa^3}{\tau}$) and capacitance c (analogous to qa^3) carrying current out of the medium to a ground point where V = 0. The conductance g_v accounts for carriers lost by volume recombination, and the

---

*This analogy has been exploited, for the non time-dependent case, by A. R. Moore and J. I. Pankove, reference 14.

capacitance c accounts for charge storage effects. The analogue is rather hard to visualize in three dimensions, but may readily be drawn for the two-dimensional case, as will be seen.

Conditions existing at the surfaces of the base volume must now be considered. At the emitter and collector surfaces, p_e is constant, so that, for the analogue, these surfaces are equipotentials. At the emitter and collector, respectively, analogous quantities are: (using Eq. 2.8)

$$V_E \rightarrow p_n\left[\exp\frac{qv_e}{kT} - 1\right]$$

$$V_c \rightarrow -\, p_n \text{ (if } v_c \text{ is sufficiently negative)} \qquad \text{(A.5)}$$

Here v_e and v_c are the voltages applied to the emitter and collector, and space-charge layer widening has been ignored. If one is interested only in the small-signal situation, the space-charge layer widening can be taken into account by using the analogous relations: see Eqs. (2.9), (2.11)

$$V_E \rightarrow p_0 \frac{qv_1}{kT}$$

$$V_C \rightarrow \frac{p_0}{K}\ \frac{qv_2}{kT} \qquad \text{(A.6)}$$

where p_0 and K are defined in Eqs. (2.10) and (2.12).

At the free base surfaces, a surface recombination mechanism may exist, which is conveniently described by defining a constant:

$$s = \frac{\text{number of carriers recombining per second per unit surface area}}{\text{excess concentration over equilibrium value just below the surface}}$$

The constant s is termed the surface recombination velocity. Since each hole carries a charge q, the current density into the surface is:

$$\underline{i} = qsp_e \quad \text{(normal to the surface)} \qquad \text{(A.7)}$$

Hence the current lost from the surrounding medium into an element of surface area a^2 is:

$$I_s = a^2 q s p_e \tag{A.8}$$

The corresponding equation for the analogue becomes:

$$I_s = g_s V \tag{A.9}$$

where the conductance g_s (analogous to qa^2s) accounts for the loss of carriers at the surface.

The analogy which has been presented is based primarily on the formal identity of Eqs. (A.1) and (A.2). The quantities p_e and V are proportional, and once a proportionality constant has been chosen, the other pairs of analogous quantities are fixed. Thus let:

$$p_e = AV$$

where it is to be noted that A has the dimensions $(\text{volts} \times \text{cc})^{-1}$. The analogous quantities may now be tabulated in terms of the transistor constants:

$$\begin{aligned} V &= p_e/A \\ \sigma &= A\ q\ D \\ g_v &= A\ \frac{q\ a^3}{\tau} \\ c &= A\ q\ a^3 \\ g_s &= A\ q\ a^2 s \end{aligned} \tag{A.10}$$

Figure A.1 shows these relationships diagrammatically. The scheme shown is exact only in the limit as $a \to 0$, however, the accuracy of representation will be excellent for sufficiently small a. The continuous material of conductivity σ can similarly be quantized. Consider a cell of dimensions a as shown in

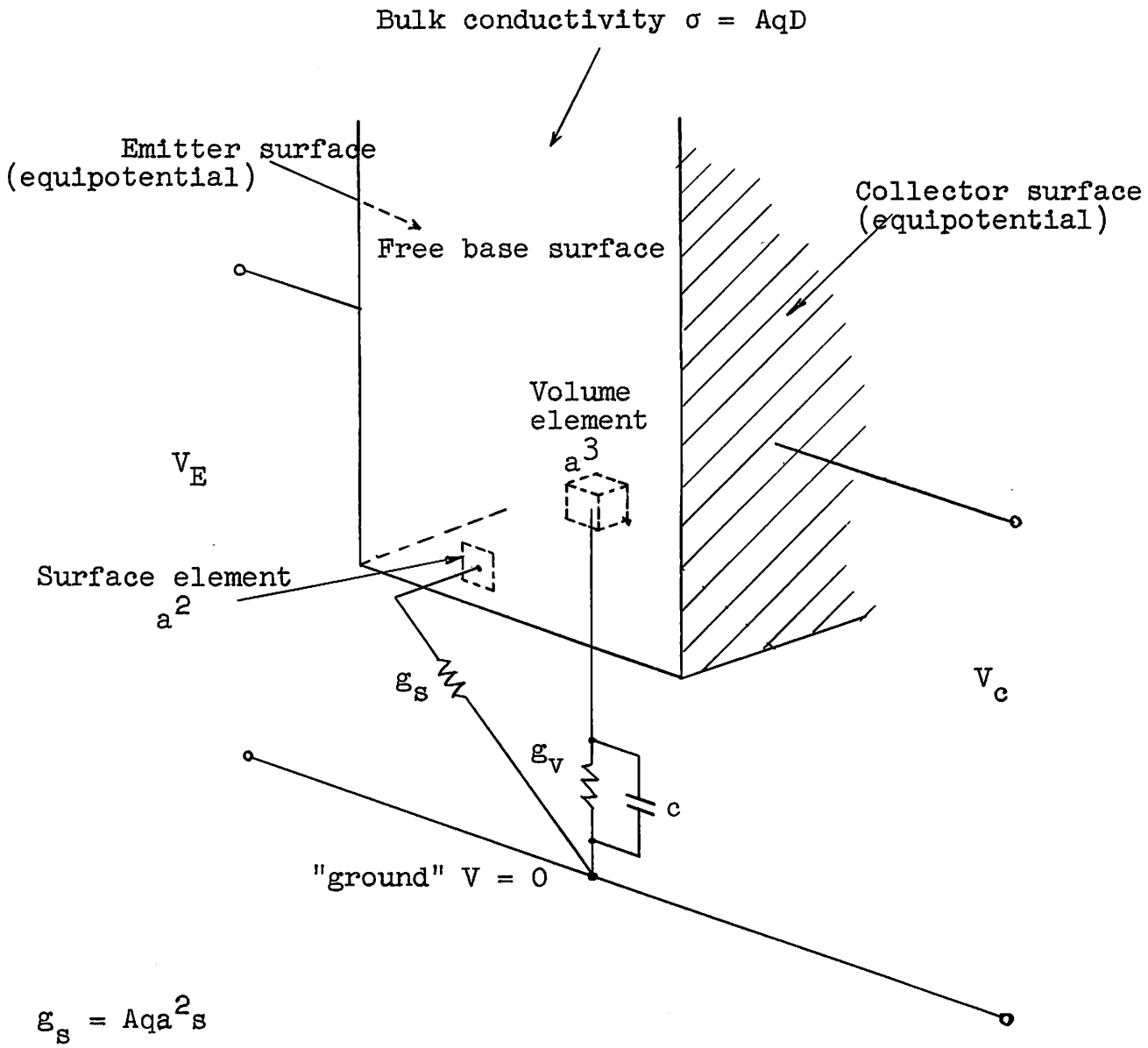

$g_s = Aqa^2 s$

$g_v = A \frac{qa^3}{\tau}$

$c = Aqa^3$

Conductances and capacitances exist from every surface and volume element to ground, as shown.

Potential V in the analogue is equivalent to excess hole density p_e in the (pnp) transistor:

$$A = \frac{p_e}{V}$$

FIG. A.1.--Electric analogue to diffusion in the base region.

Fig. A.2a, with the element g_b oriented in the direction of current flow. (This restriction is used for simplicity, but it is not essential.) Using Eq. (A.2) the total current flowing through the cell is:

$$I = a^2 i = - a^2 \sigma \nabla V \simeq a^2 \sigma \frac{V_2 - V_1}{a} = g_b (V_2 - V_1) \qquad (A.11)$$

Thus the element g_b is given by:

$$g_b = a\sigma = aAqD \qquad (A.12)$$

A small portion of the resulting circuit is shown in Fig. A.2b. Such circuits representing partial differential equations are by no means new, having been used, for example, in the solution of transient heat flow problems[40] (which are governed by a diffusion equation of the same form as occurs in transistor theory). However, these principles seem not to have been applied in full generality to the transistor situation.

As a practical matter, if it is desired to construct such an analogue, it is generally sufficient, and much easier, to work in terms of two dimensions. Referring to the coordinate system of Fig. A.2b, one assumes, for example, that p_e, and hence V, does not vary in the y-direction. Thus the potential is equal at all points lying along any line in the y-direction, and such points can be directly connected to form one point. (The various planes y = const. can be thought of as being collapsed upon one another.) If a transistor "slice" of thickness b is being represented, b/a elements g_b are connected in parallel between two such adjoining points, the resulting conductance being $(b/a)g_b$. Similarly, at a resultant surface point, the total conductance to ground is $(b/a)g_s$, and at an interior point the conductance and capacitance to ground are $(b/a)g_v$ and $(b/a)c$, respectively. This two-dimensional analogue is depicted in Fig. A.3. Such a circuit would be relatively simple to construct, and can represent any transistor geometry where planar hole flow takes place, or (approximately) a circular structure with axial symmetry, as shown in reference 14.

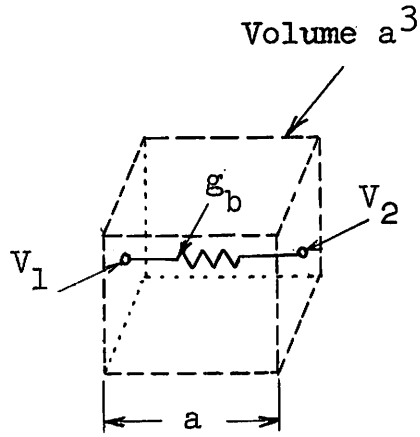

a.

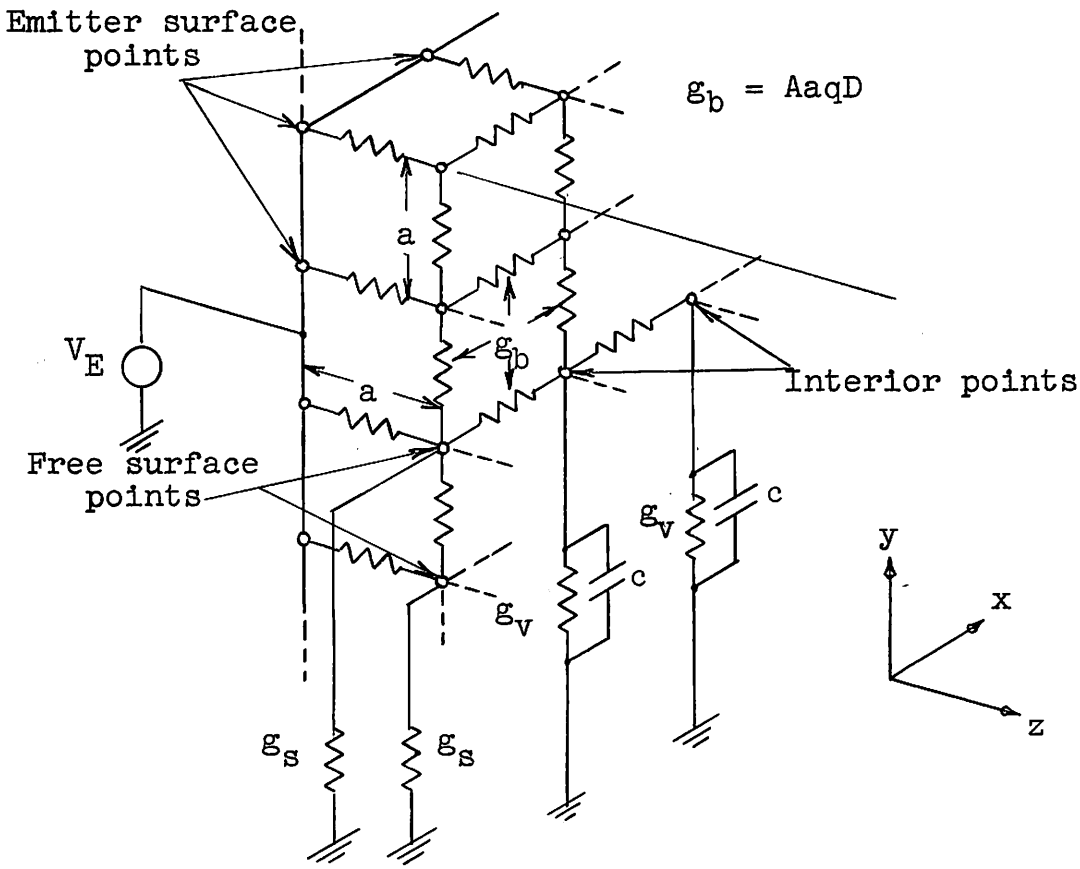

b.

FIG. A.2.--Quantization of analogue of Fig. A.1.

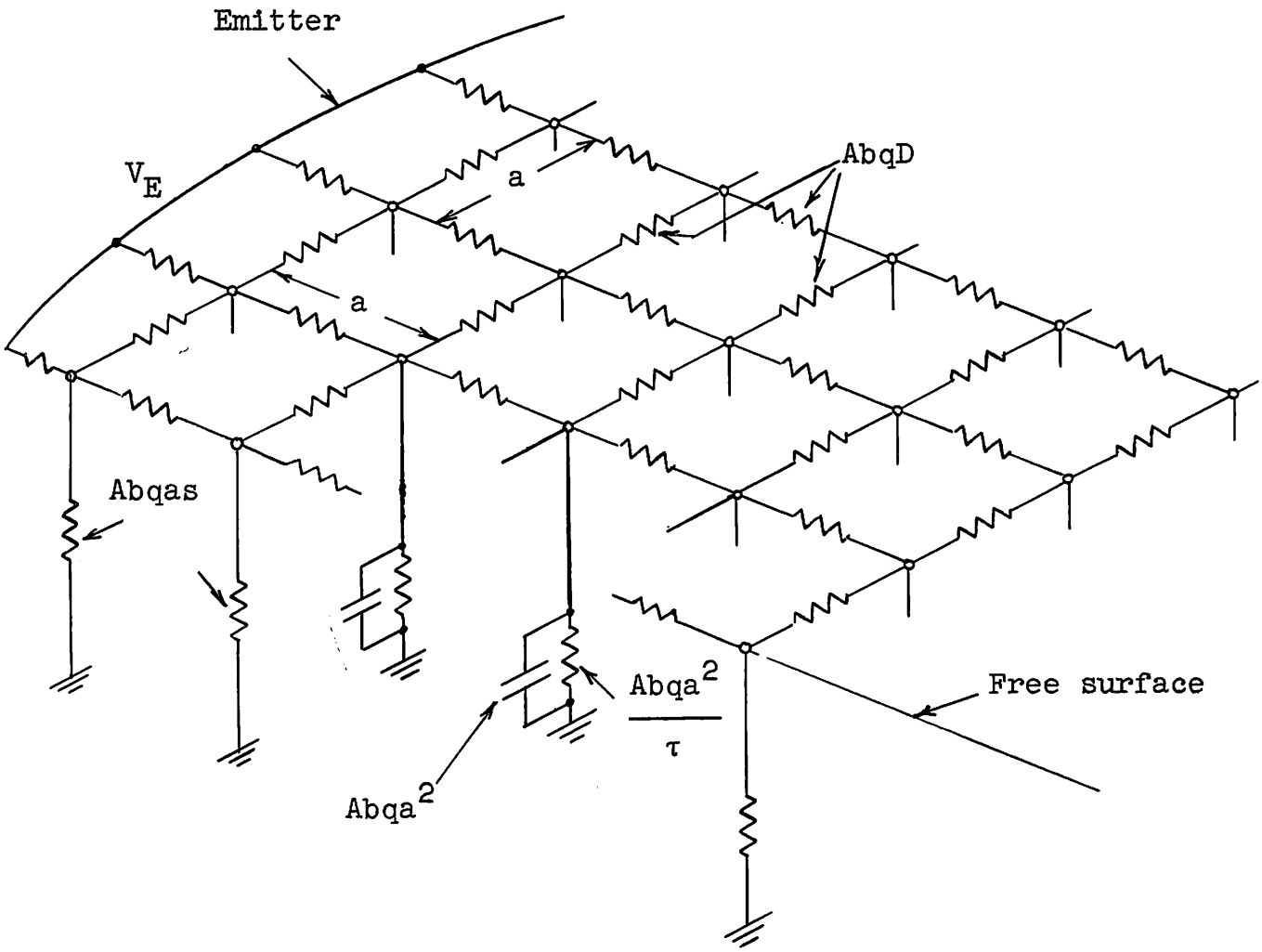

$$A = \frac{p_e}{V}$$

b = "thickness" of transistor being represented

FIG. A.3.--Two-dimensional analogue.

APPENDIX B: EFFECTS OF SURFACE RECOMBINATION

In the discussion of fundamental transistor theory given in Chapter II, an idealized one-dimensional geometry was assumed in order to obtain reasonably simple results as a basis for development of equivalent circuits. Actual high-frequency transistor structures approximate this geometry quite closely; if no surface effects occur, the minority carrier flow in the base takes place entirely in one direction and the one-dimensional analysis is accurate. In many cases, however, appreciable surface recombination is present, so that some of the minority carriers near the edge of the base are lost to the free surface during their passage from emitter to collector. It is thus of interest to attempt an analysis of this situation in order to determine the principal effects of this behavior. In particular, if the surface recombination is small, it may be accounted for by simple modifications to the one-dimensional theory.

An exact analysis will first be undertaken for a rather restrictive case where the mathematics is tractable. An approximate procedure is then introduced which yields useful results for a more general geometry.

A. PLANAR JUNCTION WITH SQUARE CROSS-SECTION*

Consider a p-n-p structure as shown in Fig. B.1, and let the small-signal hole density in the base be $p(x,y,z,t)$, which will be assumed to have a time dependence of $e^{j\omega t}$. Within the base, p satisfies the diffusion Eq. (2.6):

---

*This analytical solution is closely allied to one for a filament of infinite length given by Shockley. Refer to "The theory of p-n junctions in semi-conductors, and p-n junction transistors," Bell Syst. Tech. Jour., vol. 22, July, 1949, p. 480; also Electrons and Holes in Semiconductors, D. Van Nostrand and Co., New York, 1950, p. 318. For a similar treatment, see K. F. Stripp and A. R. Moore, reference 14.

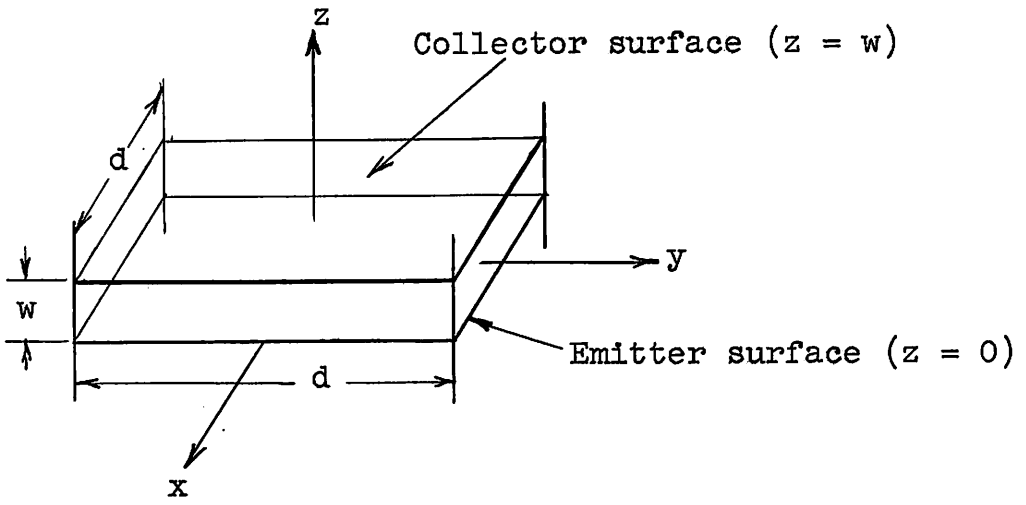

FIG. B.1.--Grown-transistor geometry.

$$\frac{\partial p}{\partial t} = j\omega p = D \nabla^2 p - \frac{p}{\tau} \qquad \text{(B.1)}$$

where τ is the volume recombination lifetime. At the emitter surface, z = 0, p is constant:

$$p\ (x, y, o, t) = p_1\ e^{j\omega t} \qquad \text{(B.2)}$$

while at the collector surface, z = w:

$$p\ (x, y, w, t) = 0 \qquad \text{(B.3)}$$

(Here, space charge layer widening has been ignored for simplicity. It will be taken into account later by a more approximate treatment.) The boundary condition to be applied at the free surfaces of the base, defined by $x = \pm d/2$, $y = \pm d/2$, is obtained from Eq. (A.7). Since the current flowing into the surface, using Eq. (2.3) is:

$$\underline{i} = - qD \frac{dp}{dn}$$

(where $\frac{d}{dn}$ refers to the derivative in the direction of the outward normal to the surface), one can write Eq. (A.7) as:

$$\frac{dp}{dn}/p = - s/D \qquad \text{(B.4)}$$

A solution of Eq. (B.1), which satisfies boundary condition (B.3) and can be made to satisfy (B.4), is: (less the time dependence)

$$p_{ij} = \sinh \gamma_{ij} (z - w) \cos \beta_i x \cos \beta_j y \tag{B.5}$$

Substitution in (B.4) at x, y = $\pm$ d/2 gives:

$$\theta_i \tan \theta_i = \frac{sd}{2D} \text{ where } \theta_i = \beta_i \, d/2 \tag{B.6}$$

A similar equation holds for $\theta_j = \beta_j \, d/2$. Substitution in (B.1) yields as a necessary condition:

$$j\omega = D[\gamma_{ij}^2 - \beta_i^2 - \beta_j^2] - \frac{1}{\tau}$$

or

$$\gamma_{ij}^2 = \frac{1 + j\omega\tau}{D\tau} + \beta_i^2 + \beta_j^2 \tag{B.7}$$

It is convenient to put this relation in the same form as results when s = 0 (i.e. no surface recombination, in which case $\beta_i = \beta_j = 0$), by defining:

$$\frac{1}{\tau_{ij}} = D(\beta_i^2 + \beta_j^2) + \frac{1}{\tau}$$

which gives:

$$\gamma_{ij}^2 = \frac{1 + j\omega\tau_{ij}}{D\tau_{ij}}$$

There exists an infinite number of roots of Eq. (B.6), and for any pair of these a partial solution p_{ij} is obtained. To satisfy boundary condition (B.2) in general, an infinite sum of these solutions is required:

$$p = \sum_{i,j} a_{ij} \, p_{ij} \tag{B.8}$$

At $z = 0$, this must reduce to a constant, p_1, so that:

$$\sum_{i,j} A_{ij} \cos \beta_i x \cos \beta_j y = p_1 \text{ for } -d/2 \leqslant x, y \leqslant d/2$$

where

$$A_{ij} = a_{ij} \sinh (-\gamma_{ij} w) \tag{B.9}$$

This is an anharmonic Fourier series,* and the coefficients A_{ij} have been given by Shockley (see footnote on page 169) as:

$$\frac{A_{ij}}{p_1} = \frac{4 \sin \theta_i \sin \theta_j}{\theta_1 \theta_j \left[1 + \frac{\sin 2\theta_i}{2\theta_i}\right]\left[1 + \frac{\sin 2\theta_j}{2\theta_j}\right]} \tag{B.10}$$

It will be instructive to evaluate the emitter and collector currents, which are obtained by integrating the expression for current density (Eq. 2.3) over the emitter and collector surfaces. For example, the emitter current is:

$$I_{e_1} = -qD \iint \frac{\partial p}{\partial z} \, dy \, dx$$

where the limits of the integral extend over the cross-section at $z = 0$. Using Eq. (B.5), (B.8), and (B.10), this procedure, applied to the emitter current results in:

$$I_{e_1} = qD \, p_1 d^2 \sum_{i,j} B_{ij} \gamma_{ij} \coth (-\gamma_{ij} w) \tag{B.11}$$

and for the collector current:

$$I_{c_1} = qDp_1 d^2 \sum_{i,j} B_{ij} \gamma_{ij} \operatorname{cosech} (\gamma_{ij} w) \tag{B.12}$$

*An example of such a series, and the method of finding the coefficients, appears in Sommerfeld, Partial Differential Equations in Physics, Academic Press Inc., New York, 1949, pp. 27-29.

where the γ_{ij} are given by (B.7), and

$$B_{ij} = \frac{4 \sin^2\theta_i \sin^2\theta_j}{\theta_i^2\theta_j^2 \left[1 + \frac{\sin 2\theta_i}{2\theta_i}\right]\left[1 + \frac{\sin 2\theta_j}{2\theta_j}\right]} \qquad \text{(B.13)}$$

As a numerical example, the following parameters are chosen, which appear to be representative of a typical grown-type transistor with a considerable amount of surface recombination:

$$d = 0.020 \text{ in.} = 0.0508 \text{ cm}$$
$$s = 1000 \text{ cm/sec}$$
$$D = 40 \text{ cm}^2/\text{sec} \text{ (for holes in n-type material)}$$
$$\frac{sd}{2D} = 0.635$$

The roots of $\theta_i \tan \theta_i = \frac{sd}{2D} = 0.635$ are found to be:

$$\theta_0 = 0.721, \quad \theta_1 = 3.32, \quad \theta_2 = 6.37 \quad \text{etc.}$$

For the higher roots:

$$\theta_n \simeq n\pi + \frac{0.635}{n\pi} \approx n\pi$$

Using these values, one finds for the B_{ij}, using (B.13):

$$B_{00} = 0.984$$

$$B_{10} = B_{01} = 0.00527$$

The higher B's are much smaller; in general:

$$B_{nm} \simeq \frac{4}{n^4 m^4 \pi^8} \left(\frac{sd}{2D}\right)^4$$

From (B.7), the γ_{ij} are:

$$\gamma_{ij}^2 = \frac{1}{D\tau} + \frac{4}{d^2}(\theta_i^2 + \theta_j^2) + j\frac{\omega}{D} \qquad (B.14)$$

Assuming zero frequency and a very large volume lifetime τ; one obtains:

$$\gamma_{00} = \frac{2.04}{d}$$

$$\gamma_{01} = \gamma_{10} = \frac{3.99}{d}$$

$$\gamma_{11} = \frac{5.26}{d} \text{ etc.}$$

These relations hold for any d, as long as $\frac{sd}{2D} = 0.635$. Since the coefficients B_{ij} diminish so rapidly, whereas the γ_{ij} do not increase rapidly, it turns out that one can ignore all but the first term in Eqs. (B.11) and (B.12) to a good approximation. Thus, the emitter current is approximately:

$$I_{e_1} \simeq qDp_1 d^2 B_{00} \gamma_{00} \coth(\gamma_{00} w) \qquad (B.15)$$

An exactly similar analysis can be applied for the d-c emitter current I_{e_0}; one then finds that the a-c emitter current above can be written in terms of I_{e_0} and the applied a-c emitter potential V_{e_1}:

$$I_{e_1} = V_{e_1} \frac{qI_{e_0}}{kT} \gamma_{00} w \coth(\gamma_{00} w) \qquad (B.16)$$

The ratio of I_{e_1} to V_{e_1}, which is the intrinsic admittance y'_{11}, has a form identical to that given in Eq. (2.14), except that in place of $\theta^2 = \frac{w^2}{D\tau} + j\omega\frac{w^2}{D}$, there appears, using (B.14):

$$\gamma_{00}^2 w^2 = \frac{w^2}{D\tau} + 8\theta_0^2 \frac{w^2}{d^2} + j\omega\frac{w^2}{D} = \frac{w^2}{D\tau_{00}} + j\omega\frac{w^2}{D}$$

It is apparent that one may define an effective lifetime τ_{00}, as above, comprising the volume lifetime τ and an apparent surface lifetime τ_s, such that:

$$\frac{1}{\tau_{00}} = \frac{1}{\tau} + \frac{1}{\tau_s} \tag{B.17}$$

The surface lifetime is thus given by:

$$\tau_s = \frac{d^2}{8D\theta_0^2} \tag{B.18}$$

where θ_0 is the first root of $\theta \tan \theta = \frac{sd}{2D}$.
For small values of $\frac{sd}{2D}$ (less than 0.25 or so), $\theta_0 \simeq (\frac{sd}{2D})^{1/2}$ and one obtains for the surface lifetime:

$$\tau_s \simeq \frac{d}{4s} \tag{B.19}$$

The conclusion to be drawn from the above analysis is that, for the particular geometry considered and for values of s which are not too large (as expressed by the parameter $\frac{sd}{2D}$), surface recombination acts to modify the volume lifetime τ to a lower effective value, as given by Eq. (B.17) and (B.19).

In order to consider the effect of surface recombination on transistor parameters which are caused by space-charge layer widening (neglected in the above treatment), an approximate procedure given by Stripp and Moore (see reference 14) is useful. The pertinent parameters are r_c and μ_{ec} (refer to Table 3.2) which are of importance chiefly at low frequencies, so that $\omega \to 0$ will be assumed. Let p represent, as before, the small-signal hole density in the base region, which satisfies the diffusion equation throughout the base volume:

$$D \nabla^2 p - \frac{p}{\tau} = 0 \tag{B.20}$$

The boundary conditions on p are:

$$p = p_1 = p_0 \frac{qV_1}{kT} \quad \text{at the emitter junction}$$

$$p = p_2 = \frac{p_0}{K} \frac{qV_2}{kT} \quad \text{at the collector junction}$$

$$\frac{\partial p/\partial n}{p} = - s/D \quad \text{at the free base surface} \qquad \text{(B.21)}$$

Here, V_1 and V_2 are the a-c emitter and collector voltages, respectively, and K is the space-charge layer widening constant:

$$1/K = \frac{kT}{qw} \frac{\partial w}{\partial V_c}$$

The rate of hole loss in the base volume owing to volume recombination is:

$$\frac{\partial p}{\partial t} = - \frac{p}{\tau}$$

so that the component of total base current from <u>volume</u> recombination is:

$$I_{b_v} = \frac{q}{\tau} \int_{\text{over base volume}} pdV \qquad \text{(B.22)}$$

Similarly, the component of base current caused by <u>surface</u> recombination is, using (B.21):

$$I_{b_s} = - qD \int \frac{\partial p}{\partial n} \, d\sigma = qs \int_{\text{over free base surface}} p \, d\sigma \qquad \text{(B.23)}$$

If the total recombination is small, the solution to (B.20) is very nearly equal to the solution obtained in the absence of all recombination, i.e. the solution to the Laplace equation $\nabla^2 p = 0$, which will be represented by p^o. One may then use this p^o to calculate the recombination currents by

means of (B.22) and (B.23), which can often be evaluated approximately, if not analytically.

As an example, consider the geometry previously investigated and shown in Fig. B.1, which is representative of a grown-type structure. To obtain an approximate p^o, the boundary condition at the collector surface $z = w$ may be taken to be $p = 0$, since K is normally large, and $p_2 \ll p_1$. In this case, one easily obtains:

$$p^o(z) = p_1 \frac{w - z}{w}$$

Evaluating (B.22) and (B.23), results in:

$$I_{b_v} = \frac{q}{\tau} \int p^o(z) dV = \frac{qd^2}{\tau} p_1 \int_o^w (1 - \frac{z}{w})\, dz = \frac{qd^2}{\tau} p_1 \frac{w}{2}$$

$$I_{b_s} = qs \int p^o(z) d\sigma = 4dqs\, p_1 \int_o^w (1 - \frac{z}{w}) dz = 4dqsp_1 \frac{w}{2}$$

The emitter current is:

$$I_e = - qD \int_{\text{emitter surface}} \frac{\partial p}{\partial z}\, d\sigma = qDd^2 \frac{p_1}{w}$$

It is convenient to calculate $\alpha = \frac{I_c}{I_e} = 1 - \frac{I_b}{I_e} = 1 - \frac{I_{b_v} + I_{b_s}}{I_e}$

Using the above relations for the base current components, one obtains:

$$\alpha = 1 - \frac{w^2}{2D} [\frac{1}{\tau} + \frac{4s}{d}] = 1 - \frac{w^2}{2D\tau_{eff}} \qquad \text{(B.24)}$$

The effective lifetime is thus $\frac{1}{\tau_{eff}} = \frac{1}{\tau} + \frac{1}{\tau_s}$, from which $\tau_s = \frac{d}{4s}$, as obtained previously. This expression is valid only for I_b small compared to I_e, or α close to unity, as is the case for most transistors.

B. ALLOY TYPE GEOMETRY

Using the approximate procedure detailed above, consider the simplified situation of Fig. B.2. The solution of $\nabla^2 p = 0$ will result in lines of constant hole density approximately as shown. Most of the volume recombination takes place in the volume directly below the emitter, where the hole density varies in nearly linear fashion from emitter to collector. Thus, as in the previous (grown) structure:

$$I_{b_v} \simeq \frac{qA_1}{\tau} p_1 \frac{w}{2}$$

where A_1 is an effective area slightly larger than the emitter area. Most of the surface recombination takes place in a small ring around the emitter, whose area is not strongly dependent on w. (This is in contrast to the grown structure where the surface recombination area depends directly on w.) Hence, since p is proportional to p_1, one can write very approximately:*

$$I_{b_s} \simeq qsp_1 A_2$$

where A_2 is the effective surface recombination area. If the emitter current is, as before, $I_e \simeq qDA_e \frac{p_1}{w}$ and $A_1 \simeq A_e$, one obtains for α:

$$\alpha = 1 - \frac{w^2}{2D\tau} - \frac{sA_2}{DA_e} w$$

or, defining $L^2 = D\tau$, as usual, and a surface diffusion length

$$L_s = \frac{DA_e}{sA_2} :$$

$$\alpha = 1 - \frac{1}{2}\frac{w^2}{L^2} - \frac{w}{L_s} \qquad \text{(B.25)}$$

---

*See W. M. Webster, reference 12.

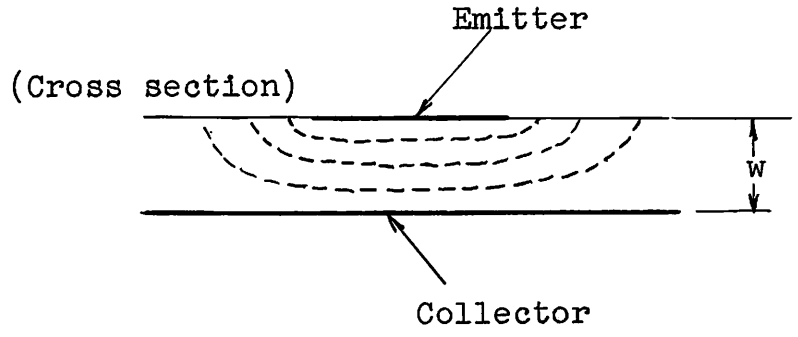

FIG. B.2.--Simplified alloy-transistor geometry.

In summary, using Eq. (B.24) and defining $L_1^2 = D\tau_{eff}$:

$$\alpha_{grown} = 1 - \frac{1}{2}\frac{w^2}{L_1^2}$$

$$\alpha_{alloy} = 1 - \frac{1}{2}\frac{w^2}{L^2} - \frac{w}{L_s} \qquad \text{(B.26)}$$

The dependence of α on w is of importance in determining the small-signal low-frequency parameters which depend on space-charge layer widening.

C. EFFECT ON LOW-FREQUENCY PARAMETERS*

Consider the intrinsic h-parameters. In the case of the grown-type geometry of Fig. B.1, the only effect of surface recombination is the change of τ to τ_{eff}. In terms of the device parameters w, τ_{eff} and the space-charge layer widening

*This analysis, which is an original contribution of the present author, has also appeared in G. H. Scithers, "The variability of some characteristics of a group of fused-junction transistors," TR-No. 92, Electronics Research Laboratory, Stanford University, September 16, 1955.

constant $1/K = \frac{kT}{q}\frac{1}{w}\frac{\partial w}{\partial V_c}$, one can write: See Eqs. (2.31), (2.32)

$$h'_{11} = 1/G \qquad G = \frac{qI_E}{kT}$$

$$h'_{21} = -\alpha \simeq -\left[1 - \frac{1}{2}\frac{w^2}{D\tau_{eff}}\right]$$

$$h'_{12} = \frac{\alpha}{K} \simeq \frac{1}{K}$$

$$h'_{22} = \frac{G}{K}\,2\,(1-\alpha) \qquad \text{(B.27)}$$

It is to be noted that these parameters are not independent, since they are expressed in terms of only 3 quantities G, α, and K.

For the alloy-type geometry of Fig. B.2, one cannot define an effective lifetime, or equivalently, an effective diffusion length, which is <u>independent</u> of w. Where w is fixed, however, as in the case of h'_{11} and h'_{21} (zero a-c collector voltage), this is of no consequence, and, as before:

$$h'_{11} = 1/G \qquad h'_{21} = -\alpha$$

From the definition of h'_{12}:

$$h'_{12} = \left.\frac{\partial V_e}{\partial V_c}\right]_{I_e = \text{const.}} = \frac{\partial V_e}{\partial w}\frac{\partial w}{\partial V_c}$$

The emitter voltage V_e depends on the (excess) hole density at emitter p_e through the relation:

$$p_e = p_n\left[e^{qV_e/kT} - 1\right]$$

and, for constant emitter current, which means constant hole

density gradient, p_e is proportional to w (very nearly), which means:

$$\frac{\partial p_e}{\partial w} = \frac{p_e}{w}$$

From the above relationships one finds $\frac{\partial V_e}{\partial w} = \frac{1}{w}\frac{kT}{q}$, so that:

$$h'_{12} = \frac{1}{w}\frac{kT}{q}\frac{\partial w}{\partial V_c} = \frac{1}{K}, \text{ as before.}$$

The definition of h'_{22} is:

$$h'_{22} = \left.\frac{\partial I_c}{\partial V_c}\right]_{I_e = \text{const.}} = -I_e \frac{\partial \alpha}{\partial V_c} = -I_e \frac{\partial \alpha}{\partial w}\frac{\partial w}{\partial V_c}$$

Using the expression for α given in Eq. (B.26), there results:

$$h'_{22} = \frac{I_e q}{kT} \cdot \frac{kT}{q} \cdot \frac{1}{w} \left[\frac{w^2}{L^2} + \frac{w}{L_s}\right] \frac{\partial w}{\partial V_c} = \frac{G}{K}\left[\frac{w^2}{L^2} + \frac{w}{L_s}\right]$$

If volume recombination predominates, $\frac{w^2}{L^2} >> \frac{w}{L_s}$, and:

$$h'_{22} = \frac{G}{K}\, 2(1 - \alpha) \qquad \text{(B.28)}$$

as before. If surface recombination predominates, $\frac{w}{L_s} >> \frac{w^2}{L^2}$, and:

$$h'_{22} = \frac{G}{K}\,(1 - \alpha) \qquad \text{(B.29)}$$

which is one-half of the value to be expected if no surface recombination were present. G. H. Scithers, (see footnote on page 179) studying the interdependence of h-parameters on a sample of 100 alloy transistors, has obtained evidence supporting this analysis.

APPENDIX C: COMPARISON OF Y-PARAMETERS WITH THOSE GIVEN IN TR-NO. 83

It is desired to compare the common-base y-parameters derived in this report, and given by Eq. (3.19) of Chapter III, with those derived by R. D. Middlebrook.[7] For this purpose, circuits representing the y-parameters will be synthesized and compared with circuits given in TR-No. 83.

To facilitate the comparison, the following changes of notation will be employed in Eq. (3.19) in order to obtain agreement with the notation of TR-No. 83:

$$r_h = \frac{1}{g_{ee}} \qquad r_b' = r \qquad C_c = C \qquad s = j\,\omega/\omega_\alpha = j\omega T$$

$$\frac{\mu_b}{r_h} = g_{ec} \qquad \frac{1}{r_c}\,\frac{r_h + r_c\,\alpha_0\mu_b}{r_h} = g_{cc} \tag{C.1}$$

With these changes, Eq. (3.19) can be written in the form:

$$y_{11} = g_{ee}\,\frac{1 + j\omega T}{1 + 1.21\,r\,g_{ee}\,j\omega T}$$

$$y_{21} = -\,\alpha_0\,g_{ee}\,\frac{1 - 0.2\,j\omega T}{1 + 1.21\,r\,g_{ee}\,j\omega T}$$

$$y_{12} = -\,g_{ec}\,\frac{1 + g_{ee}/g_{ec}\;rCj\omega + g_{ee}/g_{ec}\;rCT\;(j\omega)^2}{1 + 1.21\,r\,g_{ee}\,j\omega T}$$

$$y_{22} = g_{cc}\,\frac{1 + g_{ee}/g_{cc}(\alpha_0 + 1/rg_{ee})\;rCj\omega + g_{ee}/g_{cc}\;rCT\;(j\omega)^2}{1 + 1.21\,r\,g_{ee}\,j\omega T} \tag{C.2}$$

For purposes of synthesizing circuits, the above equations are rearranged in such a form that the circuit elements can be readily visualized:

$$y_{11} = \frac{1}{1.21r} + \frac{g_{ee} - 1/1.21r}{1 + 1.21r\, g_{ee}\, j\omega T}$$

$$-y_{21} = -\frac{0.2\ \alpha_0}{1.21r} + \frac{\alpha_0 g_{ee} + \dfrac{0.2\alpha_0}{1.21r}}{1 + 1.21r\, g_{ee}\, j\omega T}$$

$$-y_{12} = g_{ec} + j\omega \frac{C}{1.21} + \frac{(g_{ee}r - \frac{1}{1.21})\ j\omega C}{1 + 1.21r\, g_{ee}\, j\omega T}$$

$$y_{22} = g_{cc} + j\omega \frac{C}{1.21} + \frac{(1 + \alpha_0 r g_{ee} - \frac{1}{1.21})\ j\omega C}{1 + 1.21r\, g_{ee}\, j\omega T} \qquad (C.3)$$

From Eq. (C.3), the circuits given in Fig. C.1 may be drawn. Reference to TR-No. 83* shows substantial agreement,** the differences being the following:

1. The capacitances $C^b = C/1.19$ are omitted across y_{11} and y_{21}, principally because the approximation which Eq. (3.18) used for h_{21}, ignores terms in $\omega_\alpha r_b' C_c = \frac{rC}{T}$ compared to unity, for simplicity. The error in doing this is not great at frequencies below ω_α.

2. Also because of the above approximations, quantities $\frac{rC}{T}$ are ignored relative to unity in y_{11} and y_{21}.

3. The number 1.19 in TR-No. 83 appears here as 1.21, because of a different scheme of approximating the hyperbolic functions. The difference is not significant.

It remains to evaluate the quantities g_{ec} and g_{cc}. In TR-No. 83,

---

*In TR-No. 83, the circuits are given in Fig. 5.5 on p. 89, and the element values in Eqs.(7.6) to (7.21) on pp. 113-114.

**Note that in Eqs. (7.15) and (7.16) of TR-No. 83, the quantity $\frac{1}{k} + r\, g_{ee}$ becomes, on reference to Eq. (7.3), $1 + \alpha_0 r g_{ee}$.

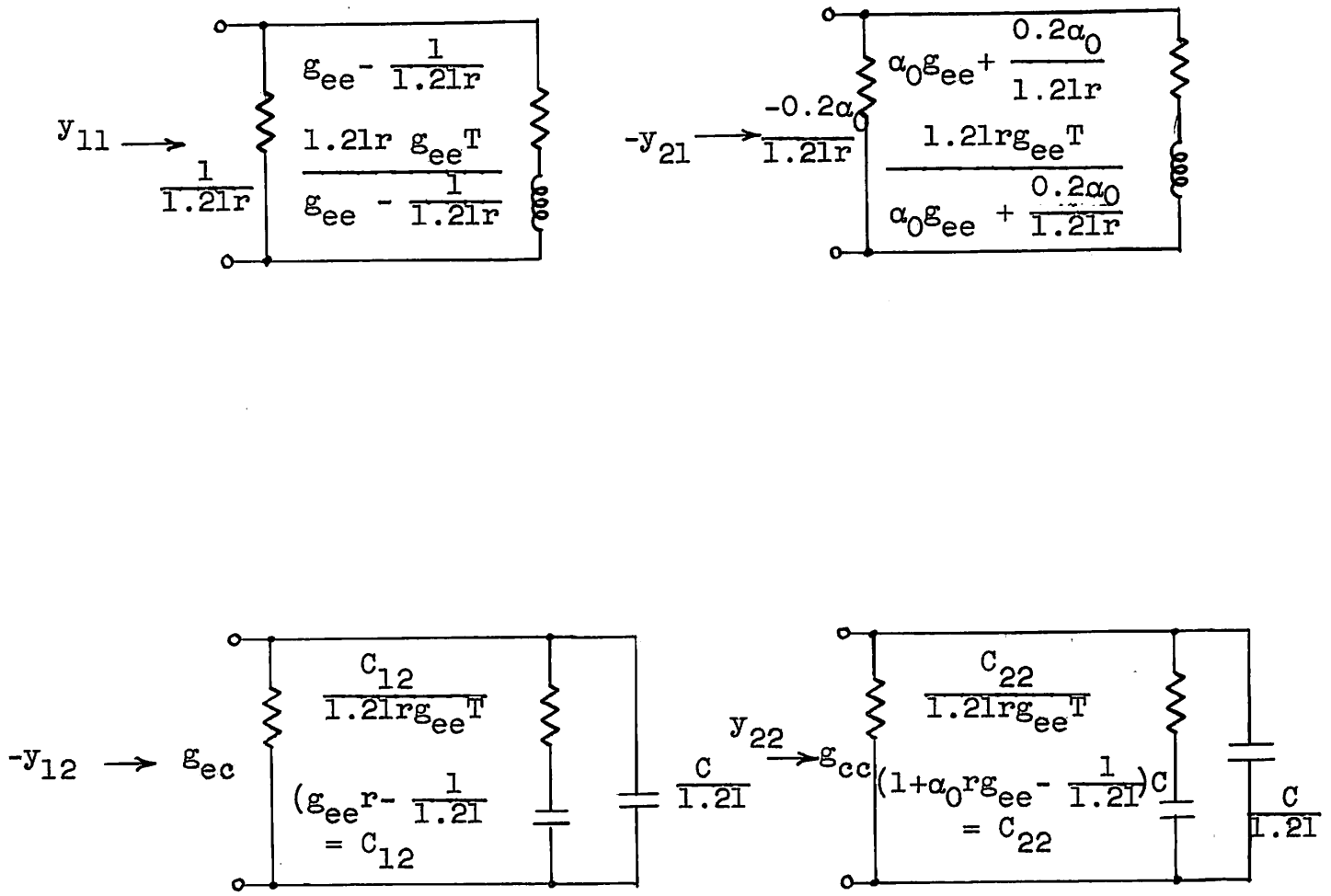

FIG. C.1.--Circuits representing the y-parameters of Eq. C.3.

these quantities are given in terms of g_c, which is the low-frequency value of the intrinsic collector admittance y'_{22}. Reference to Eqs.(2.14), (2.27), and (3.15), yields:

$$g_c = \frac{G}{K} = \frac{1}{Kr'_e} = \frac{1}{2(1 - \alpha_0)r_c} \simeq \frac{1}{(1 - \alpha_0^2)r_c} \qquad (C.4)$$

Here, $1 - \alpha_0^2$ has been written for $2(1 - \alpha_0)$, the difference between the two expressions being only 2 per cent for $\alpha_0 = 0.95$ and 5 per cent for $\alpha_0 = 0.90$. From Eqs. (C.1) and (3.15), using (C.4), one obtains:

$$g_{ec} = \frac{\mu_b}{r_h} \simeq \frac{1}{r_h Kr'_e} [\alpha_0 r'_e + r'_b (1 - \alpha_0^2)]$$

$$= g_c \frac{\alpha_0[r'_e + r'_b (1 - \alpha_0)] + r'_b (1 - \alpha_0)}{r_h}$$

Using the notation of Eq. (C.1):

$$g_{ec} = g_c [\alpha_0 + r\, g_{ee} (1 - \alpha_0)] \qquad (C.5)$$

Similarly:

$$g_{cc} = \frac{1}{r_c} + \alpha_0 \frac{\mu_b}{r_h} = (1 - \alpha_0^2)\, g_c + \alpha_0\, g_{ec}$$

Using Eq. (C.5):

$$g_{cc} = g_c [1 + \alpha_0 r g_{ee}(1 - \alpha_0)] \qquad (C.6)$$

Equations (C.5) and (C.6) are identical to Eqs. (7.14) and (7.18) of TR-No. 83. Thus, this Appendix has shown that the common-base h-parameters obtained in this report (Eq. 3.16) are equivalent to the y-parameters of TR-No. 83 within the limits of the approximations used in converting from one set to the other. As noted in connection with Eq. (3.19), one of these approximations indicates that the h-parameters derived here are a more general representation.

REFERENCES

1. L. C. Peterson, "Equivalent circuits of linear active four-terminal networks," Bell System Tech. Jour., vol. 27, October 1948, pp. 593-622.
2. C. W. Mueller and J. I. Pankove, "A p-n-p triode alloy-junction transistor for radio-frequency amplification," Proc. IRE, vol. 42, February 1954, pp. 386-391.
3. W. E. Bradley, "Principles of the surface-barrier transistor," Proc. IRE, vol. 41, December 1953, pp. 1702-1706.
4. J. M. Early, "P-n-i-p and n-p-i-n junction transistor triodes," Bell System Tech. Jour., vol. 33, May 1954, p. 517.
5. R. L. Wallace, L. G. Schimpf and E. Dickten, "A junction transistor tetrode for high frequency use," Proc. IRE, vol. 40, November 1952, p. 1395.
6. J. M. Early, "Design theory of junction transistors," Bell System Tech. Jour., vol. 32, November 1953, pp. 1271-1312.
7. R. D. Middlebrook, "A junction-transistor high-frequency equivalent circuit," TR-No. 83, Contract N6onr 251(07), Stanford University (Electronics Research Laboratory), May 2, 1955.
8. W. Shockley, "Transistor electronics: imperfections, unipolar and analog transistors," Proc. IRE, vol. 40, November 1952, p. 1302.
9. E. M. Conwell, "Properties of silicon and germanium," Proc. IRE, vol. 40, November 1952, p. 1335.
10. W. Shockley, M. Sparks, and G. K. Teal, "P-n junction transistors," Phys. Rev., vol. 83, July 1951, p. 154.
11. J. M. Early, "Effects of space charge layer widening in junction transistors," Proc. IRE, vol. 40, November 1952, pp. 1404-1405.
12. W. M. Webster, "On the variation of junction-transistor current-amplification factor with emitter current," Proc. IRE, vol. 42, June 1954, pp. 914-920.
13. R. Kansas, "On the high-frequency performance of transistors," Proc. IRE, vol. 41, December 1953, pp. 1712-1714.
14. A. R. Moore and J. I. Pankove, "The effect of junction shape and surface recombination on transistor current gain," Proc. IRE, vol. 42, June 1954, pp. 907-913. Also, see Part II of the above paper by K. F. Stripp and A. R. Moore, Proc. IRE, vol. 43, July 1955, pp. 856-866.

15. H. Statz, E. A. Guillemin, and R. A. Pucel, "Design considerations of junction transistors at higher frequencies," Proc. IRE, vol. 42, November 1954, pp. 1623-1625.

16. R. L. Pritchard, "Frequency variations of current-amplification factor for junction transistors," Proc. IRE, vol. 40, November 1952, p. 1480.

17. E. A. Guillemin, The Mathematics of Circuit Analysis, John Wiley and Sons, Inc., New York, N. Y., 1949, p. 287.

18. Dwight, Tables of Integrals and Other Mathematical Data, Macmillan, New York, 1947, p. 146.

19. R. L. Pritchard, "Frequency variations of junction transistor parameters," Proc. IRE, vol. 42, May 1954, p. 798.

20. D. Haneman, "Expression for the 'Alpha cut-off' frequency in junction transistors," Proc. IRE, vol. 42, December 1954, p. 1808.

21. R. L. Pritchard and W. N. Coffey, "Small-signal parameters of grown-junction transistors at high frequencies," Convention Record of the IRE, vol. 2, part 3, pp. 89-96.

22. J. M. Early, "P-n-i-p and n-p-i-n junction transistor triodes," Bell System Tech. Jour., vol. 33, May 1954, p. 517.

23. R. L. Pritchard, "Effect of base-contact overlap and parasitic capacities on small-signal parameters of junction transistors," Proc. IRE, vol. 43, January 1955, pp. 38-40.

24. A. P. Stern, C. A. Aldridge, and W. F. Chow, "Internal feedback and neutralization of transistor amplifiers," Proc. IRE, vol. 43, July 1955, p. 843.

25. R. L. Pritchard, "Frequency response of theoretical models of junction transistors," Trans. IRE PGCT, vol. CT-2, June 1955, p. 187.

26. Jacob Shekel, "Matrix representation of transistor circuits," Proc. IRE, vol. 40, November 1952, pp. 1493-1497.

27. Jacob Shekel, "Two network theorems concerning change of voltage reference terminal," Proc. IRE, vol. 42, July 1954, p. 1125.

28. G. Knight, R. A. Johnson, and R. B. Holt, "Measurement of the small-signal parameters of transistors," Proc. IRE, vol. 41, August 1953, p. 983.

29. Shepard Roberts, "Conjugate-image impedances," Proc. IRE, vol. 34, April 1946, p. 198P.

30. J. G. Linvill, "The relationship of transistor parameters to amplifier performance," presented at IRE/AIEE -- University of Pennsylvania Conference on Transistor Circuits, Philadelphia, Pa., February 17, 1955.

31. L. J. Giacolletto, "Study of p-n-p alloy junction transistor from d-c through medium frequencies," RCA Review, vol. 15, December 1954, p. 555.

32. S. J. Mason, "Power gain in feedback amplifiers," Trans. IRE, vol. CT-1, June 1954, pp. 20-25.

33. P. R. Drouilhet, Jr., "Predictions based on the maximum oscillation frequency of a transistor," Trans. IRE, vol. CT-2, June 1955, pp. 178-183.

34. J. B. Angell and F. P. Keiper, Jr., "Circuit applications of surface-barrier transistors," Proc. IRE, vol. 41, December 1953, pp. 1709-1712.

35. Valley and Wallman, Vacuum Tube Amplifiers, (vol. 18, MIT Radiation Lab. Series), McGraw-Hill, New York, 1948, p. 169.

36. H. W. Bode, Network Analysis and Feedback Amplifier Design, D. Van Nostrand, New York, 1945, pp. 211-212.

37. Valley and Wallman, op. cit., p. 176.

38. W. A. Edson, "The single-layer solenoid as an rf transformer," Proc. IRE, vol. 43, August 1955, pp. 932-936.

39. M. Tanenbaum and D. E. Thomas, "Diffused emitter and base silicon transistors," Bell Syst. Tech. Jour., vol. 35, January 1956, pp. 1-22.

40. Gabriel Kron, "Numerical solution of ordinary and partial differential equations by means of equivalent circuits," J. Appl. Phys., vol. 16, March 1945, pp. 172-186.

Distribution List

Technical Reports (Circuits) #6onr 251(07)

cc	Addressee
	Chief of Naval Research Department of the Navy Washington 25, D. C.
2	Attn: Code 427
	Commanding Officer Office of Naval Research 1000 Geary Street
1	San Francisco 9, California
	Commanding Officer Office of Naval Research Branch Office 1030 E. Green Street
1	Pasadena, California
	Commanding Officer Office of Naval Research Branch Office John Crerar Library Building 86 E. Randolph Street
1	Chicago 1, Illinois
	Commanding Officer Office of Naval Research Branch Office 346 Broadway
1	New York 13, New York
	Officer in Charge Office of Naval Research Navy 100, Fleet Post Office
3	New York, New York
	Director Naval Research Laboratory Washington 25, D. C.
6	Attn: Code 2000
1	Attn: Code 5240
1	Attn: Code 7100
1	Attn: Code 5490
1	Attn: Code 5200
1	Attn: Code 5300
1	Attn: Code 5400
1	Attn: Code 5261OA
	Chief, Bureau of Ships Navy Department Washington 25, D. C.
3	Attn: Code 810
1	Attn: Code 816
1	Attn: Code 820
1	Attn: Code 840
	Chief, Bureau of Aeronautics Navy Department Washington 25, D. C.
1	Attn: Code EL 4
1	Attn: Code EL 45
1	Attn: Code EL 43
	Chief, Bureau of Ordnance Navy Department Washington 25, D. C.
1	Attn: Code Re 4
1	Attn: Code Re 9
	Chief of Naval Operations Navy Department Washington 25, D. C.
1	Attn: Code Op 30X
1	Attn: Code Op 55
1	Attn: Code Op 371C
	Director Naval Ordnance Laboratory White Oak, Maryland
	Director Naval Electronics Laboratory
1	San Diego 52, California
	U. S. Naval Post Graduate School
1	Monterey, California
	Commander Naval Air Missile Test Center Point Mugu, California
1	Attn: Code 366
	U. S. Naval Proving Ground
1	Dahlgren, Virginia
	Commander U. S. Naval Air Development Center
1	Johnsville, Pennsylvania
	Commanding Officer New York Naval Shipyard Material Laboratory Library Naval Base
1	Brooklyn, New York
	Naval Ordnance Laboratory Corona, California
1	Attn: Ralph A. Lunn, Chief, Missile Development Div.
	Scientific Research Section Research Branch, R and D Division Office of Asst. Chief of Staff, G4 Department of the Army
1	Washington 25, D. C.
	Chief, E and T Division Office of the Chief Signal Officer Washington 25, D. C.
1	Attn: SIGGD
	Chief, P and O Division Office of the Chief Signal Officer Department of the Army Washington 25, D. C.
1	Attn: SIGOT-5
	Office of the Chief of Engineers Department of the Army
1	Washington 25, D. C.
	Office of the Chief of Ordnance Department of the Army Washington 25, D. C.
2	Attn: ORDTU

cc	Addressee
	Director Signal Corps Engineering Laboratories Evans Signal Laboratory Supply Receiving Section Building No. 42 Belmar, New Jersey
28	Attn: Countermeasures Branch
	Commanding Officer Eng. Research and Development Lab.
1	Ft. Belvoir, Virginia
	Commanding Officer Frankford Arsenal Bridesburg, Philadelphia, Pennsylvania
1	
	Ballistics Research Laboratory Aberdeen Proving Ground, Maryland
2	Attn: D. W. Delassso
	Commanding General Wright Air Development Center Wright-Patterson Air Force Base, Ohio
1	Attn: WCRED-2
4	Attn: WCLOL
1	Attn: WCLRA
1	Attn: WCRR
1	Attn: WCRRH
	Chief of Staff United States Air Force Washington 25, D. C.
2	Attn: AFDRD-SC-3
	Commanding General Rome Air Development Center Griffiss Air Force Base Rome, New York
2	Attn: RCRW
	Commanding General Air Force Cambridge Research Center Air Research and Development Command L. G. Hanscom Field Bedford, Massachusette
8	Attn: CRTOTT-2, Electronics
	Commander Patrick Air Force Base
1	Cocoa, Florida
	Air Force Special Weapons Center Kirtland Air Force Base Albuquerque, New Mexico
2	Attn: SWOI
	Chief, European Office Air Research and Development Command c/o Hq. USAFE APO 633, c/o Postmaster
1	New York, New York
	Director Air University Library Maxwell Air Force Base, Alabama
1	Attn: CR 4582
	Commanding General Air Research and Development Command Post Office Box 1395 Baltimore 3, Maryland
1	Attn: RDTDR
1	Attn: RDTDRE
1	Attn: RDTDRR
1	Attn: SROFF
	Assistant Secretary of Defense (Research and Development) Research and Development Board Department of Defense Washington 25, D. C.
1	Attn: Technical Library
	Secretary, Committee on Electronics Office of the Assistant Secretary of Defense (Research and Development) Department of Defense
1	Washington 25, D. C.
	Advisory Group on Electron Tubes 346 Broadway, 8th Floor East New York 13, New York
1	Attn: William J. McDonald, Chief, Technical Reference Section
	Armed Services Technical Information Agency Document Service Center Knott Building Dayton 2, Ohio
5	Attn: DSC-SA
	Office of Technical Services Department of Commerce
1	Washington 25, D. C.
	Commanding Officer Diamond Fuse Laboratories Connecticut Ave. and Van Ness St.,N.W. Washington 25, D. C.
1	Attn: Division 10, Librarian
1	Attn: ORDTL-52.0
	Library Boulder Laboratories National Bureau of Standards
1	Boulder, Colorado
	Chief, West Coast Office Signal Corps Engineering Labs. 75 S. Grand Ave., Bldg. 6
1	Pasadena, California
	Polytechnic Institute of Brooklyn Microwave Research Institute 55 Johnson Street Brooklyn 1, New York
1	Attn: Prof. E. Weber
	California Institute of Technology Department of Electrical Engineering Pasadena, California
1	Attn: Prof. L. M. Field

cc	Addressee
	University of California Electrical Engineering Department Berkeley 4, California
1	Attn: Prof. J. R. Whinnery
	Georgia Institute of Technology Atlanta, Georgia
1	Attn: Mrs. J. Henley Crosland, Librarian
	Harvard University Technical Reports Collection Room 303A, Pierce Hall Cambridge 38, Massachusetts
1	Attn: H. L. Cox, Librarian
	University of Illinois Control Systems Laboratories Urbana, Illinois
1	Attn: Profs. P. Seitz and R. E. Norberg
	University of Illinois Department of Physics Urbana, Illinois
1	Attn: Dr. John Bardeen
	Johns Hopkins University Radiation Laboratory 1315 St. Paul Street Baltimore 2, Maryland
1	Attn: Dr. D. D. King
	Loyola University Department of Physics New Orleans 18, La.
1	Attn: Dr. Paul D. Pickar
	Linfield Research Institute McMinnville, Oregon
1	Attn: Dr. W. P. Dyke, Director
	Massachusetts Institute of Technology Cambridge 39, Massachusetts
1	Research Laboratory of Electronics
1	Laboratory for Insulation Research
1	Lincoln Laboratory
	New York University University Heights College of Engineering New York 53, New York
1	Attn: L. S. Schwartz,Res. Div.
	Ohio State University Department of Electrical Engineering Columbus 10, Ohio
1	Attn: Prof. K. M. Boone
	Purdue University Research Library Lafayette, Indiana
1	Attn: H. J. Oorthuys
	Stanford Research Institute Stanford, California
1	Attn: Bryon Bennett
1	Attn: Technical Library
	Syracuse University Department of Electrical Engineering Syracuse 10, New York
1	Attn: Dr. Herbert Hellerman
	University of California at Los Angeles West Los Angeles, California
1	Attn: Dr. D. L. Trautman
	Director Electronics Defense Group Engineering Research Institute University of Michigan
1	Ann Arbor, Michigan
	Engineering Research Institute 351 East Engineering Building University of Michigan Ann Arbor, Michigan
1	Attn: Joseph E. Rowe, Res. Assoc.
	University of Michigan Willow Run Research Center Engineering Research Institute Ypsilanti, Michigan
1	Attn: Dr. H. Goode
	Commanding Officer Signal Corps Electronics Research Unit 9560th TU (Sylvania) P. O. Box 205
1	Mountain View, California
	Airborne Instrument Laboratory 160 Old Country Road Mineola, L. I., New York
1	Attn: Mr. John Dyer
	Bell Telephone Laboratories Murray Hill Laboratory Murray Hill, New Jersey
1	Attn: Technical Library
1	Attn: Dr. S. Darlington
	CBS Laboratories 485 Madison Avenue
1	New York 22, New York
	Columbia Radiation Laboratory 538 West 120th Street
1	New York 27, New York
	Cornell Aeronautical Labs.,Inc. Cornell Research Foundation
2	Buffalo 21, New York
	Federal Telecommunications Labs., Inc. 500 Washington Avenue Nutley, New Jersey
1	Attn: Librarian
	Gilfillan Brothers 1815 Venice Boulevard Los Angeles, California
1	Attn: Countermeasures Laboratory

cc	Addressee
	General Electric Company Research Laboratory P. O. Box 1088 Schenectady, New York
1	Attn: Alice V. Neil, Librarian
	General Electric Microwave Laboratory at Stanford Stanford Industrial Park Palo Alto, California
1	Attn: Technical Library
	Hewlett-Packard Company 275 Page Mill Road Palo Alto, California
1	
	Hughes Aircraft Company Research and Development Library Culver City, California
1	Attn: Mr. John T. Milek
	Philco Corporation 22nd Street and Lehigh Avenue Philadelphia 32, Pa.
1	Attn: Mr. F. H. Sherman, Tech.Editor, Tech. Rep. Div. Bulletin
	RCA Laboratories Princeton, New Jersey
1	Attn: E. W. Herold and Harwell Johnson
	The Rand Corporation 1700 Main Street Santa Monica, California
1	Attn: Margaret Anderson, Librarian
	Raytheon Corporation Waltham, Massachusetts
1	Attn: W. Welsh
	Sperry Gyroscope Company Engineering Library Mail Station C-39
1	Great Neck, L. I., New York
	Tektronix, Inc. P. O. Box 831
1	Portland 7, Oregon
	Texas Instruments, Inc. 6000 Lemmon Avenue
1	Dallas 9, Texas
	Varian Associates 611 Hansen Way Palo Alto, California
1	Attn: Technical Library
	Stanford University
25	Stanford, California